Lecture Note #3 (Spring, 2020)

Experimental Probes and Techniques

1. Ultrahigh vacuum, sources
2. Probe techniques
3. Electron diffraction
4. Electron spectroscopy
5. Vibrational spectroscopy

Reading: Kolasinski, ch.2

The techniques of surface science

- AES, AFM, EELS, ESCA, EXAFS, FEM, FIM, FTIR, HEIS, HPXPS, HREELS, IRAS, ISS, LEED, LEIS, NEXAFS, NMR, RBS, SERS, SEXAFS, SFG, SHG, SIMS, STM, TEM, TDS, UPS, XANES, SPS, XRD…

- Surface properties: structure, composition, oxidation states, chemical properties, electronic properties, mechanical properties → atomic resolution, smaller energy resolution, shorter time scales, in situ, high pressure

- Sources: electrons, atoms, ions, photons

Ultrahigh vacuum (UHV)

- Ultra-high vacuum (UHV) conditions → atomically clean surfaces

the Flux, F, of molecules striking the surface of unit area at pressure P

M: average molecular weight of gases species, N_A: Avogadro's number
$m = M/N_A$, $k_B = R/N_A$

$$\boxed{Z_w = P/(2\pi m k_B T)^{1/2}}$$ (1.0.1) in textbook

- UHV ($<1.33 \times 10^{-7}$ Pa $= 10^{-9}$ Torr) → to maintain a clean surface for ~ 1h
- Mean free path: distance that a particle travels on average between collisions → longer mean free path for electron in e^- spectroscopy

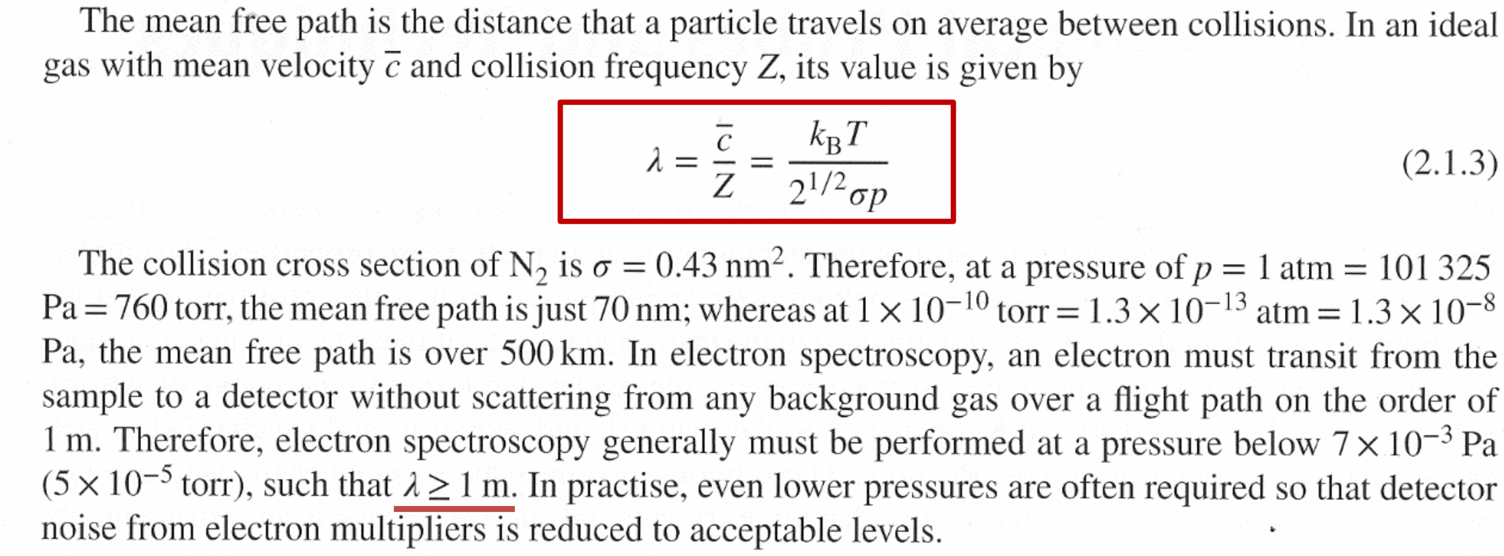

The mean free path is the distance that a particle travels on average between collisions. In an ideal gas with mean velocity $\bar{c}$ and collision frequency Z, its value is given by

$$\boxed{\lambda = \frac{\bar{c}}{Z} = \frac{k_B T}{2^{1/2} \sigma p}} \tag{2.1.3}$$

The collision cross section of N_2 is $\sigma = 0.43\ \mathrm{nm}^2$. Therefore, at a pressure of $p = 1$ atm = 101 325 Pa = 760 torr, the mean free path is just 70 nm; whereas at 1×10^{-10} torr $= 1.3 \times 10^{-13}$ atm $= 1.3 \times 10^{-8}$ Pa, the mean free path is over 500 km. In electron spectroscopy, an electron must transit from the sample to a detector without scattering from any background gas over a flight path on the order of 1 m. Therefore, electron spectroscopy generally must be performed at a pressure below 7×10^{-3} Pa (5×10^{-5} torr), such that $\underline{\lambda \geq 1\ \mathrm{m}}$. In practise, even lower pressures are often required so that detector noise from electron multipliers is reduced to acceptable levels.

Light and electron sources

Electromagnetic radiation (light, photon)

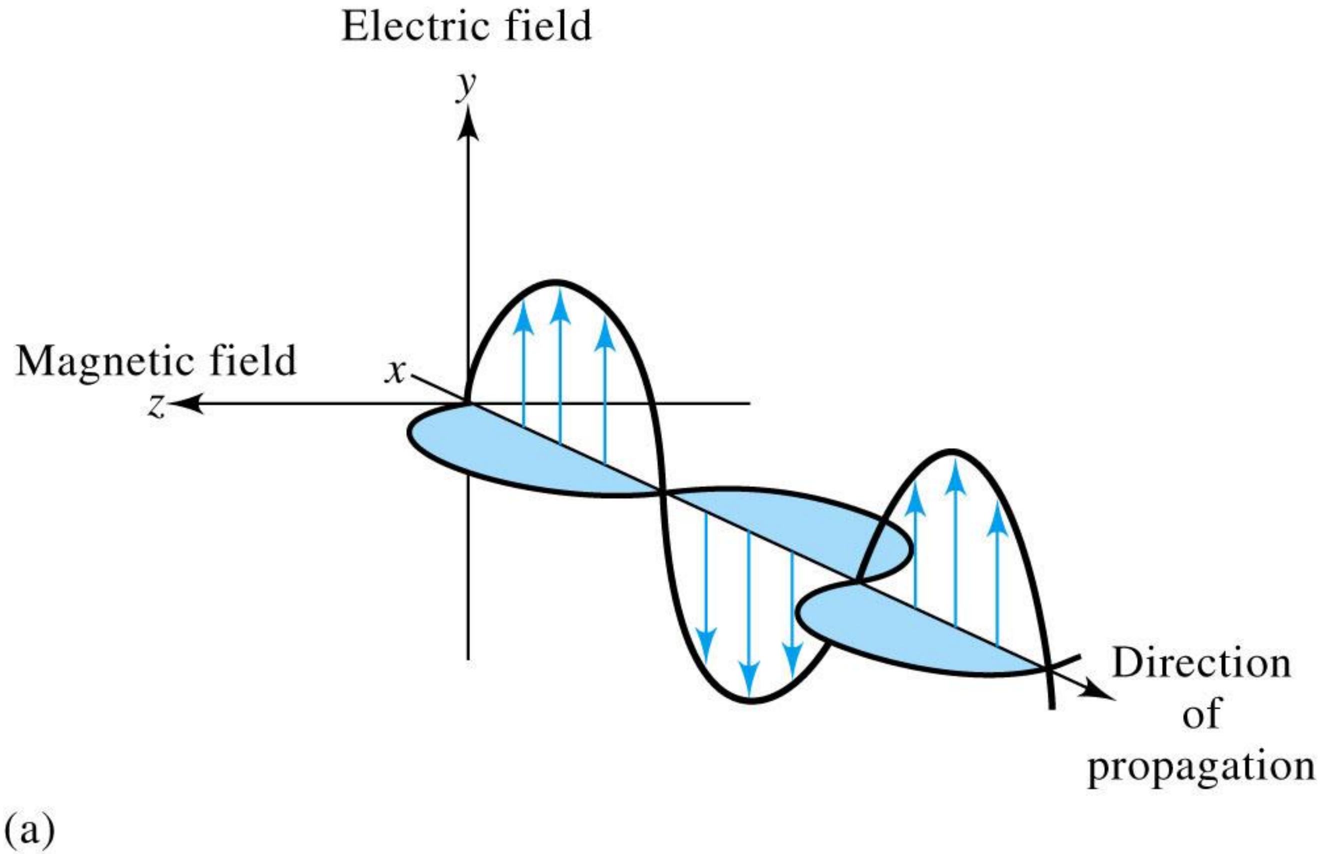

Skoog, Holler, Crouch, Principles of Instrumental Analysis (Thomson)

Electric component of electromagnetic wave

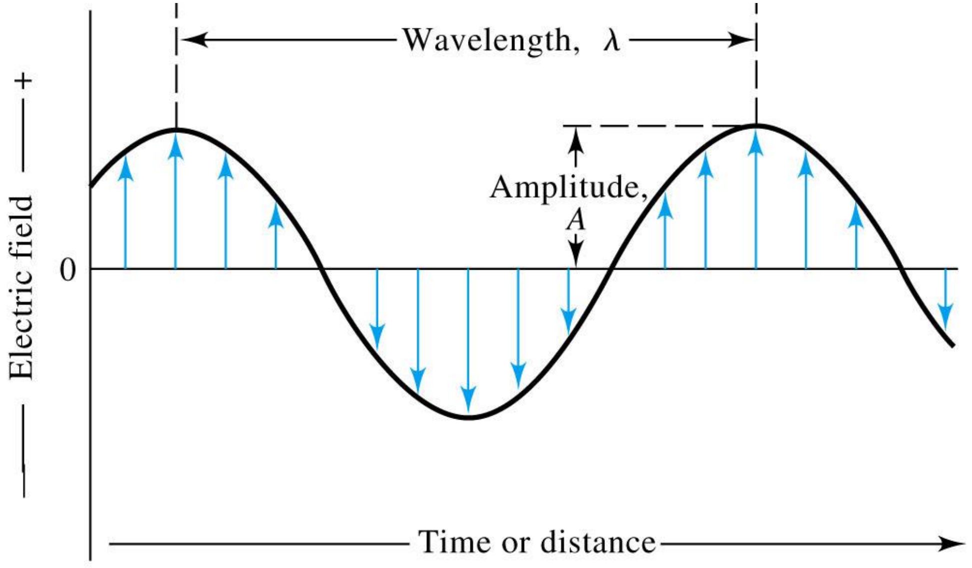

(b)

© 2007 Thomson Higher Education

$$v_i = v\lambda_i \qquad (6\text{-}1)$$

velocity of propagation v_i
frequency v: number of oscillations per second

In a vacuum, v_i is independent of wavelength and a maximum → $c = 2.99792 \times 10^8$ m/s

In a air, v_i differs only slightly from c (about 0.03% less): ~ c

$$c = v\lambda = 3.00 \times 10^8 \text{ m/s} = 3.00 \times 10^{10} \text{ cm/s} \qquad (6\text{-}2)$$

wavenumber $\bar{v}$: the reciprocal of wavelength in cm (cm^{-1})

$$\boxed{E = hv = h(c/\lambda) = hc\bar{v}}$$

Skoog, Holler, Crouch, Principles of Instrumental Analysis (Thomson)

The electromagnetic spectrum

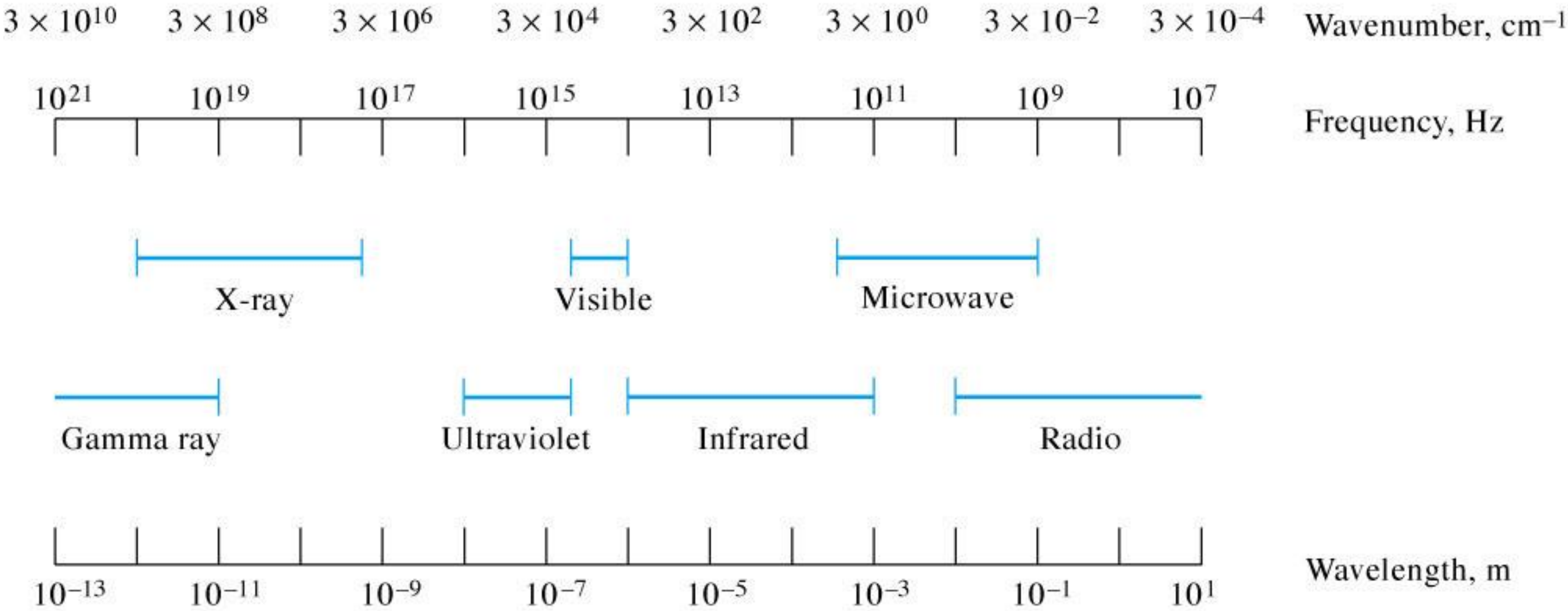

© 2007 Thomson Higher Education

eV **nm** **cm^{-1}** **Hz**

Skoog, Holler, Crouch, Principles of Instrumental Analysis (Thomson)

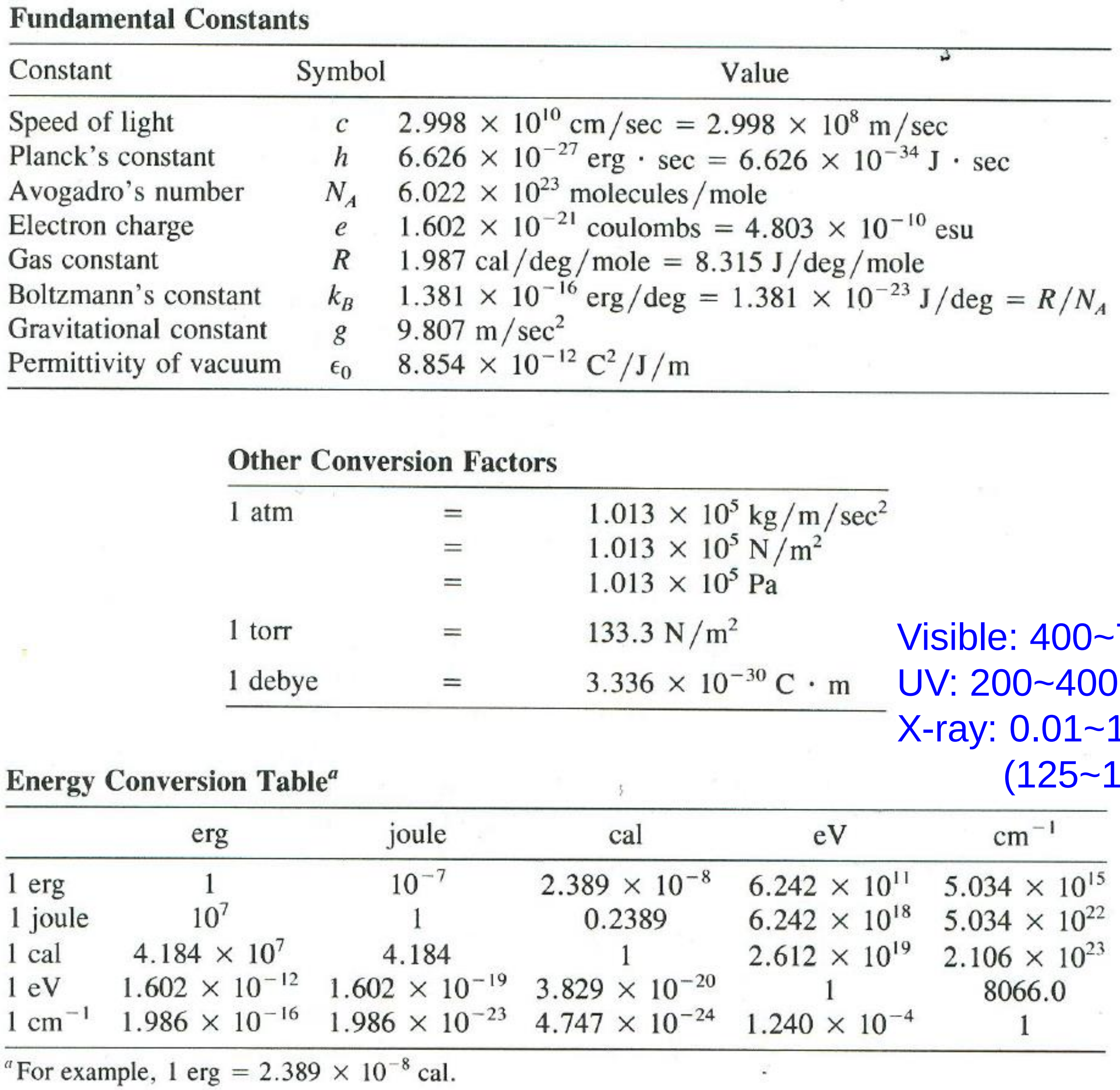

Fundamental Constants

Constant	Symbol	Value
Speed of light	c	2.998×10^{10} cm/sec = 2.998×10^{8} m/sec
Planck's constant	h	6.626×10^{-27} erg · sec = 6.626×10^{-34} J · sec
Avogadro's number	N_A	6.022×10^{23} molecules/mole
Electron charge	e	1.602×10^{-21} coulombs = 4.803×10^{-10} esu
Gas constant	R	1.987 cal/deg/mole = 8.315 J/deg/mole
Boltzmann's constant	k_B	1.381×10^{-16} erg/deg = 1.381×10^{-23} J/deg = R/N_A
Gravitational constant	g	9.807 m/sec^2
Permittivity of vacuum	ϵ_0	8.854×10^{-12} C^2/J/m

Other Conversion Factors

1 atm = 1.013×10^{5} kg/m/sec^2
= 1.013×10^{5} N/m^2
= 1.013×10^{5} Pa

1 torr = 133.3 N/m^2

1 debye = 3.336×10^{-30} C · m

Energy Conversion Table[a]

	erg	joule	cal	eV	cm^{-1}
1 erg	1	10^{-7}	2.389×10^{-8}	6.242×10^{11}	5.034×10^{15}
1 joule	10^{7}	1	0.2389	6.242×10^{18}	5.034×10^{22}
1 cal	4.184×10^{7}	4.184	1	2.612×10^{19}	2.106×10^{23}
1 eV	1.602×10^{-12}	1.602×10^{-19}	3.829×10^{-20}	1	8066.0
1 cm^{-1}	1.986×10^{-16}	1.986×10^{-23}	4.747×10^{-24}	1.240×10^{-4}	1

[a] For example, 1 erg = 2.389×10^{-8} cal.

Visible: 400~700 nm (1.8~3.1 eV)
UV: 200~400 nm (3.1~6.2 eV)
X-ray: 0.01~10 nm
(125~125,000 eV)

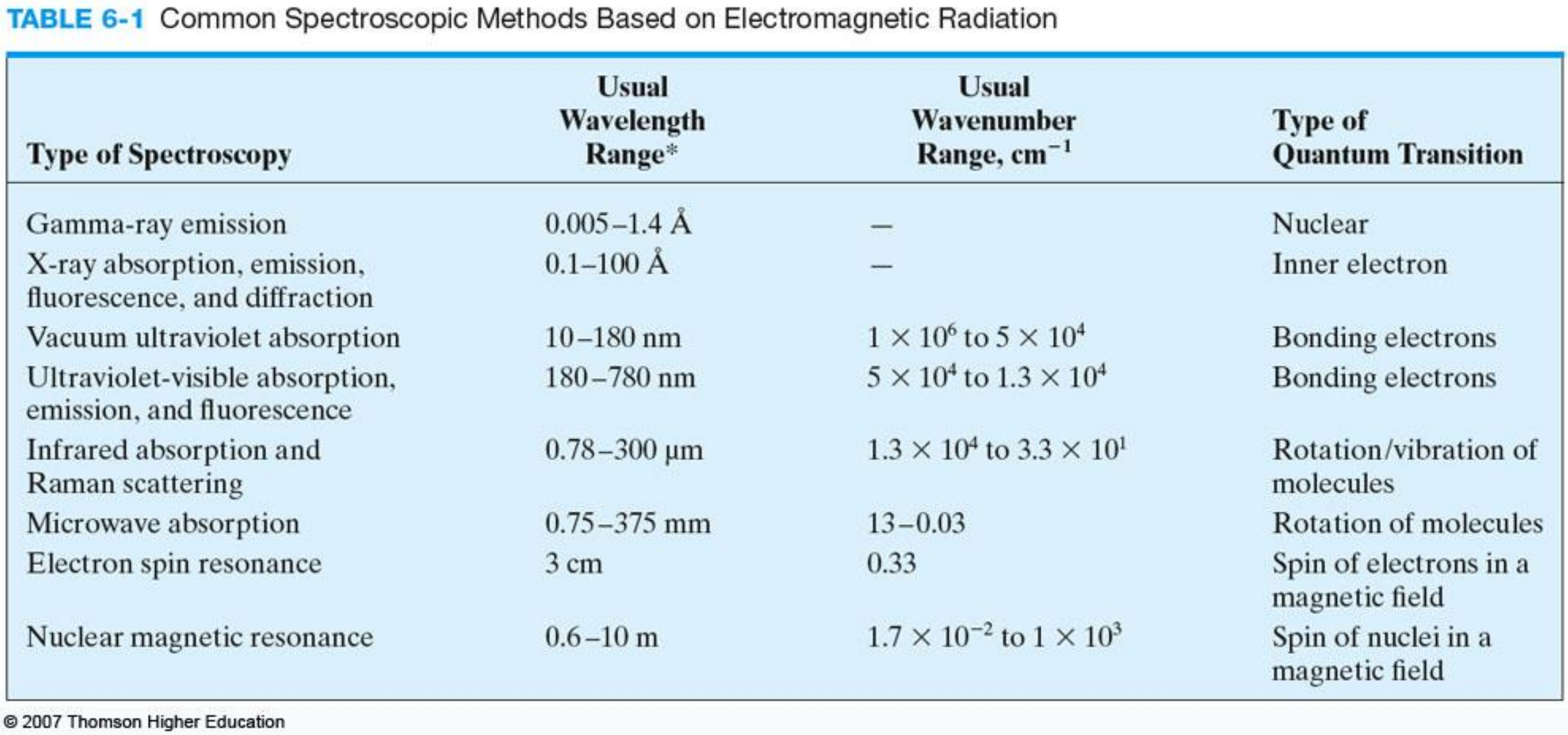

TABLE 6-1 Common Spectroscopic Methods Based on Electromagnetic Radiation

Type of Spectroscopy	Usual Wavelength Range*	Usual Wavenumber Range, cm^{-1}	Type of Quantum Transition
Gamma-ray emission	0.005–1.4 Å	—	Nuclear
X-ray absorption, emission, fluorescence, and diffraction	0.1–100 Å	—	Inner electron
Vacuum ultraviolet absorption	10–180 nm	1×10^6 to 5×10^4	Bonding electrons
Ultraviolet-visible absorption, emission, and fluorescence	180–780 nm	5×10^4 to 1.3×10^4	Bonding electrons
Infrared absorption and Raman scattering	0.78–300 μm	1.3×10^4 to 3.3×10^1	Rotation/vibration of molecules
Microwave absorption	0.75–375 mm	13–0.03	Rotation of molecules
Electron spin resonance	3 cm	0.33	Spin of electrons in a magnetic field
Nuclear magnetic resonance	0.6–10 m	1.7×10^{-2} to 1×10^3	Spin of nuclei in a magnetic field

Skoog, Holler, Crouch, Principles of Instrumental Analysis (Thomson)

Types of lasers

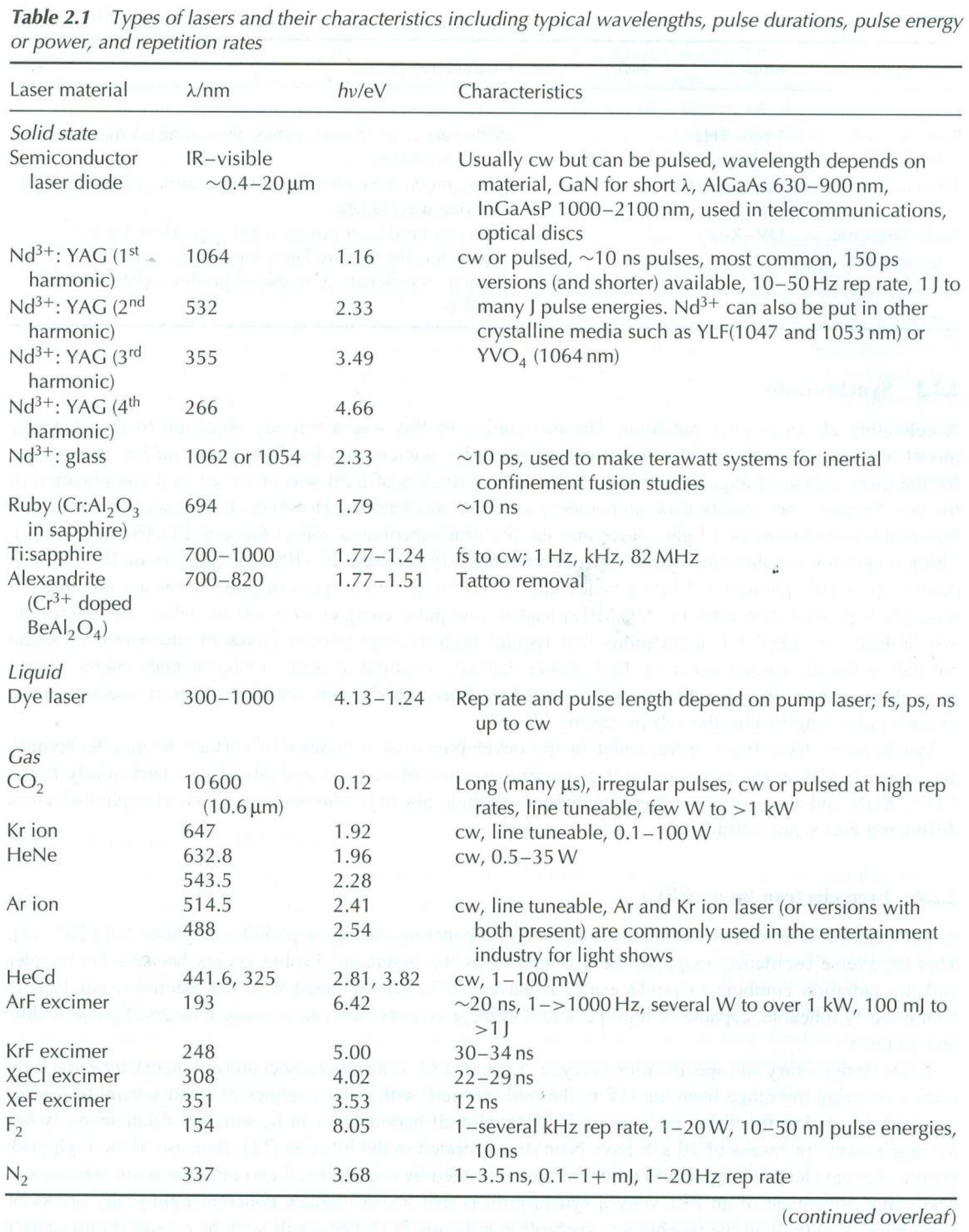

Table 2.1 Types of lasers and their characteristics including typical wavelengths, pulse durations, pulse energy or power, and repetition rates

Laser material	λ/nm	hν/eV	Characteristics
Solid state			
Semiconductor laser diode	IR–visible ~0.4–20 μm		Usually cw but can be pulsed, wavelength depends on material, GaN for short λ, AlGaAs 630–900 nm, InGaAsP 1000–2100 nm, used in telecommunications, optical discs
Nd^{3+}: YAG (1st harmonic)	1064	1.16	cw or pulsed, ~10 ns pulses, most common, 150 ps versions (and shorter) available, 10–50 Hz rep rate, 1 J to many J pulse energies. Nd^{3+} can also be put in other crystalline media such as YLF(1047 and 1053 nm) or YVO_4 (1064 nm)
Nd^{3+}: YAG (2nd harmonic)	532	2.33	
Nd^{3+}: YAG (3rd harmonic)	355	3.49	
Nd^{3+}: YAG (4th harmonic)	266	4.66	
Nd^{3+}: glass	1062 or 1054	2.33	~10 ps, used to make terawatt systems for inertial confinement fusion studies
Ruby ($Cr:Al_2O_3$ in sapphire)	694	1.79	~10 ns
Ti:sapphire	700–1000	1.77–1.24	fs to cw; 1 Hz, kHz, 82 MHz
Alexandrite (Cr^{3+} doped $BeAl_2O_4$)	700–820	1.77–1.51	Tattoo removal
Liquid			
Dye laser	300–1000	4.13–1.24	Rep rate and pulse length depend on pump laser; fs, ps, ns up to cw
Gas			
CO_2	10 600 (10.6 μm)	0.12	Long (many μs), irregular pulses, cw or pulsed at high rep rates, line tuneable, few W to >1 kW
Kr ion	647	1.92	cw, line tuneable, 0.1–100 W
HeNe	632.8 543.5	1.96 2.28	cw, 0.5–35 W
Ar ion	514.5 488	2.41 2.54	cw, line tuneable, Ar and Kr ion laser (or versions with both present) are commonly used in the entertainment industry for light shows
HeCd	441.6, 325	2.81, 3.82	cw, 1–100 mW
ArF excimer	193	6.42	~20 ns, 1–>1000 Hz, several W to over 1 kW, 100 mJ to >1 J
KrF excimer	248	5.00	30–34 ns
XeCl excimer	308	4.02	22–29 ns
XeF excimer	351	3.53	12 ns
F_2	154	8.05	1–several kHz rep rate, 1–20 W, 10–50 mJ pulse energies, 10 ns
N_2	337	3.68	1–3.5 ns, 0.1–1+ mJ, 1–20 Hz rep rate

(continued overleaf)

X-ray

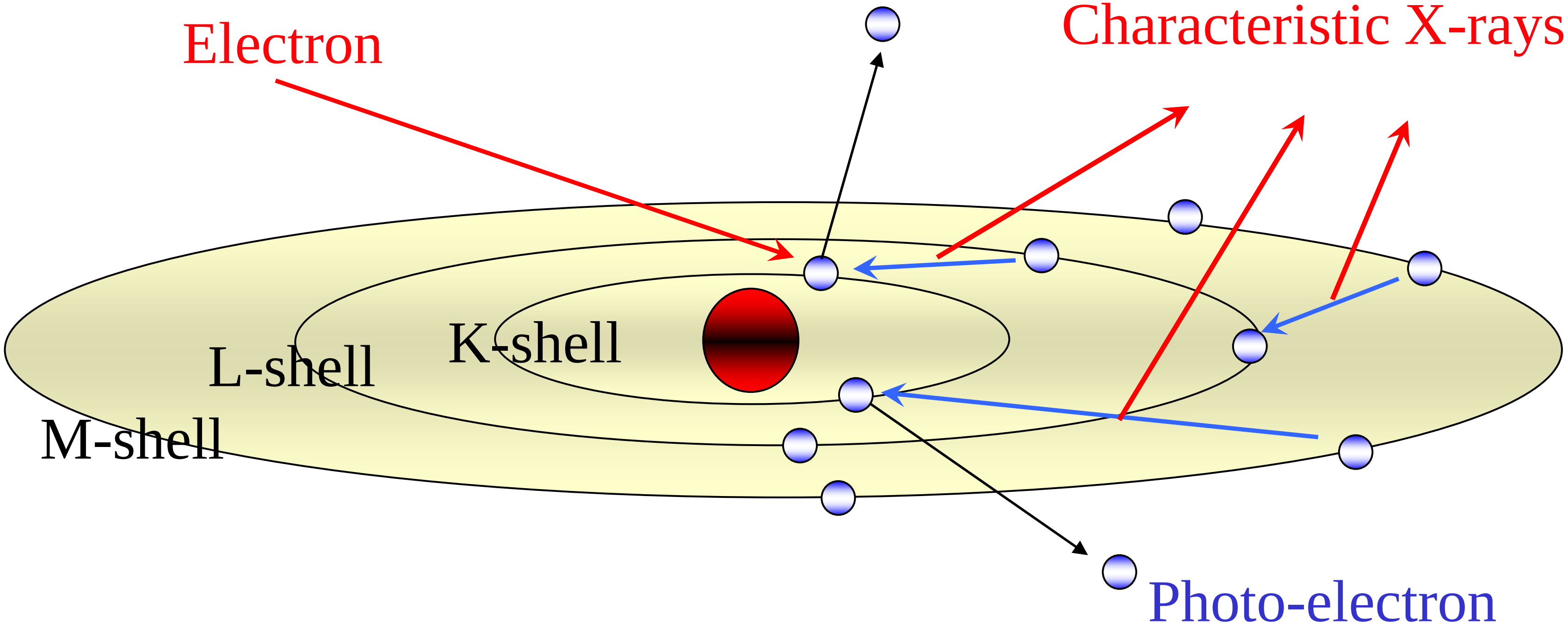
Electron
Characteristic X-rays
K-shell
L-shell
M-shell
Photo-electron

X-ray sources

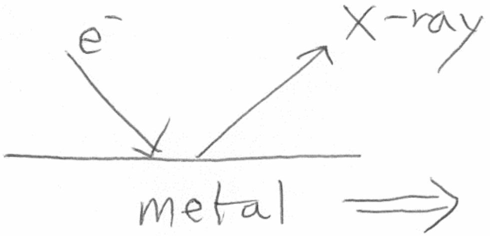

⟹ Mg Kα 1253.6 eV

Al Kα 1486.6 eV

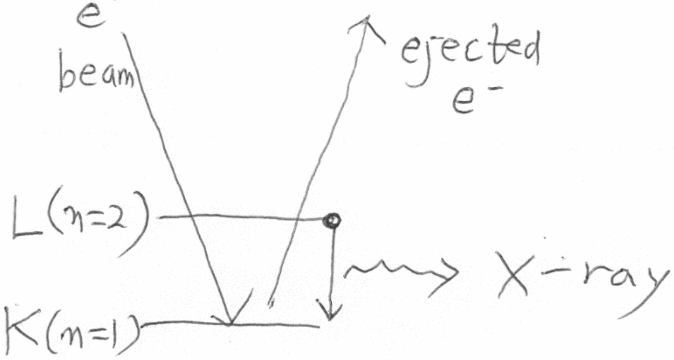

L → K ⟹ Kα

M → K ⟹ Kβ

$2P_{3/2} \rightarrow 1s$ $K\alpha_1$

$2P_{1/2} \rightarrow 1s$ $K\alpha_2$

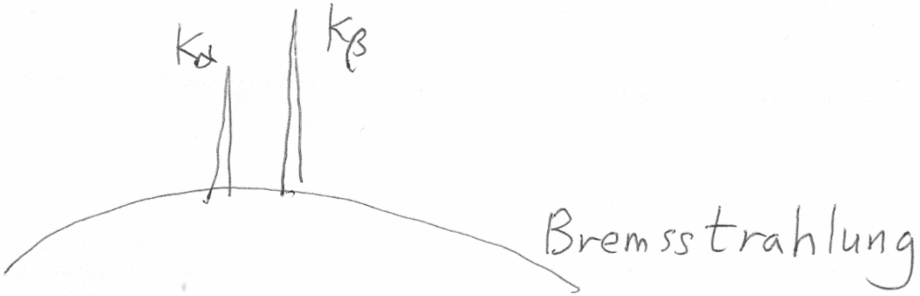

Synchrotron

X-ray absorption spectroscopy

Absorption edge (energy that is just need to eject a particular core electron, e.g., 1s (K edge), $2p_{3/2}$ e^- (L_3 edge)

Fe & Fe oxides
K-edge: 7.112 keV

Within 10-40 eV: X-ray absorption near-edge structure (**XANES**) (or near-ed absorption fine structure (**NEXAFS**))
→ oxidation state & ligand environment

About 50 keV: extended X-ray absorption Fine structure (**EXAFS**)
→ distance & arrangement of atoms

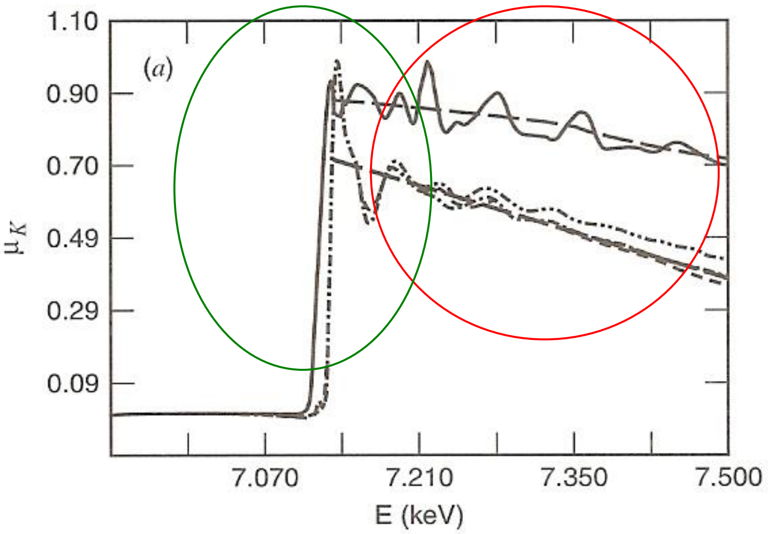

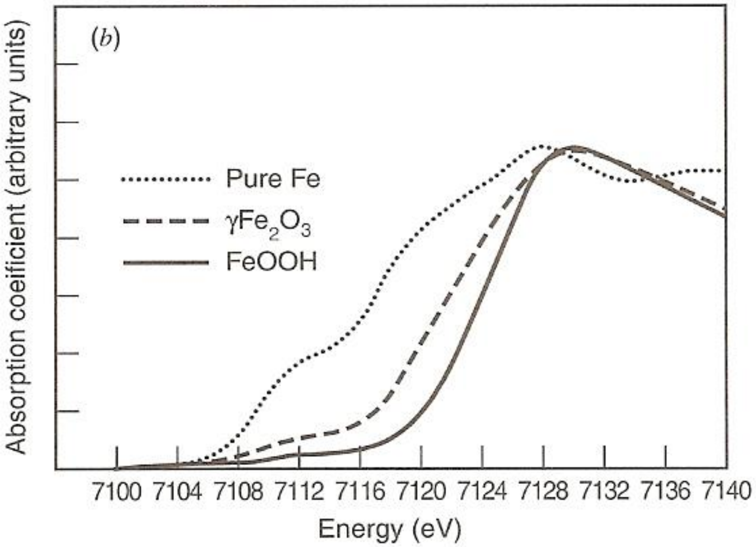

Spectroscopic surface methods

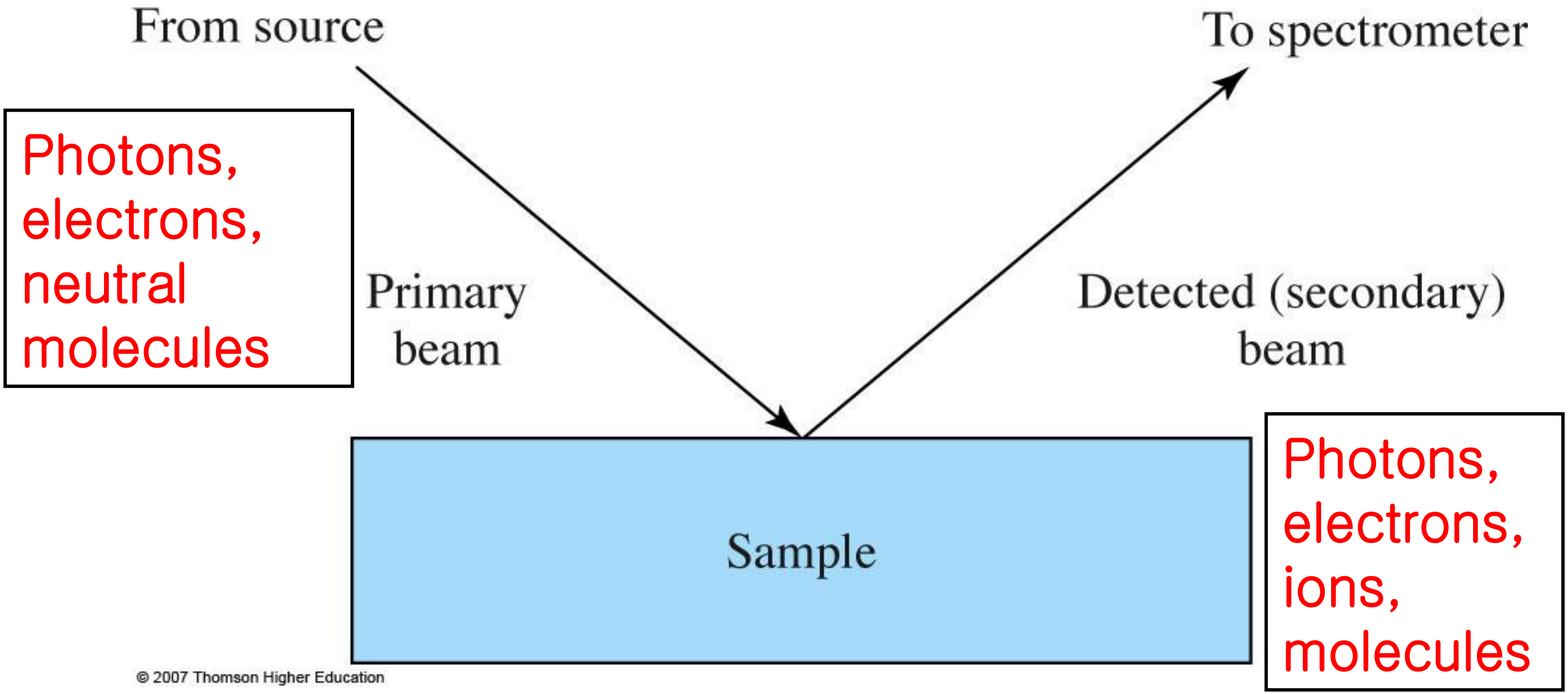

Photons, electrons, neutral molecules

Photons, electrons, ions, molecules

Atomic lamps: H (10.2 eV)
He (21.1, 42.82 eV) → UV sources, UPS
Xe lamp (170~3000 nm)

Skoog, Holler, Crouch, Principles of Instrumental Analysis (Thomson)

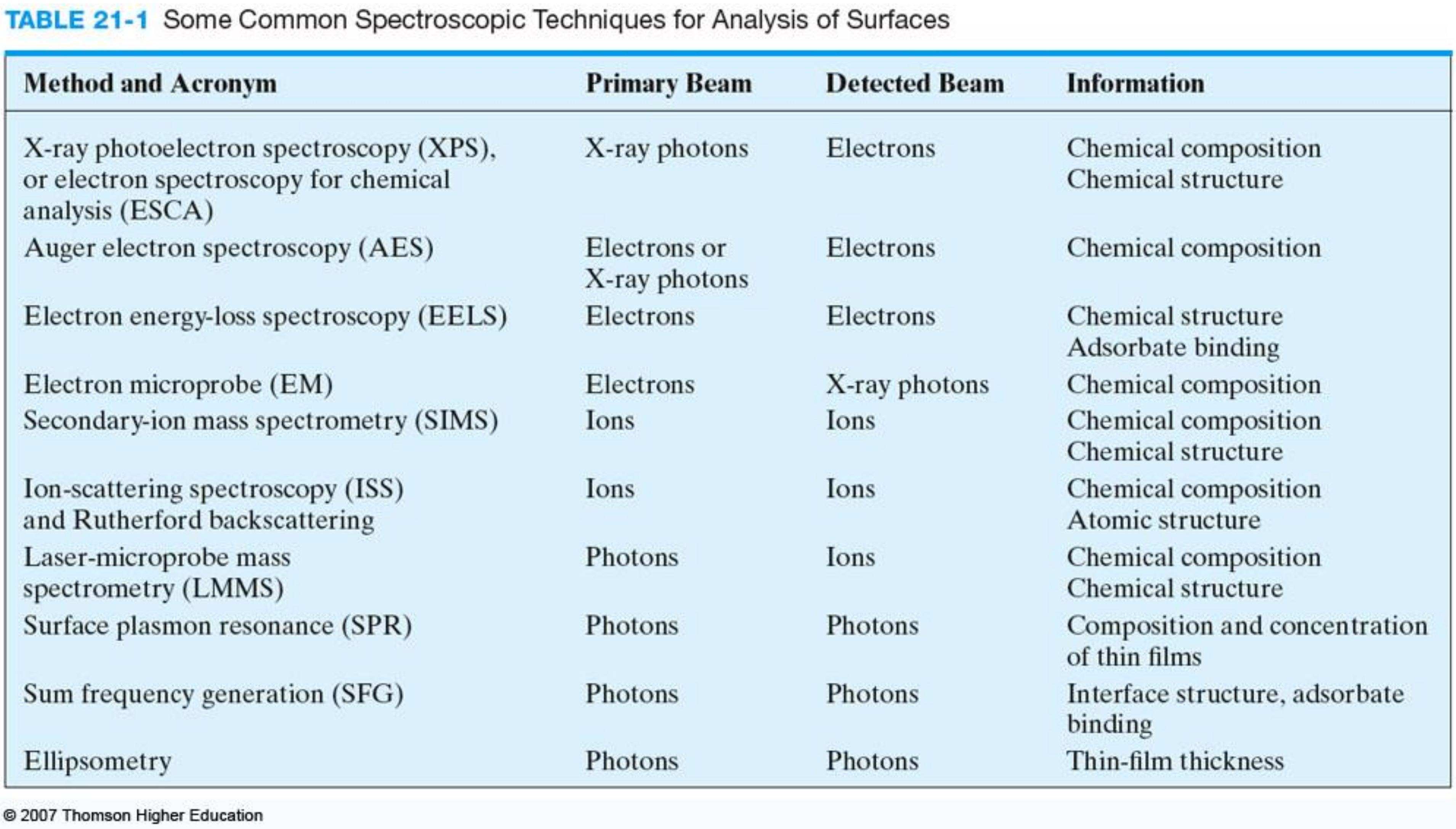

TABLE 21-1 Some Common Spectroscopic Techniques for Analysis of Surfaces

Method and Acronym	Primary Beam	Detected Beam	Information
X-ray photoelectron spectroscopy (XPS), or electron spectroscopy for chemical analysis (ESCA)	X-ray photons	Electrons	Chemical composition Chemical structure
Auger electron spectroscopy (AES)	Electrons or X-ray photons	Electrons	Chemical composition
Electron energy-loss spectroscopy (EELS)	Electrons	Electrons	Chemical structure Adsorbate binding
Electron microprobe (EM)	Electrons	X-ray photons	Chemical composition
Secondary-ion mass spectrometry (SIMS)	Ions	Ions	Chemical composition Chemical structure
Ion-scattering spectroscopy (ISS) and Rutherford backscattering	Ions	Ions	Chemical composition Atomic structure
Laser-microprobe mass spectrometry (LMMS)	Photons	Ions	Chemical composition Chemical structure
Surface plasmon resonance (SPR)	Photons	Photons	Composition and concentration of thin films
Sum frequency generation (SFG)	Photons	Photons	Interface structure, adsorbate binding
Ellipsometry	Photons	Photons	Thin-film thickness

Skoog, Holler, Crouch, Principles of Instrumental Analysis (Thomson)

Electron and ion

Ultra high vacuum (UHV)

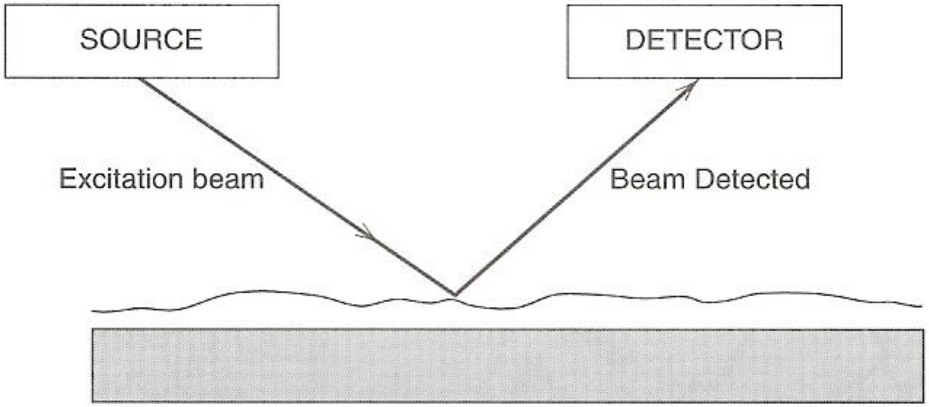

	Excitation	Detection
X-ray photoelectron spectroscopy (XPS)	Photons(X-ray)	Electrons
UV photoelectron spectroscopy (UPS)	Photons (UV)	Electrons
Auger electron spectroscopy (AES)	Electrons	Electrons
Low-energy electron diffraction (LEED)	Electrons	Electrons
High resolution e^- E loss spec. (HREELS)	Electrons	Electrons
Rutherford backscattering (RBS)	H+ or He+	H+ or He+
Secondary ion mass spec. (SIMS)	Ions	Ions
Laser desorption mass spec. (LDMS)	Photons	Ions

Scanning probe techniques

→ Surface structure, manipulation of atoms & molecules at surface

-Microscopy: a sharp tip close to the surface → scanning electron or force and so on → STM, AFM and so on

-Similar idea: NSOM (Near field scanning optical microscopy) → a small-diameter optical fiber close to the surface (diameter/distance < wavelength of the light) → image resolution far below light wavelength

-SP techniques: current, van der Waals force, chemical force, magnetic force, capacitance, phonon, photon

-UHV or at atmosphere or in solution, *in situ vs. ex situ* techniques

Scanning tunneling microscopy (STM)

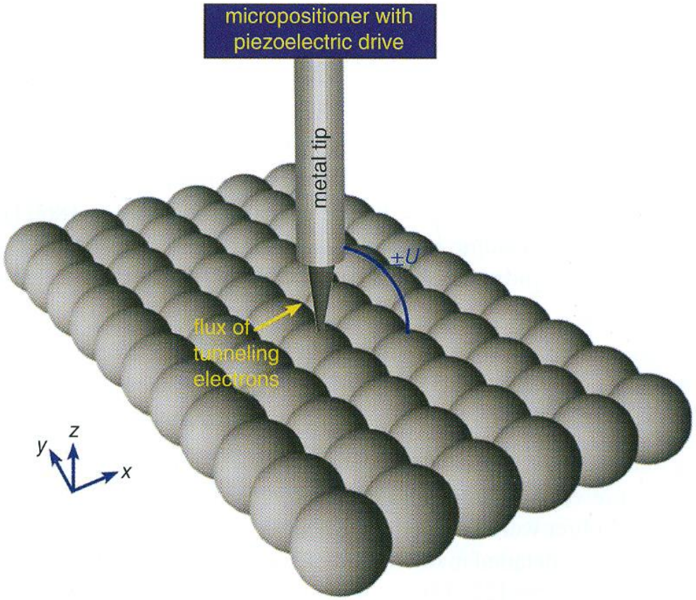

Tersoff and Hamann [31, 32] set the theoretical basis for interpretation of STM images. The tunnelling current, I, depends exponentially on the tip to surface distance d according to

$$\boxed{I \propto e^{-2\kappa d}} \tag{2.4.3}$$

where the decay constant κ is given by

$$\kappa = \frac{1}{\hbar}\sqrt{2m_e(\Phi_s + E_F^S - E)}. \tag{2.4.4}$$

E is the energy of the state from which tunnelling occurs, and the barrier height is given by the sum of the average work function of the sample surface Φ_s and its Fermi energy E_F^S. κ is on the order of 1 Å^{-1}, hence, a change in separation of just 1 Å leads to an order of magnitude change in the tunnelling current. Importantly, STM does not rely on simple one-dimensional tunnelling but is instead sensitive

cf. Tunnelling

- if the potential energy of a particle does not rise to infinite in the wall & E < V → Ψ does not decay abruptly to zero
- if the walls are thin → Ψ oscillate inside the box & on the other side of the wall outside the box → particle is found on the outside of a container: leakage by penetration through classically forbidden zones "tunnelling"

cf) C.M.: insufficient energy to escape

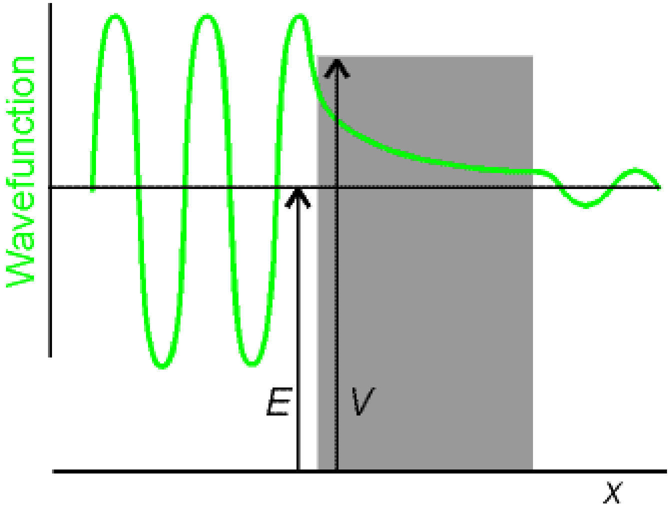

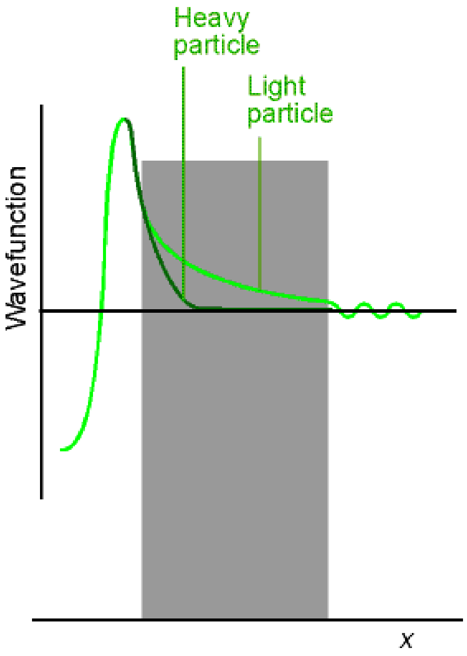

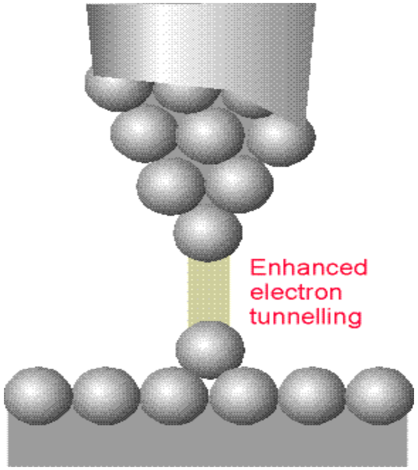

Electron flow between tip and surface

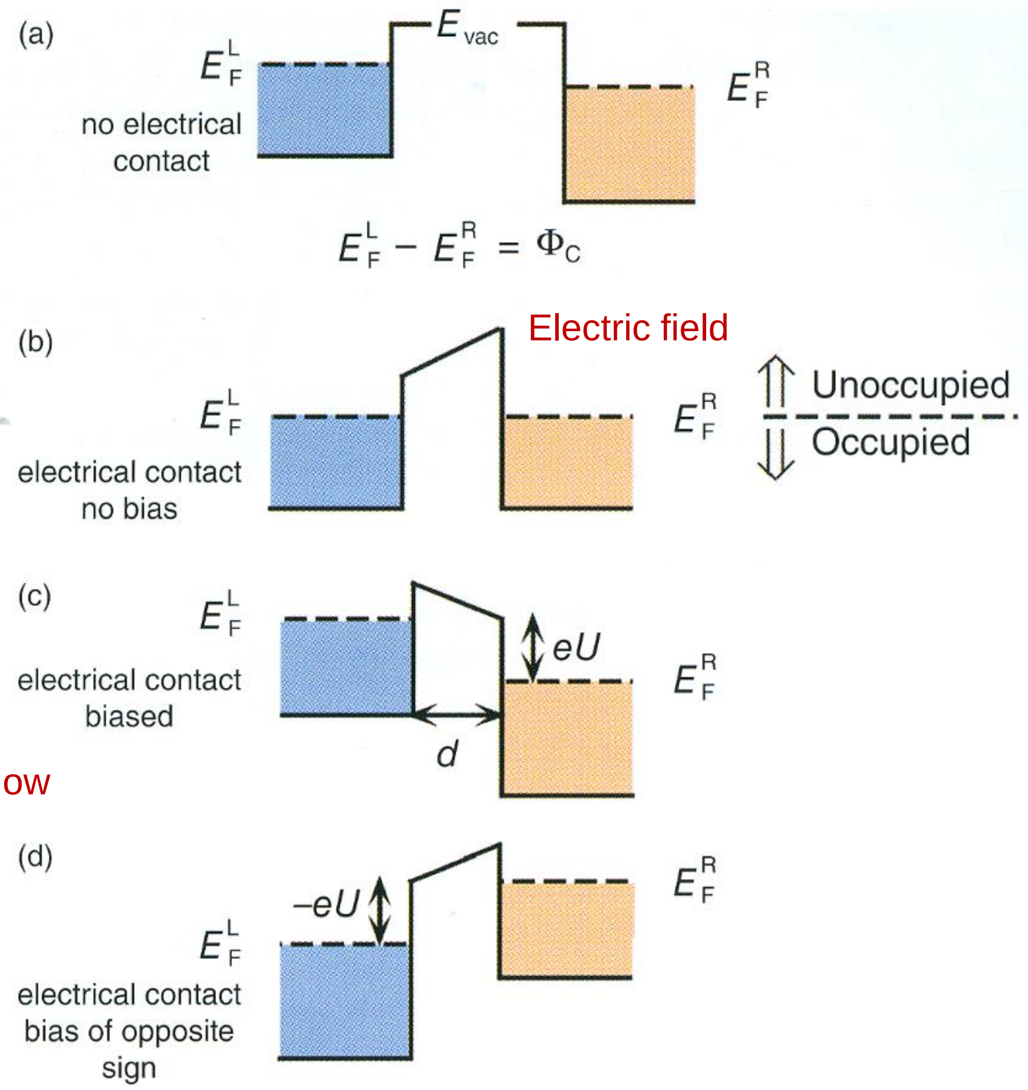

Electric field

Tunneling current flow

Figure 2.7 *Illustrations of the Fermi and vacuum level positions for two metals separated by distance* d. *(a) Isolated metals. (b) After electrical contact, in the absence of an applied bias. (c) Biasing shifts the relative positions of the Fermi levels and makes available unoccupied states in an energy window* eU *into which electrons can tunnel. (d) The direction of tunnelling is switched compared to the previous case simply by changing the sign of the applied bias.*

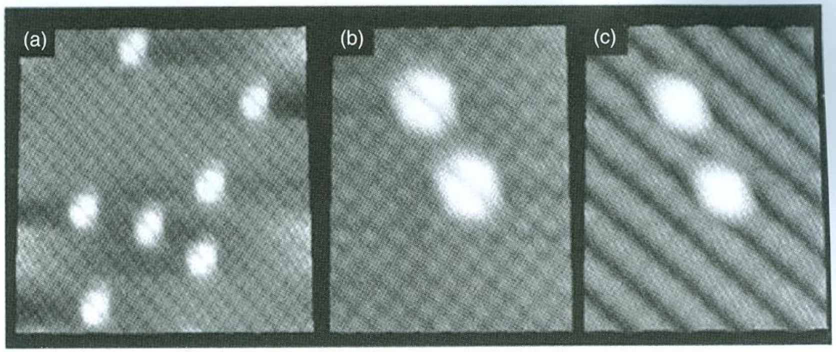

Figure 2.4 *An STM image of occupied states on a Si(100)-(2 × 1) surface nearly completely covered with adsorbed H atoms. The uncapped Si dangling bonds (sites where H is not adsorbed) appear as lobes above the plane of the H-terminated sites. The rows of the (2 × 1) reconstruction are clearly visible in the H-terminated regions. Source: Reproduced from J.J. Boland,* Phys. Rev. Lett. ***67*** *(1991) 1539. (c) 1991, with permission from the American Physical Society.*

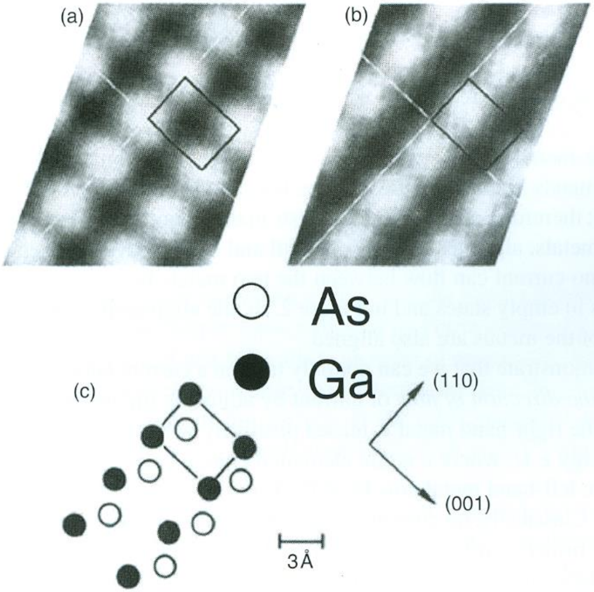

Figure 2.5 *Constant current STM images of the clean GaAs(110) surface. (a) The normally unoccupied states imaged at V = +1.9 V. (b) The normally occupied states imaged at V = −1.9 V. (c) Schematic representation of the positions of the Ga (•) and As (o) atoms. The rectangle is at the same position in (a), (b) and (c). This is an unusual example of chemically specific imaging based simply on the polarity of the tip. Source: Reproduced from R.M. Feenstra, J.A. Stroscio, J. Tersoff and A.P. Fein,* Phys. Rev. Lett. ***58*** *(1987) 1192. (c) 1987, with permission from the American Physical Society.*

Electrochemical STM

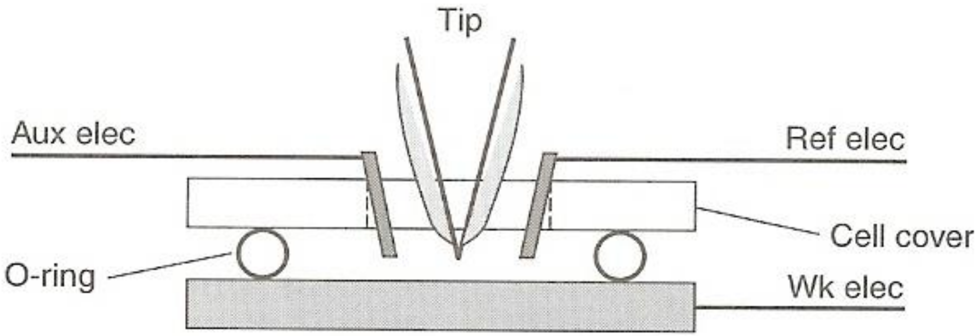

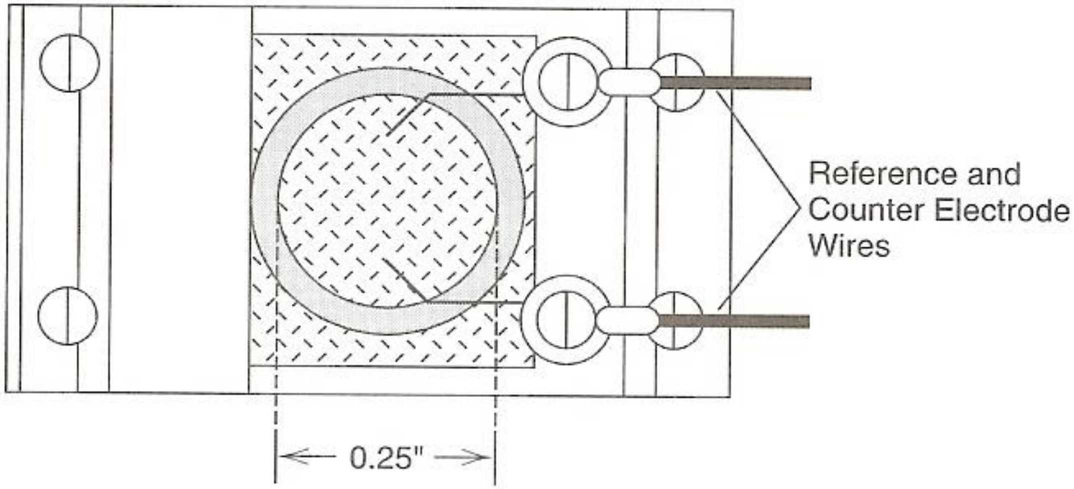

Scanning tunneling spectroscopy (STS)

STM image depends on the voltage on the tip → control of the voltage → to determine the electronic states with atomic resolution (STS)

Chemisorption changes the electronic structure of the surface

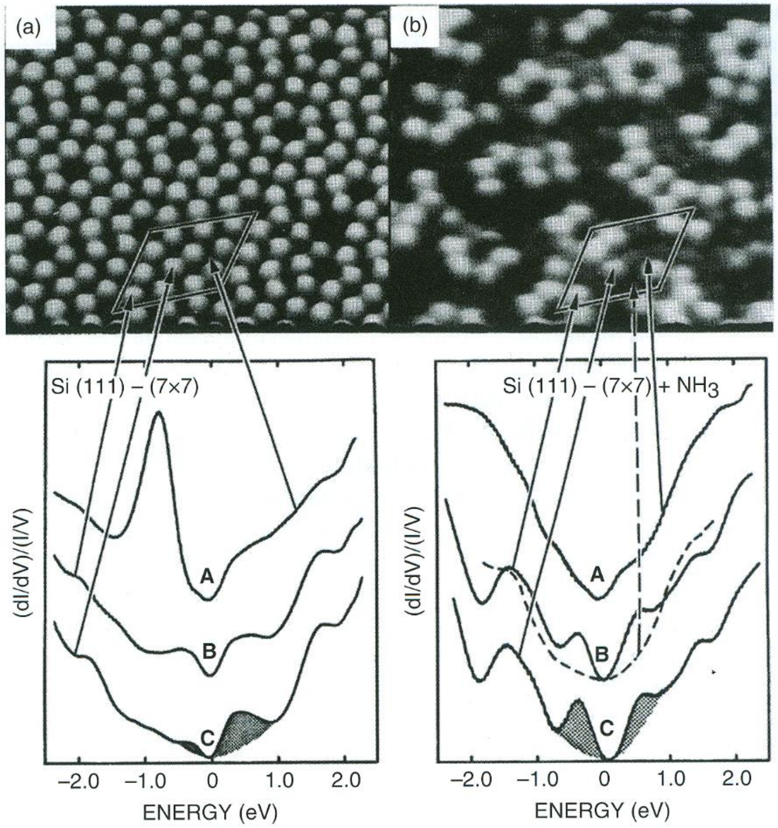

Figure 2.8 Left-hand side: Topography of the unoccupied states of the clean (7 × 7) surface (top panels) and atom resolved tunnelling spectra (bottom panels). The curves represent spectra acquired over different sites in the reconstructed surface (Curve A: restatom, Curve B: corner adatom, Curve C: middle adatom). Negative energies correspond to occupied states, positive to empty states. Right-hand side: Same types of images and spectra obtained after exposure of a Si(111)-(7 × 7) surface to NH_3. The different sites exhibit different reactivities with respect to NH_3 adsorption with the restatoms being the most reactive and the middle adatoms being the least reactive. Source: Reproduced with permission from Ph. Avouris and R. Wolkow, Phys. Rev. B 39 (1989) 5091. © 1989 American Physical Society.

Scanning electrochemical microscopy (SECM)

Using ultra-micro electrode or nano-electrode

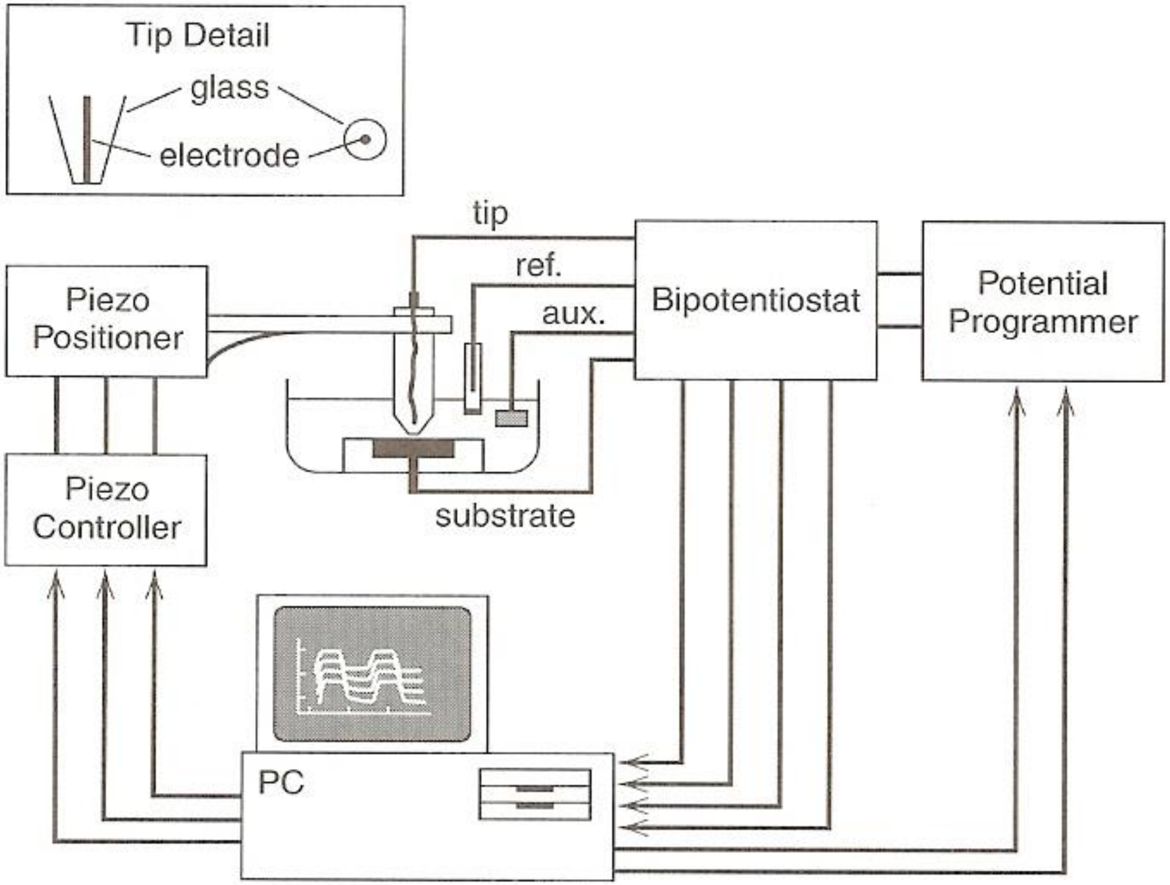

Atomic force microscopy (AFM)

- -using attractive or repulsive interactions with the surface (Table 2.2): van der Waals….
- -AFM can image conducting as well as insulating surfaces (soft, polymer, biological)
- -Force curve: function of distance of the tip from the surface

Force

$$\boxed{F_N = k_N \cdot \Delta z}$$

k_N: force constant
Δz: displacement of the tip

Table 2.2 *Interaction forces appropriate to scanning force microscopy and their ranges.*

Force	Range (nm)
Electrostatic	100
Double layer in electrolyte	100
van der Waals	10
Surface-induced solvent ordering	5
Hydrogen bonding	0.2
Contact	0.1

Values taken from Takano et al. [45].

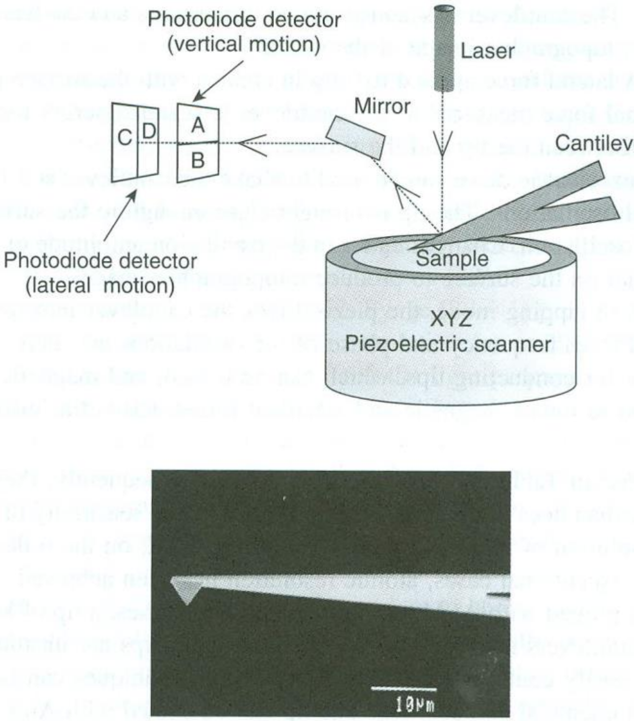

Figure 2.9 *Principal components for an optical lever type AFM. Detection of the reflected laser beam with a quadrant, position sensitive photodiode facilitates the simultaneous detection of bending and torsion of the cantilever. A scanning electron micrograph of a typical AFM cantilever and tip is shown in the lower panel. Reproduced from H. Takano, J. R. Kenseth, S.-S. Wong, J. C. O'Brien, M. D. Porter,* Chem. Rev. *99 (1999) 2845. © 1999, with permission from the American Chemical Society.*

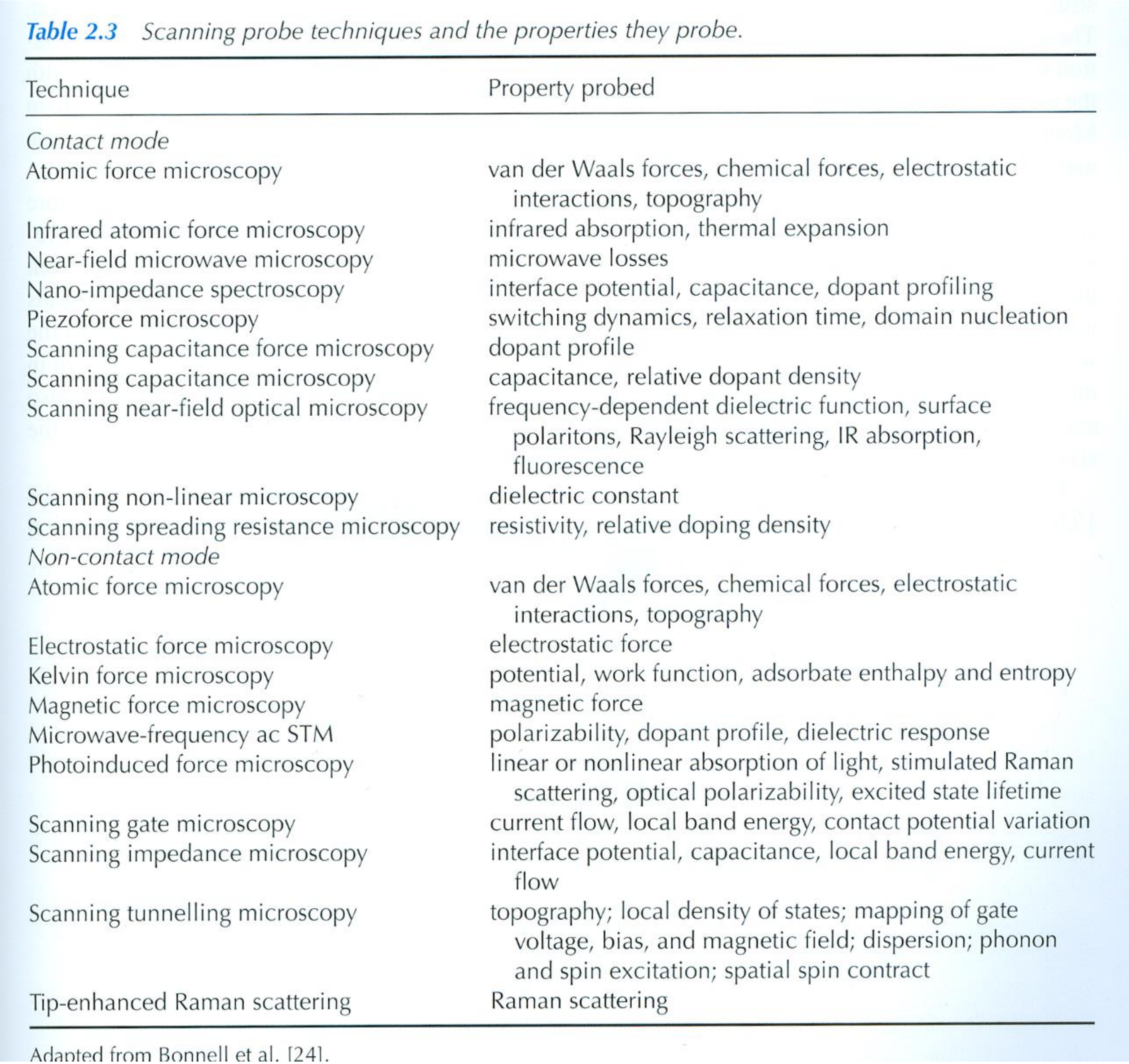

Table 2.3 *Scanning probe techniques and the properties they probe.*

Technique	Property probed
Contact mode	
Atomic force microscopy	van der Waals forces, chemical forces, electrostatic interactions, topography
Infrared atomic force microscopy	infrared absorption, thermal expansion
Near-field microwave microscopy	microwave losses
Nano-impedance spectroscopy	interface potential, capacitance, dopant profiling
Piezoforce microscopy	switching dynamics, relaxation time, domain nucleation
Scanning capacitance force microscopy	dopant profile
Scanning capacitance microscopy	capacitance, relative dopant density
Scanning near-field optical microscopy	frequency-dependent dielectric function, surface polaritons, Rayleigh scattering, IR absorption, fluorescence
Scanning non-linear microscopy	dielectric constant
Scanning spreading resistance microscopy	resistivity, relative doping density
Non-contact mode	
Atomic force microscopy	van der Waals forces, chemical forces, electrostatic interactions, topography
Electrostatic force microscopy	electrostatic force
Kelvin force microscopy	potential, work function, adsorbate enthalpy and entropy
Magnetic force microscopy	magnetic force
Microwave-frequency ac STM	polarizability, dopant profile, dielectric response
Photoinduced force microscopy	linear or nonlinear absorption of light, stimulated Raman scattering, optical polarizability, excited state lifetime
Scanning gate microscopy	current flow, local band energy, contact potential variation
Scanning impedance microscopy	interface potential, capacitance, local band energy, current flow
Scanning tunnelling microscopy	topography; local density of states; mapping of gate voltage, bias, and magnetic field; dispersion; phonon and spin excitation; spatial spin contract
Tip-enhanced Raman scattering	Raman scattering

Adapted from Bonnell et al. [24].

Optical and electron microscopy

Optical microscopy

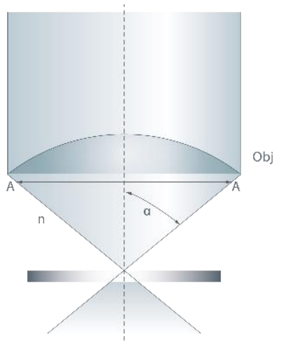

- Limit of resolution(δ): mainly by the wavelength λ of the light

$$\boxed{\delta = \lambda / 2n \sin \alpha}$$

α: the angular aperture (half the angle subtended at the object by the objective lens),
n: the refractive index of the medium between the object and the objective lens,
n sin α: the numerical aperture of the objective lens for a given immersion medium

Numerical aperture: generally less than unity
up to 1.5 with oil-immersion objectives → 600 nm light: 200 nm
(0.2 μm) resolution limit
Serious error in particle size less than 2 μm (Table 3.1)

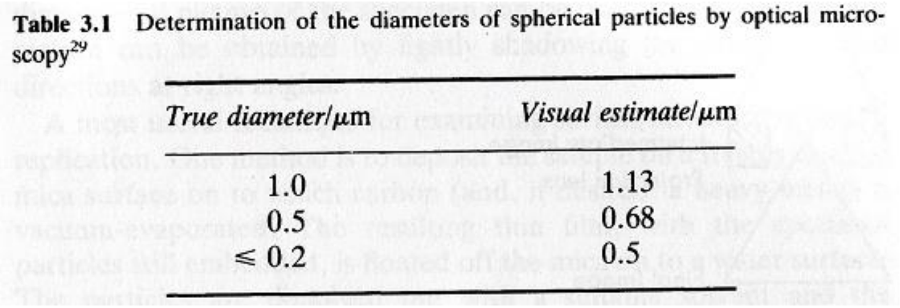

Table 3.1 Determination of the diameters of spherical particles by optical microscopy[29]

True diameter/μm	*Visual estimate/μm*
1.0	1.13
0.5	0.68
≤ 0.2	0.5

- Limitation: resolution power & contrast

Transmission electron microscopy(TEM)

- e-beam: wavelength λ ~ 0.01 nm
- resolution: 0.2 nm
- limitation: high vacuum system

Scanning electron microscopy(SEM)

- resolution: ~ 5 nm

SEM

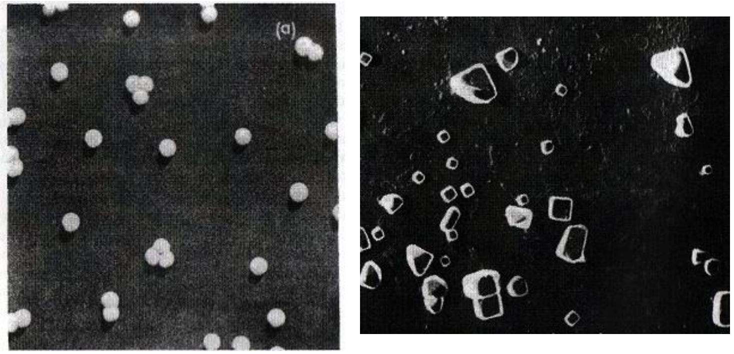

Figure 3.2 Electron micrographs. (a) Shadowed polystyrene latex particles (×50 000). (b) Shadowed silver chloride particles (× 15 000)

Near-field scanning optical microscopy (NSOM or SNOM)

a small-diameter optical fiber close to the surface (diameter/distance < wavelength of the light) → image resolution far below light wavelength (can be exceeded by using near-field technique)

Optical fiber + laser + AFM techniques
Resolution ~ 50 nm, ultimate resolution ~ 12 nm
(By working close enough to the aperture, resolution close to the size of the aperture and far below the wavelength of the light can be obtained)

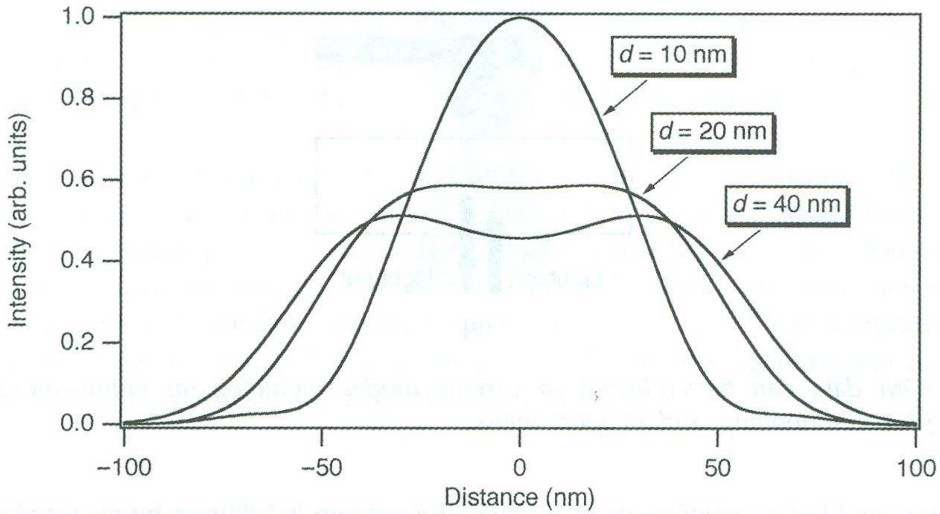

Figure 2.10 *Near-field intensity distributions are shown for 532 nm light that has passed through an aperture with a diameter of 100 nm at distances d from the aperture of 10, 20 and 40 nm. The distributions are normalized such that they all have the same integrated intensity.*

NSOM:
-high brightness of light (laser)
-optical fiber

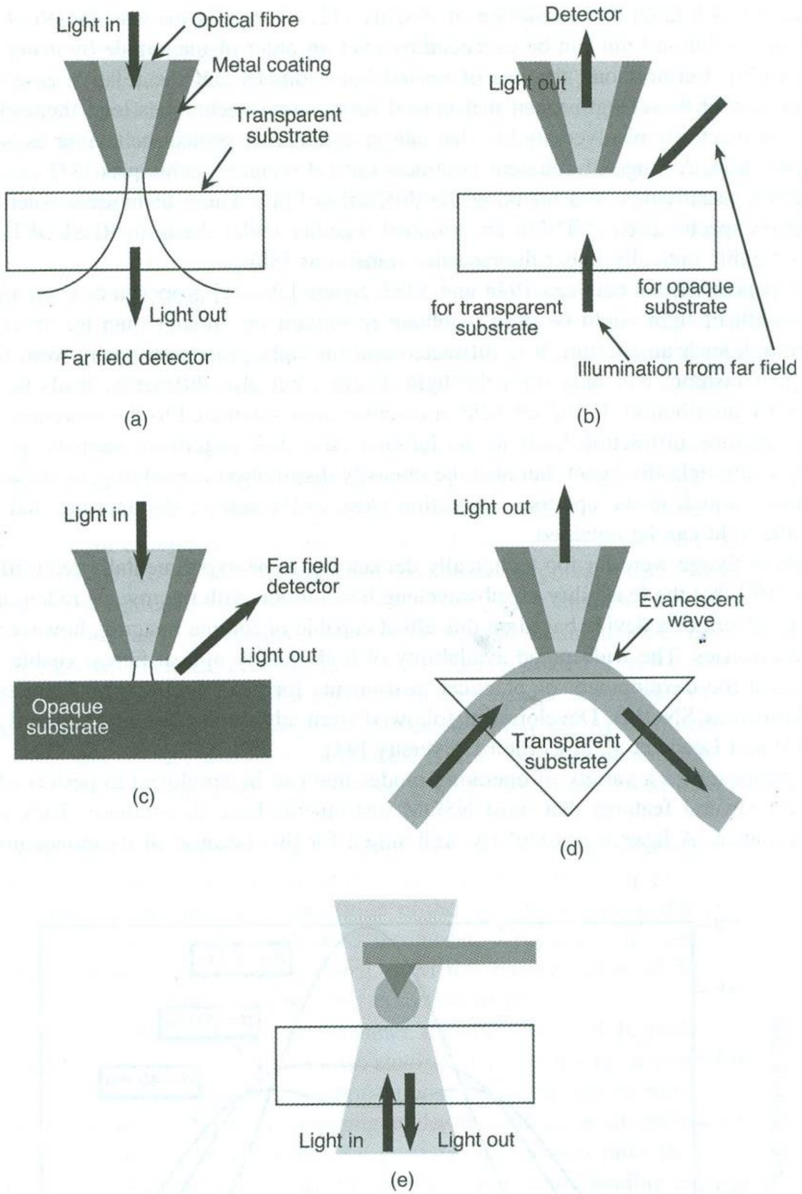

Figure 2.11 *NSOM data can be collected in various modes including (a) illumination; (b) collection; (c) reflection; (d) photon tunnelling; and (e) apertureless.*

Small aperture diameter (typically 80~100 nm) → few tens of nW light power → ultimate resolution ~12 nm (practically ~50 nm)

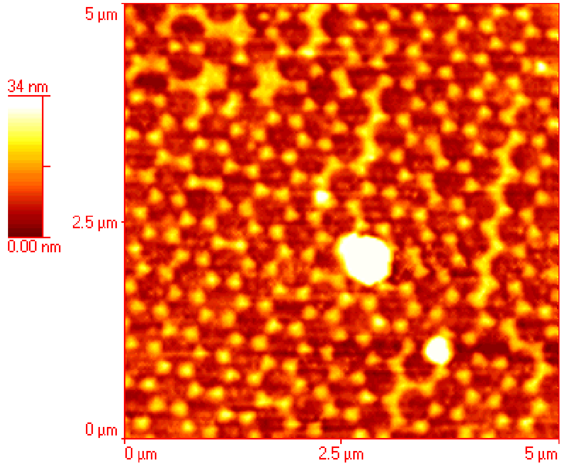

elchem.kaist.ac.kr

Electron diffraction

LEED(low energy): surface & adsorbate structure
TED(transmission): crystal structure

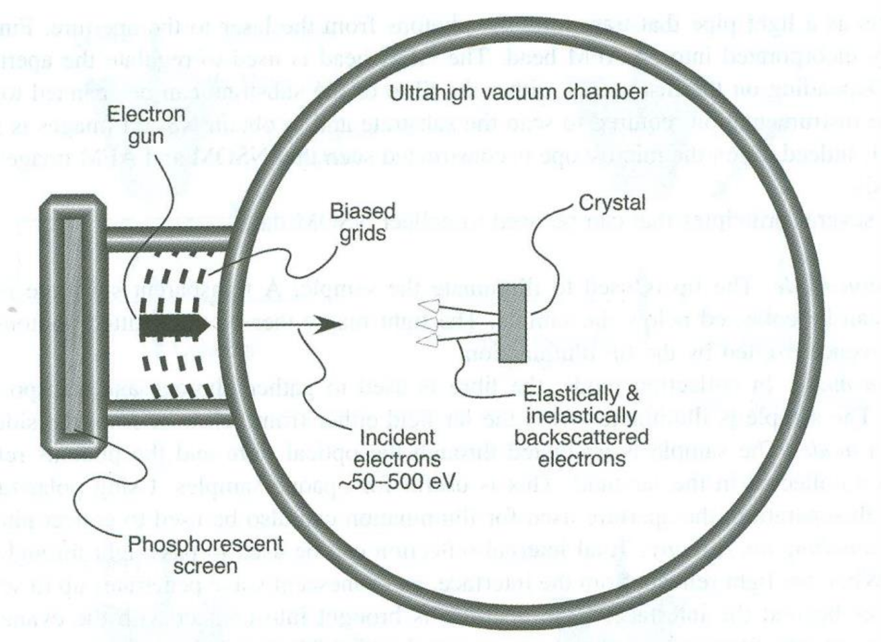

Figure 2.12 *Schematic drawing of a LEED chamber.*

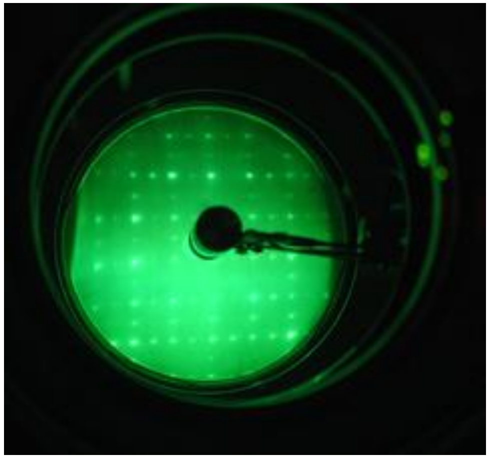

Si(100), LEED

en.wikipedia.org

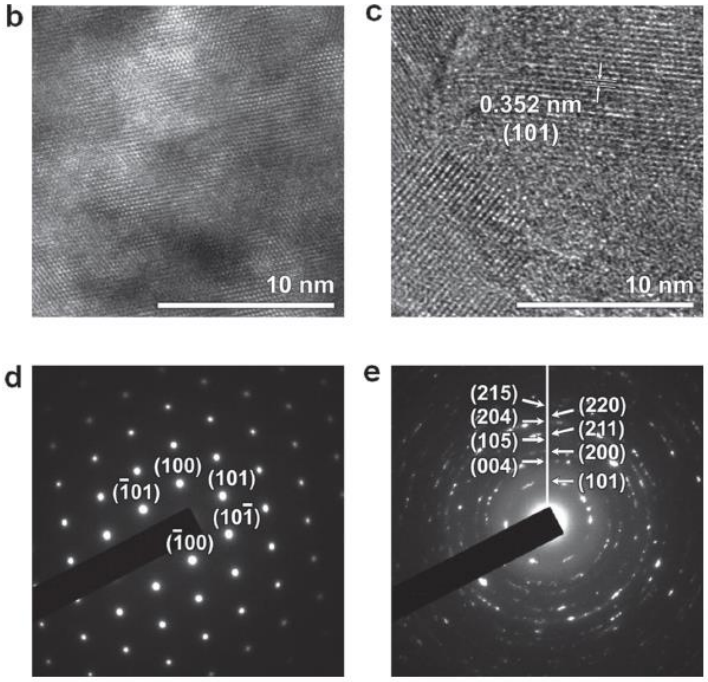

TEM & SAED

Small (2017)

Surface diffraction

- Low energy electron diffraction (LEED), X-ray diffraction, atomic diffraction

de Broglie wavelength, λ, of a particle $\boxed{\lambda = h/p}$

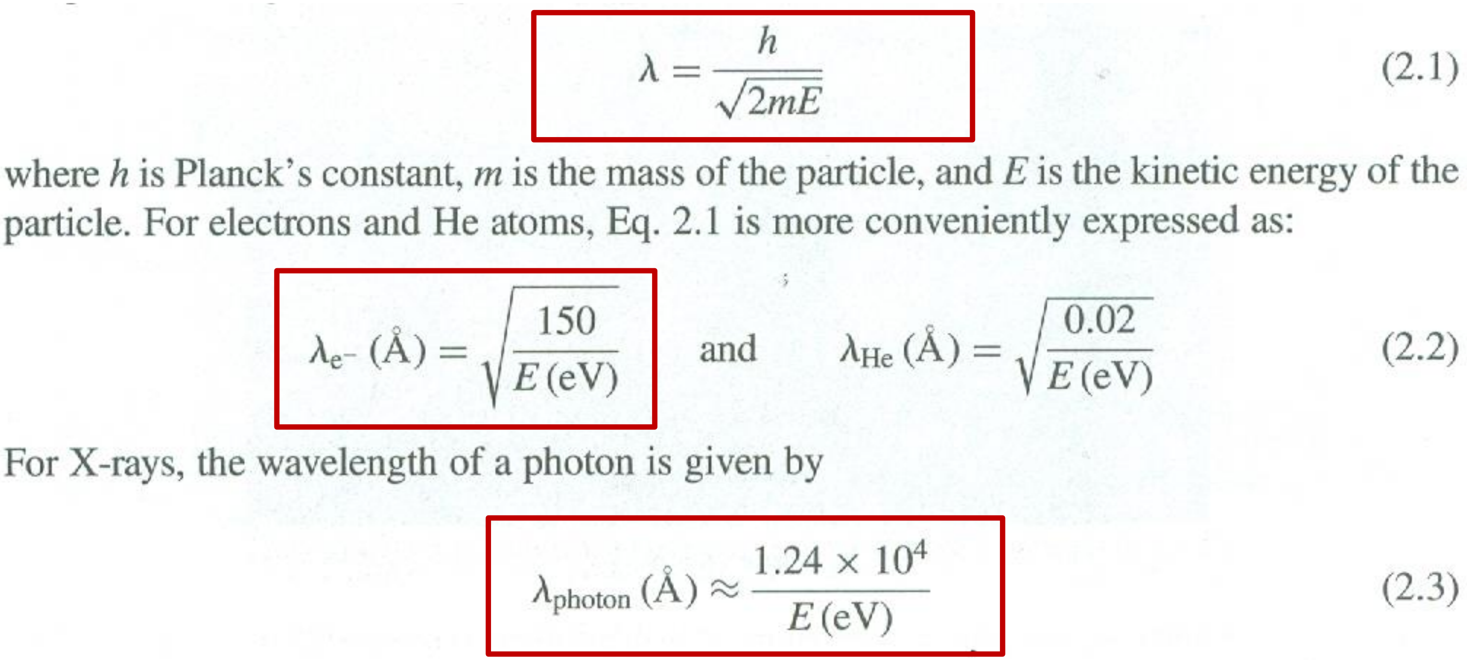

$$\boxed{\lambda = \frac{h}{\sqrt{2mE}}} \tag{2.1}$$

where *h* is Planck's constant, *m* is the mass of the particle, and *E* is the kinetic energy of the particle. For electrons and He atoms, Eq. 2.1 is more conveniently expressed as:

$$\boxed{\lambda_{e^-}\,(\text{Å}) = \sqrt{\frac{150}{E\,(\text{eV})}}} \quad \text{and} \quad \lambda_{\text{He}}\,(\text{Å}) = \sqrt{\frac{0.02}{E\,(\text{eV})}} \tag{2.2}$$

For X-rays, the wavelength of a photon is given by

$$\boxed{\lambda_{\text{photon}}\,(\text{Å}) \approx \frac{1.24 \times 10^4}{E\,(\text{eV})}} \tag{2.3}$$

Electrons with 10~200 eV energies and He atoms with thermal energies (~0.026 eV at 300K) → atomic diffraction condition (λ < interatomic distance, ~1 Å)

X-rays at the high intensities available at a synchrotron radiation suitable for surface and interface structure studies (grazing angle X-ray diffraction). X-ray bombardment-induced emission of electrons also shows diffraction (photoelectron diffraction)

LEED: electron beam of 10~200 eV is back-scattered → atomic structure of surface

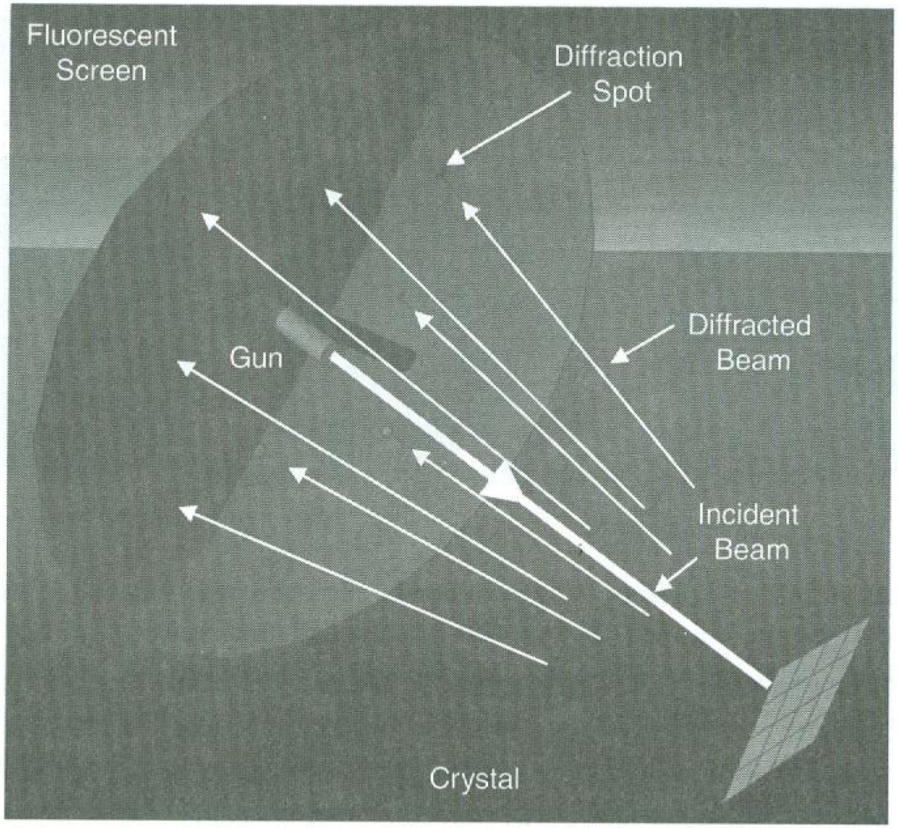

Figure 2.7. A scheme illustration of LEED surface crystallography.

Low energy electron diffraction (LEED):

Why low energy electron used?

- The penetration depth of x-ray is ~ 1 μm. So x-ray diffraction give structural information of a bulk solid (3D). It does not have any surface sensitivity
- The penetration depth of low energy electron is ≤ 20 Å; a rather good surface sensitivity
- In any diffraction the employed wavelength λ should ~ d

- De Broglie wavelength of **e^-** is

$$\boxed{\lambda = h/p = h/mv = h/(2mE_k)^{1/2}}$$

If E_k= 150 eV, λ =~ 1 Å

- Since diffraction can be observed in elastic scattering, the inelastically scattered electrons have to be removed by setting up an potential barrier (grid assembly).
- The LEED pattern is usually recorded by taking a picture.

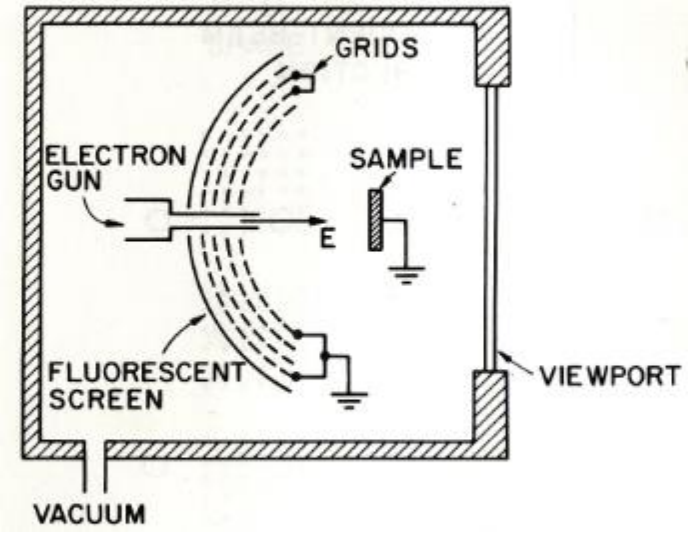

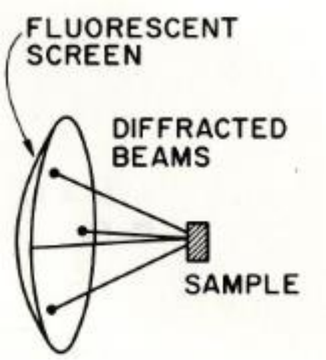

Instrument

Reciprocal lattice

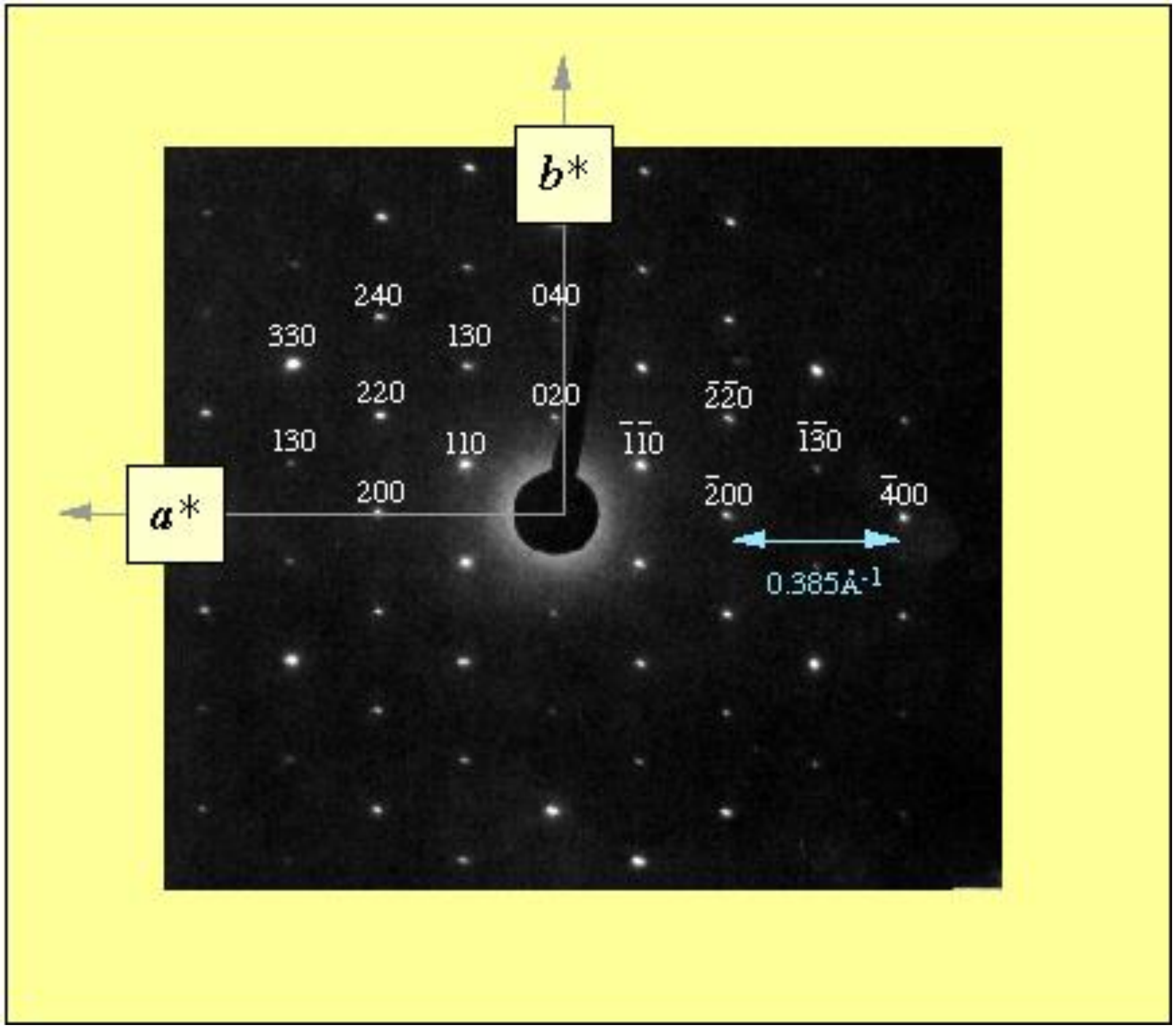

clay.uga.edu

Reciprocal lattice

Basis vectors $\mathbf{a_1}$, $\mathbf{a_2}$ in the unit cell in real space
Basis vectors $\mathbf{a_1^*}$, $\mathbf{a_2^*}$ in a reciprocal space

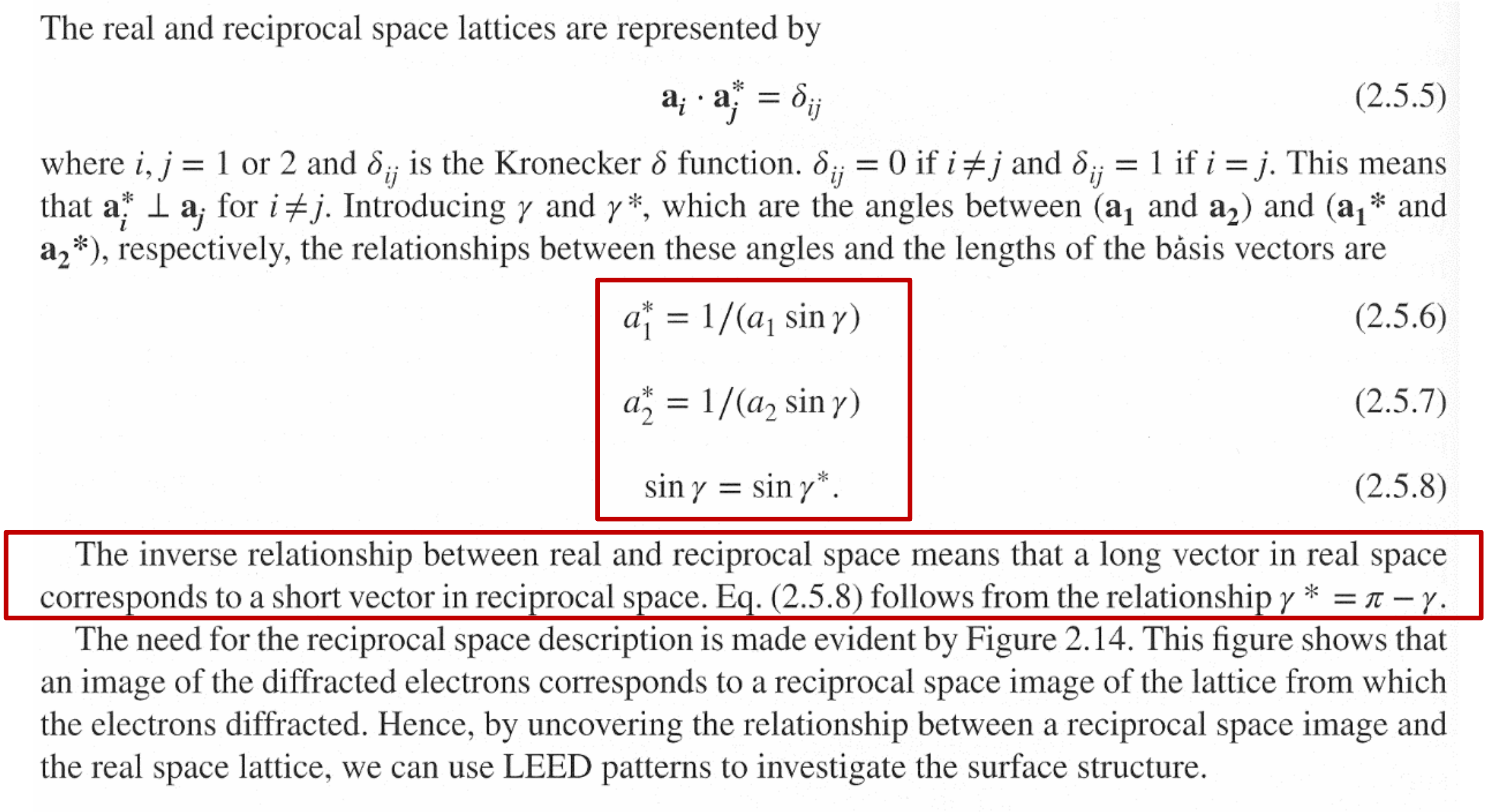

The real and reciprocal space lattices are represented by

$$\mathbf{a}_i \cdot \mathbf{a}_j^* = \delta_{ij} \tag{2.5.5}$$

where $i, j = 1$ or 2 and δ_{ij} is the Kronecker δ function. $\delta_{ij} = 0$ if $i \neq j$ and $\delta_{ij} = 1$ if $i = j$. This means that $\mathbf{a}_i^* \perp \mathbf{a}_j$ for $i \neq j$. Introducing γ and γ^*, which are the angles between ($\mathbf{a}_1$ and $\mathbf{a}_2$) and ($\mathbf{a}_1$* and $\mathbf{a}_2$*), respectively, the relationships between these angles and the lengths of the basis vectors are

$$a_1^* = 1/(a_1 \sin\gamma) \tag{2.5.6}$$

$$a_2^* = 1/(a_2 \sin\gamma) \tag{2.5.7}$$

$$\sin\gamma = \sin\gamma^*. \tag{2.5.8}$$

The inverse relationship between real and reciprocal space means that a long vector in real space corresponds to a short vector in reciprocal space. Eq. (2.5.8) follows from the relationship $\gamma^* = \pi - \gamma$.

The need for the reciprocal space description is made evident by Figure 2.14. This figure shows that an image of the diffracted electrons corresponds to a reciprocal space image of the lattice from which the electrons diffracted. Hence, by uncovering the relationship between a reciprocal space image and the real space lattice, we can use LEED patterns to investigate the surface structure.

Reciprocal lattice

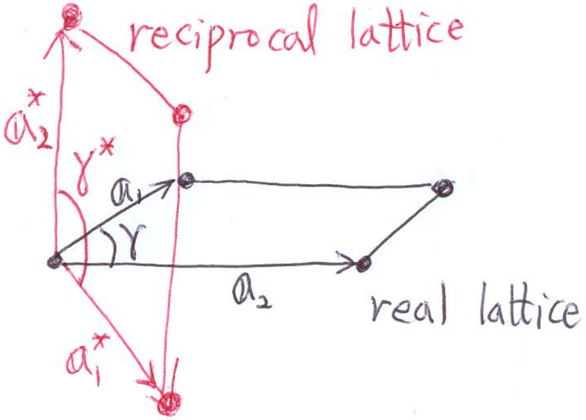

A: real lattice → unit cell

A^*: reciprocal lattice → unit cell

$$A = |a_1 \times a_2| = a_1 a_2 \sin\gamma$$

$$A^* = |a_1^* \times a_2^*| = a_1^* a_2^* \sin\gamma^* = \frac{1}{A}$$

$$(\sin\gamma = \sin\gamma^*)$$

$$AA^* = (a_1 a_1^* \sin\gamma)(a_2 a_2^* \sin\gamma) = 1$$

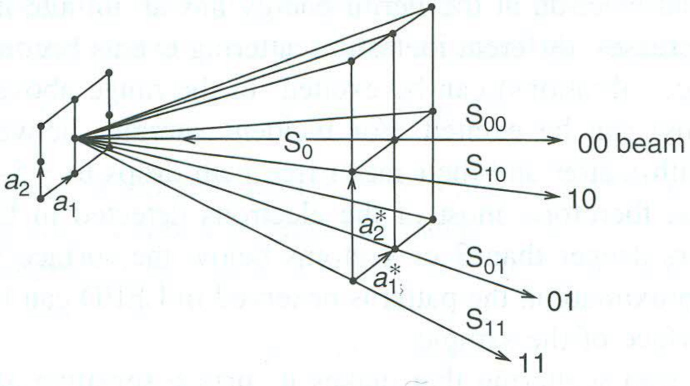

Figure 2.14 *The principle of diffraction pattern formation in a LEED experiment. The incident electron beam approaches along* s_0*. The specular beam exits along* s_{00}*. Reproduced from G. Ertl, J. Küppers,* Low Energy Electrons and Surface Chemistry, *2nd ed., VCH, Weinheim. © 1985, with permission from John Wiley & Sons, Ltd.*

The diffraction condition from a one-dimensional lattice of periodicity a leads to constructive interference at angles φ when

$$\boxed{a \sin \varphi = n\lambda} \qquad \text{Bragg's law} \qquad (2.5.18)$$

for an electron with a wavelength λ incident at normal incidence. n is an integer denoting the diffraction order. The wavelength of the electron is given by the de Broglie relationship, Eq. (2.4.9). The Bragg condition of Eq. (2.5.18) needs to be generalized to two dimensions. This leads to the Laue conditions

$$\mathbf{a_1} \cdot (\mathbf{s} - \mathbf{s_0}) = h_1 \lambda \qquad (2.5.19)$$

$$\mathbf{a_2} \cdot (\mathbf{s} - \mathbf{s_0}) = h_2 \lambda \qquad (2.5.20)$$

where $\mathbf{s_0}$ defines the direction of the incident beam (generally along the surface normal) and s defines the direction of the diffracted beam intensity maxima. h_1 and h_2 are integers. They are used to identify the diffraction reflexes that appear in the LEED pattern. The specular reflex at (00) is used as the origin and arises from electrons that are elastically scattered without diffraction.

Matrix notation for adsorbate

$b_1 = m_{11} a_1 + m_{12} a_2$ in matrix notation, $b = \mathfrak{M} \cdot a$ $\quad \mathfrak{M} = \begin{pmatrix} m_{11} & m_{12} \\ m_{21} & m_{22} \end{pmatrix}$

$b_2 = m_{21} a_1 + m_{22} a_1$

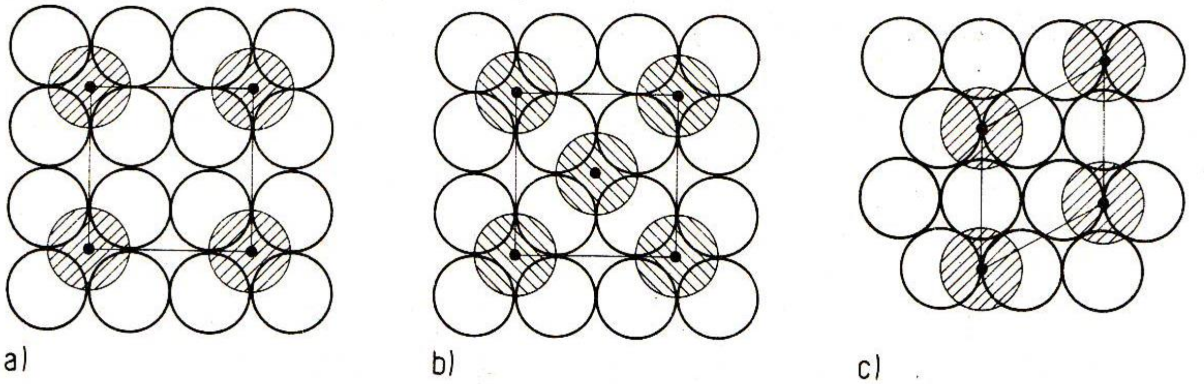

Fig. 9.2. Examples for overlayer structures. a) 2×2, b) $c(2 \times 2)$, c) $\sqrt{3} \times \sqrt{3}/R\ 30°$.

$$\mathfrak{M} = \begin{pmatrix} 2 & 0 \\ 0 & 2 \end{pmatrix}, \begin{pmatrix} 1 & 1 \\ -1 & 1 \end{pmatrix} \text{ and } \begin{pmatrix} 1 & 1 \\ -1 & 2 \end{pmatrix}$$

2D real vs. reciprocal lattices of adsorbate

$$\begin{aligned} b_1 &= m_{11}a_1 + m_{12}a_2 \\ b_2 &= m_{21}a_1 + m_{22}a_2 \, . \end{aligned} \qquad \begin{aligned} b_1^* &= m_{11}^* a_1^* + m_{12}^* a_2^* \\ b_2^* &= m_{21}^* a_1^* + m_{22}^* a_2^* \, . \end{aligned}$$

$\mathfrak{M}^* = \tilde{\mathfrak{M}}^{-1}$, and so $\mathfrak{M} = \tilde{\mathfrak{M}}^{*-1}$

m*: inverse transposed matrix of m

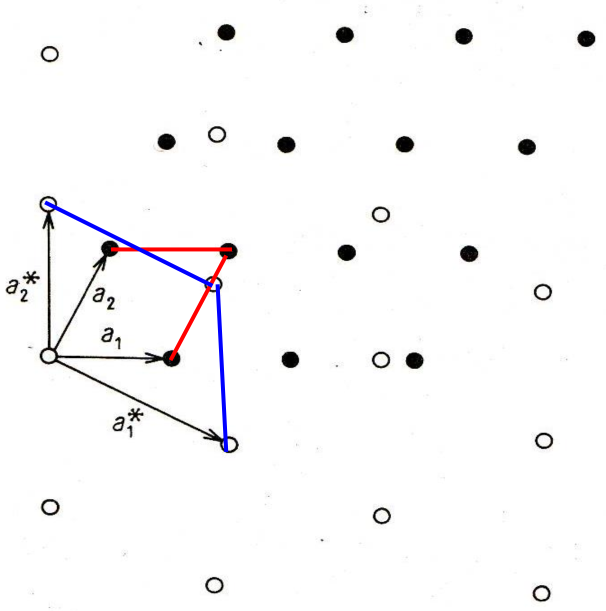

Fig. 9.11. A two-dimensional real lattice, described by a_1, a_2 (dark circles), and its reciprocal lattice a_1^*, a_2^* (open circles).

$$m_{11} = \frac{1}{\det \mathfrak{M}^*} \cdot m_{22}^*$$

$$m_{12} = -\frac{1}{\det \mathfrak{M}^*} \cdot m_{21}^*$$

$$m_{21} = -\frac{1}{\det \mathfrak{M}^*} \cdot m_{12}^*$$

$$m_{22} = \frac{1}{\det \mathfrak{M}^*} \cdot m_{11}^*$$

where det **M*** = $m_{11}^* \cdot m_{22}^* - m_{21}^* \cdot m_{12}^*$

m_{ij}^* can be measured directly from LEED pattern

→

Target: m_{ij} can be calculated from reciprocal pattern real $\mathbb{b} = \mathbb{M} \cdot a \Rightarrow \begin{pmatrix} \mathbb{b}_1 \\ \mathbb{b}_2 \end{pmatrix} = \overset{\overset{\mathbb{M}}{\|}}{\begin{pmatrix} m_{11} & m_{12} \\ m_{21} & m_{22} \end{pmatrix}} \begin{pmatrix} a_1 \\ a_2 \end{pmatrix}$

reciprocal $\mathbb{b}^* = \mathbb{M}^* \cdot a^* \Rightarrow \begin{pmatrix} \mathbb{b}_1^* \\ \mathbb{b}_2^* \end{pmatrix} = \underset{\underset{\mathbb{M}^*}{\|}}{\begin{pmatrix} m_{11}^* & m_{12}^* \\ m_{21}^* & m_{22}^* \end{pmatrix}} \begin{pmatrix} a_1^* \\ a_2^* \end{pmatrix}$

cf. Inverse matrix : $A = \begin{bmatrix} a & b \\ c & d \end{bmatrix} \Rightarrow A^{-1} = \frac{1}{ad-bc} \begin{bmatrix} d & -b \\ -c & a \end{bmatrix}$, $ad-bc$: determinant of A

transposed matrix : $A = \begin{bmatrix} a & b \\ c & d \end{bmatrix} \Rightarrow \widehat{A} = \begin{bmatrix} a & c \\ b & d \end{bmatrix}$

inverse matrix $\mathbb{M}^{-1} = \frac{1}{\det \mathbb{M}^*} \begin{pmatrix} m_{22}^* & -m_{12}^* \\ -m_{21}^* & m_{11}^* \end{pmatrix}$, $\mathbb{M}^{*-1} = \frac{1}{\det \mathbb{M}} \begin{pmatrix} m_{22} & -m_{12} \\ -m_{21} & m_{11} \end{pmatrix}$

inversed transposed matrix

$$\widetilde{M}^{-1} = \frac{1}{\det \mathbb{M}^*} \begin{pmatrix} m_{22}^* & -m_{21}^* \\ -m_{12}^* & m_{11}^* \end{pmatrix}, \quad \widetilde{\mathbb{M}}^{*-1} = \frac{1}{\det M} \begin{pmatrix} m_{22} & -m_{21} \\ -m_{12} & m_{11} \end{pmatrix}$$

$$\boxed{\mathbb{M} = \widetilde{\mathbb{M}}^{*-1}.}$$

$\mathfrak{M}^* = \tilde{\mathfrak{M}}^{-1}$, and so $\mathfrak{M} = \tilde{\mathfrak{M}}^{*-1}$

$$\begin{aligned} \boldsymbol{b}_1 &= m_{11}\boldsymbol{a}_1 + m_{12}\boldsymbol{a}_2 & \quad \boldsymbol{b}_1^* &= m_{11}^*\boldsymbol{a}_1^* + m_{12}^*\boldsymbol{a}_2^* \\ \boldsymbol{b}_2 &= m_{21}\boldsymbol{a}_1 + m_{22}\boldsymbol{a}_2 \,. & \quad \boldsymbol{b}_2^* &= m_{21}^*\boldsymbol{a}_1^* + m_{22}^*\boldsymbol{a}_2^* \,. \end{aligned}$$

$\mathbf{b}_i \cdot \mathbf{b}_j = \delta_{ij}$ $\qquad \delta_{ij} = 0$ if $i \neq j$

$a_i \cdot a_j = \delta_{ij}$ $\qquad \delta_{ij} = 1$ if $i = j$

$\Rightarrow$ prove $\mathbb{M}^* \cdot \tilde{\mathbb{M}} = 1$

$$\begin{pmatrix} m_{11}^* & m_{12}^* \\ m_{21}^* & m_{22}^* \end{pmatrix} \begin{pmatrix} m_{11} & m_{21} \\ m_{12} & m_{22} \end{pmatrix} = \begin{pmatrix} m_{11}^* m_{11} + m_{12}^* m_{12} & m_{11}^* m_{21} + m_{12}^* m_{22} \\ m_{21}^* m_{11} + m_{22}^* m_{12} & m_{21}^* m_{21} + m_{22}^* m_{22} \end{pmatrix} = \begin{pmatrix} 1 & 0 \\ 0 & 1 \end{pmatrix}$$

$$1 = \mathbf{b}_1 \cdot \mathbf{b}_1^* = (m_{11} a_1 + m_{12} a_2)(m_{11}^* a_1^* + m_{12}^* a_2^*) = m_{11} m_{11}^* + m_{12} m_{12}^* \qquad \left(\begin{aligned} &\because a_1 \cdot a_1^* = a_2 \cdot a_2^* = 1 \\ &\quad a_1 \cdot a_2^* = a_2 \cdot a_1^* = 0 \end{aligned} \right)$$

$$0 = \mathbf{b}_1 \cdot \mathbf{b}_2^* = (\qquad)(\qquad) = m_{11}^* m_{21} + m_{12}^* m_{22}$$

$$0 = \mathbf{b}_2 \cdot \mathbf{b}_1^* = (\qquad)(\qquad) = m_{21}^* m_{11} + m_{22}^* m_{12}$$

$$1 = \mathbf{b}_2 \cdot \mathbf{b}_2^* = (\qquad)(\qquad) = m_{21}^* m_{21} + m_{22}^* m_{22}$$

//

We represent a surface overlayer by the basis vectors $\mathbf{b_1}$ and $\mathbf{b_2}$ and the corresponding reciprocal lattice vectors are given stars. The substrate and overlayer lattices are related by

$$\mathbf{b_1} = m_{11}\mathbf{a_1} + m_{12}\mathbf{a_2} \tag{2.5.9}$$

$$\mathbf{b_2} = m_{21}\mathbf{a_1} + m_{22}\mathbf{a_2} \tag{2.5.10}$$

$$\mathbf{b_1^*} = m_{11}^*\mathbf{a_1^*} + m_{12}^*\mathbf{a_2^*} \tag{2.5.11}$$

$$\mathbf{b_2^*} = m_{21}^*\mathbf{a_1^*} + m_{22}^*\mathbf{a_2^*}. \tag{2.5.12}$$

This can be written in matrix notation as

$$\mathbf{b} = \mathbf{M} \cdot \mathbf{a} \rightarrow \begin{pmatrix} \mathbf{b}_1 \\ \mathbf{b}_2 \end{pmatrix} = \begin{pmatrix} m_{11} & m_{12} \\ m_{21} & m_{22} \end{pmatrix} \cdot \begin{pmatrix} \mathbf{a}_1 \\ \mathbf{a}_2 \end{pmatrix}. \tag{2.5.13}$$

A similar relationship holds for the reciprocal space representation

$$\mathbf{b}^* = \mathbf{M}^* \cdot \mathbf{a}^* \rightarrow \begin{pmatrix} \mathbf{b}_1^* \\ \mathbf{b}_2^* \end{pmatrix} = \begin{pmatrix} m_{11}^* & m_{12}^* \\ m_{21}^* & m_{22}^* \end{pmatrix} \cdot \begin{pmatrix} \mathbf{a}_1^* \\ \mathbf{a}_2^* \end{pmatrix}. \tag{2.5.14}$$

It can be shown that **M*** is related to **M** (and vice versa) by

$$\boxed{\begin{aligned} \mathbf{M} &= \frac{1}{\det \mathbf{M}^*} \begin{pmatrix} m_{22}^* & -m_{21}^* \\ -m_{12}^* & m_{11}^* \end{pmatrix} && (2.5.15) \\ \mathbf{M}^* &= \frac{1}{\det \mathbf{M}} \begin{pmatrix} m_{22} & -m_{21} \\ -m_{12} & m_{11} \end{pmatrix} && (2.5.16) \end{aligned}}$$

The determinant of **M*** is define as

$$\det \mathbf{M}^* = m_{11}^*\, m_{22}^* - m_{21}^*\, m_{12}^*, \tag{2.5.17}$$

and analogously for the determinant of **M**. Experimentally, the challenge is to determine the elements of **M** from the diffraction pattern measured on the LEED screen.

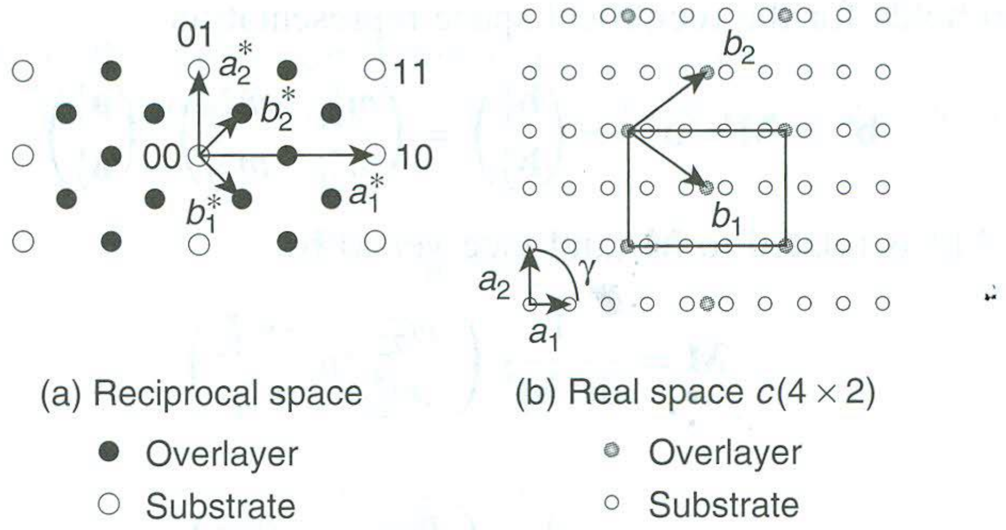

(a) Reciprocal space

(b) Real space $c(4 \times 2)$

Figure 2.15 *Real space and reciprocal space patterns. (a) Reciprocal lattice (LEED pattern) composed o substrate (normal) spots ○ and overlayer (extra) spots ●. (b) Real lattice of the substrate (○) and overlayer (●) The solid line delineates the c(4 × 2) cell and the arrows depict the unit vectors.*

From (a)

i) $\mathbb{b}_1^* = \frac{1}{4}a_1^* - \frac{1}{2}a_2^* = m_{11}^* a_1^* + m_{12}^* a_2^*$

$\mathbb{b}_2^* = \frac{1}{4}a_1^* + \frac{1}{2}a_2^* = m_{21}^* a_1^* + m_{22}^* a_2^*$

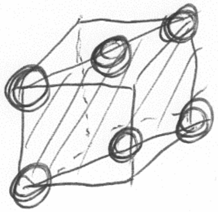

fcc(110)

ii) $a_1 \perp a_2^*$, $a_2 \perp a_1^*$

Substrate
↓
position
area

$a_1 = \frac{1}{a_1^* \sin\gamma} = \frac{1}{a_1^*}$, $a_2 = \frac{1}{a_2^* \sin\gamma} = \frac{1}{a_2^*} = \frac{\sqrt{2}}{a_1^*} = \sqrt{2}\,a_1$

$(\gamma = 90^\circ)$

iii) $\mathbb{b}_1^*, \mathbb{b}_2^* \longrightarrow \mathbb{b}_1, \mathbb{b}_2$, $\det \mathbb{M}^* = \begin{vmatrix} \frac{1}{4} & -\frac{1}{2} \\ \frac{1}{4} & \frac{1}{2} \end{vmatrix} = \frac{1}{4}$

adsorbate

$m_{11} = \frac{m_{22}^*}{\det M^*} = \frac{1}{2}\Big/\left(\frac{1}{4}\right) = 2$, $m_{12} = \frac{-m_{21}^*}{\det \mathbb{M}^*} = -1$, $m_{21} = \frac{-m_{12}^*}{\det \mathbb{M}^*} = 2$, $m_{22} = 1$

$\mathbb{M} = \begin{pmatrix} 2 & -1 \\ 2 & 1 \end{pmatrix}$ $\therefore$ $\mathbb{b}_1 = 2a_1 - a_2$

$\mathbb{b}_2 = 2a_1 + a_2$ (Fig 2.15 (b))

LEED image

Bisulfate/Pt(111)

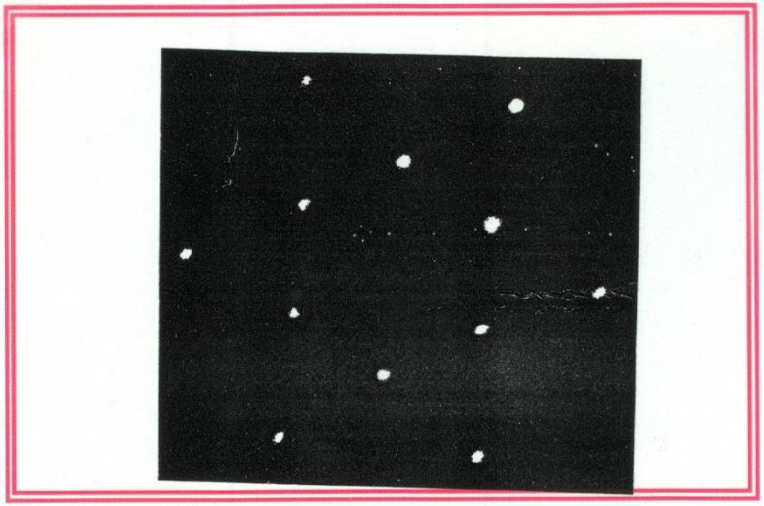

E = 0.34 V in 50 mM sulfuric acid 49.4 eV

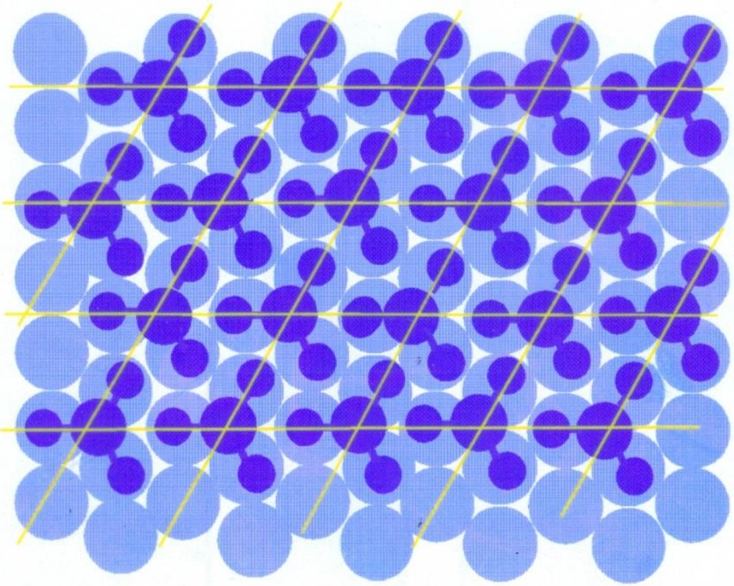

$(\sqrt{3} \times \sqrt{3})R30^\circ$

Sung's Ph.D thesis

Electron spectroscopy

XPS (X-ray photoelectron spectroscopy)
UPS (UV photoelectron spectroscopy)
AES (Auger electron spectroscopy)

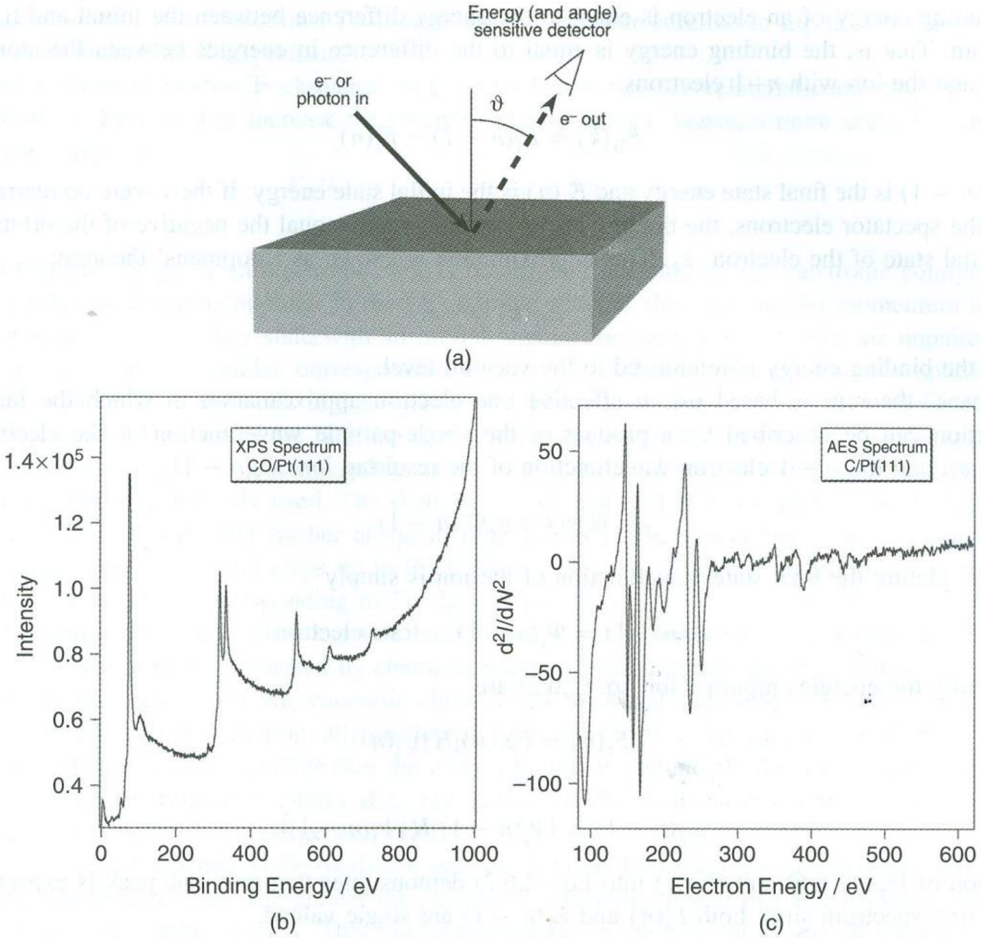

Figure 2.17 *(a) Schematic representation of electron spectroscopy. (b) A sample XPS spectrum of CO/Pt(111). (c) A sample AES spectrum of CO/Pt(111).*

X-ray photoelectron spectroscopy (XPS)
or electron spectroscopy for chemical analysis (ESCA)

Binding energy of core electron ~ photon energy of X-ray region

$$\boxed{E_b = h\nu - E_k - w} \qquad (21\text{-}2)$$

w: work function of spectrometer

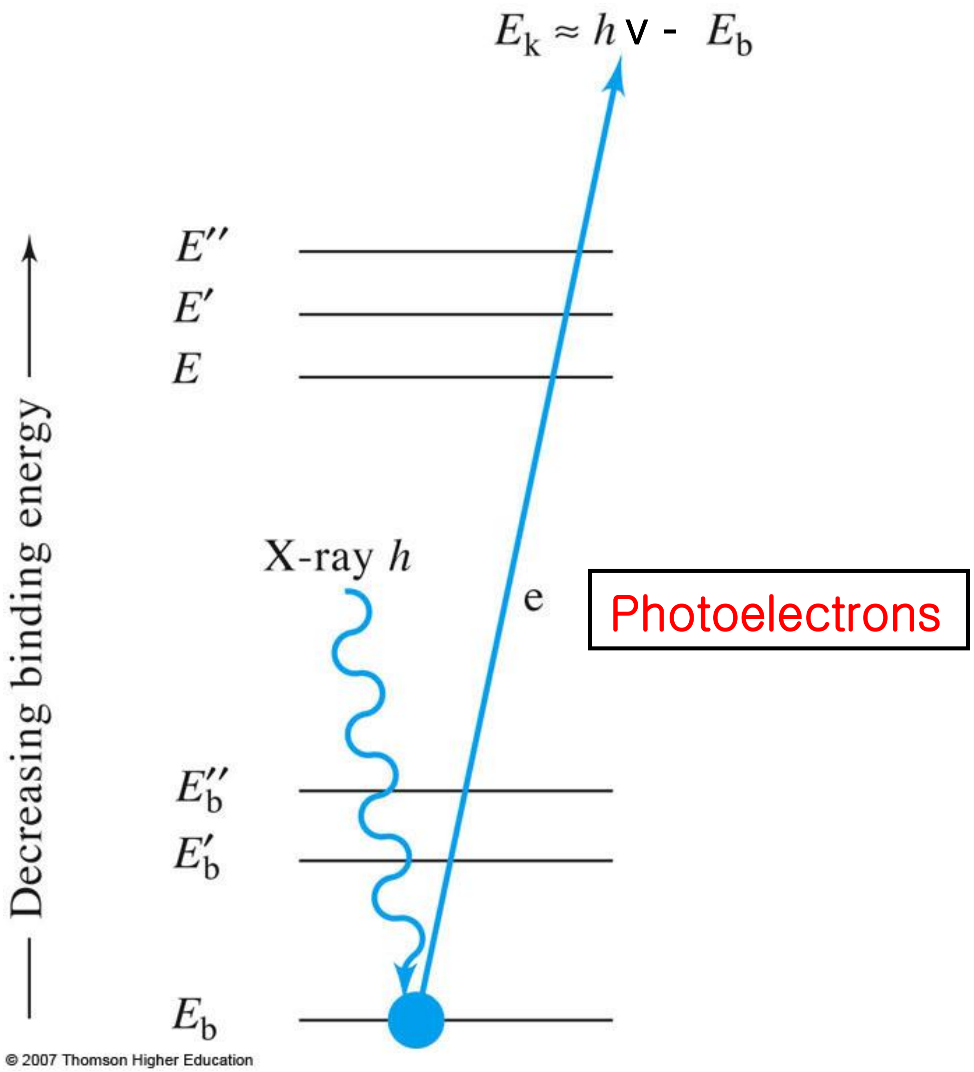

© 2007 Thomson Higher Education

Skoog, Holler, Crouch, Principles of Instrumental Analysis (Thomson)

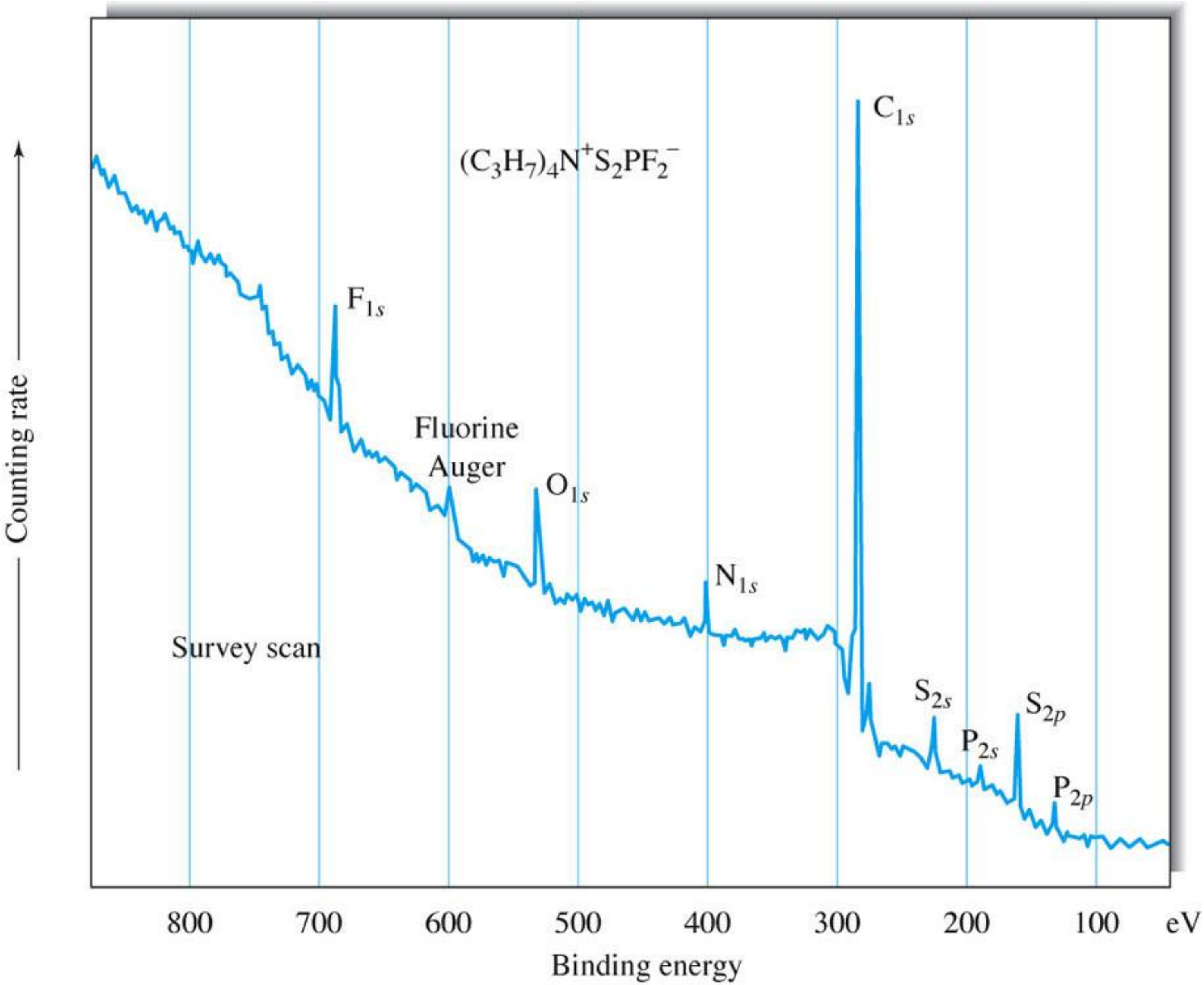

Skoog, Holler, Crouch, Principles of Instrumental Analysis (Thomson)

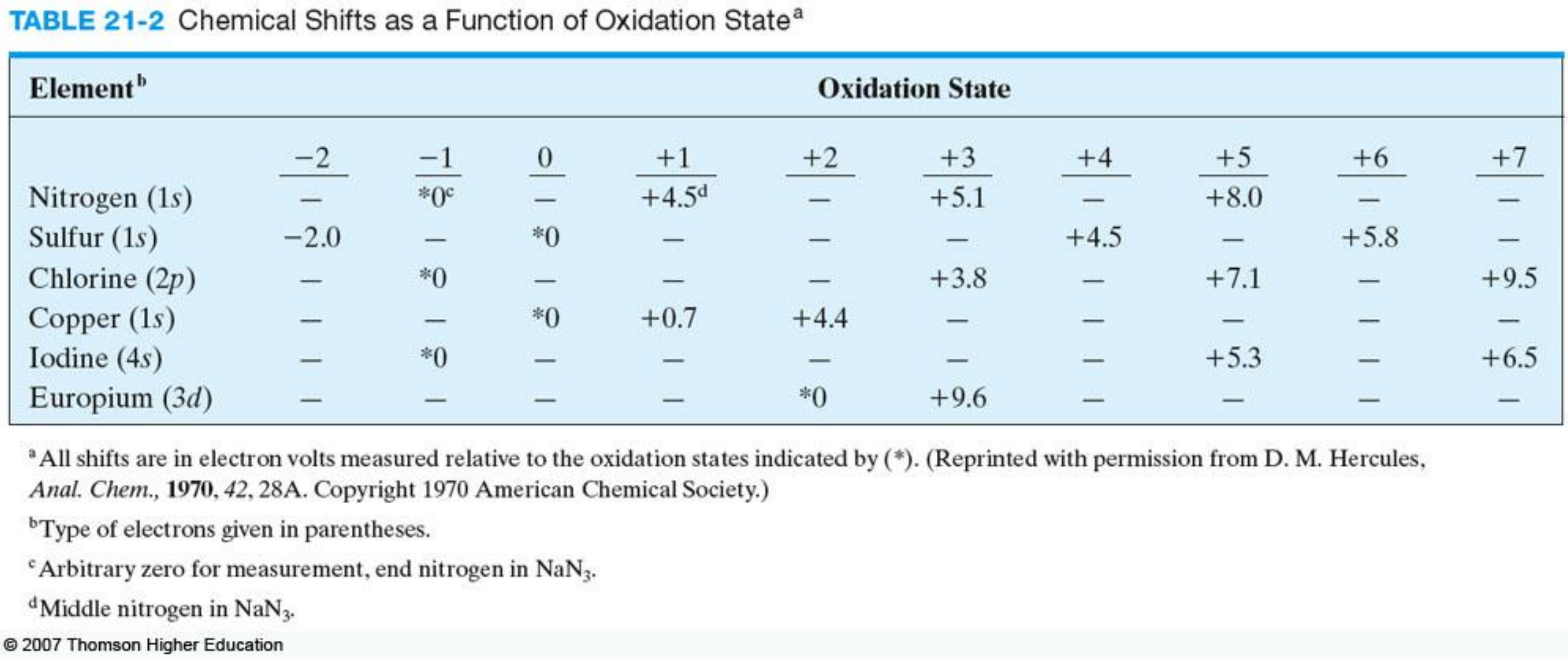

TABLE 21-2 Chemical Shifts as a Function of Oxidation State[a]

Element[b]	**Oxidation State**									
	−2	−1	0	+1	+2	+3	+4	+5	+6	+7
Nitrogen (1*s*)	—	*0[c]	—	+4.5[d]	—	+5.1	—	+8.0	—	—
Sulfur (1*s*)	−2.0	—	*0	—	—	—	+4.5	—	+5.8	—
Chlorine (2*p*)	—	*0	—	—	—	+3.8	—	+7.1	—	+9.5
Copper (1*s*)	—	—	*0	+0.7	+4.4	—	—	—	—	—
Iodine (4*s*)	—	*0	—	—	—	—	—	+5.3	—	+6.5
Europium (3*d*)	—	—	—	—	*0	+9.6	—	—	—	—

[a] All shifts are in electron volts measured relative to the oxidation states indicated by (*). (Reprinted with permission from D. M. Hercules, *Anal. Chem.*, **1970**, *42*, 28A. Copyright 1970 American Chemical Society.)

[b] Type of electrons given in parentheses.

[c] Arbitrary zero for measurement, end nitrogen in NaN_3.

[d] Middle nitrogen in NaN_3.

Oxidation state↑ → electron의 binding energy↑

Skoog, Holler, Crouch, Principles of Instrumental Analysis (Thomson)

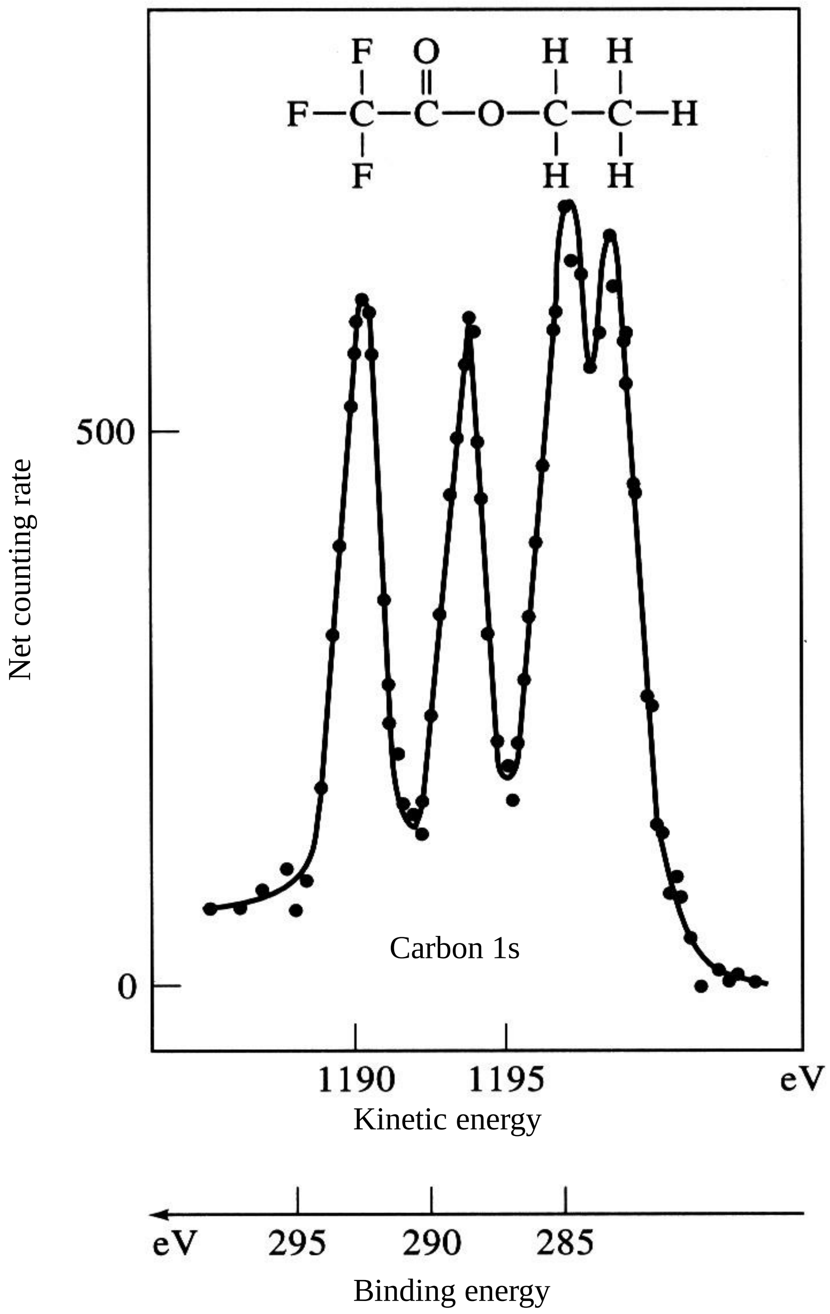
F
O
H
H
F—C—C—O—C—C—H
F
H
H
Net counting rate
500
0
Carbon 1s
1190
1195
eV
Kinetic energy
eV
295
290
285
Binding energy

XPS quantitative analysis

$$I = n\phi\sigma\varepsilon\eta ATl \tag{21-3}$$

Sensitivity factor

$$S = \sigma\varepsilon\eta ATl \tag{21-4}$$

n: number density of atoms of the sample (atoms/cm^3)
φ: flux of the incident X-ray beam (photons/cm^2·s)
σ: photoelectric cross section (cm2/atom)
ε: angular efficiency factor for the instrument
η: the efficiency of producing photoelectrons (photoelectrons/photon)
A: area of sample which photoelectrons are detected (cm^2)
T: the efficiency detection of the photoelectrons
l: mean free path of photoelectrons in the sample (cm)

→ for a given transition, last six terms are constant → atomic sensitivity factor S (XPS Handbook)

$I/S \propto$ concentration

XPS quantitative analysis

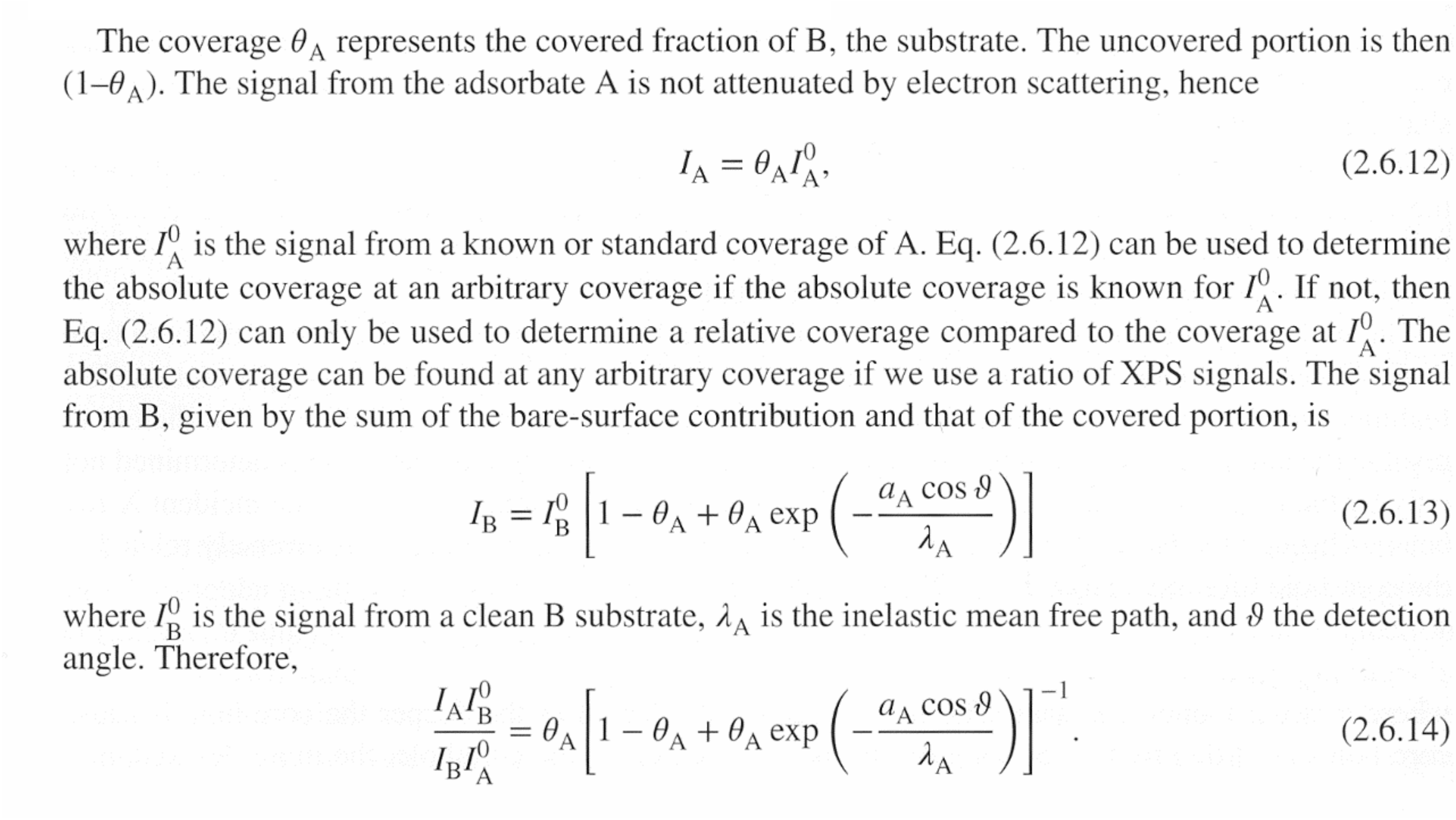

The coverage θ_A represents the covered fraction of B, the substrate. The uncovered portion is then $(1-\theta_A)$. The signal from the adsorbate A is not attenuated by electron scattering, hence

$$I_A = \theta_A I_A^0, \tag{2.6.12}$$

where I_A^0 is the signal from a known or standard coverage of A. Eq. (2.6.12) can be used to determine the absolute coverage at an arbitrary coverage if the absolute coverage is known for I_A^0. If not, then Eq. (2.6.12) can only be used to determine a relative coverage compared to the coverage at I_A^0. The absolute coverage can be found at any arbitrary coverage if we use a ratio of XPS signals. The signal from B, given by the sum of the bare-surface contribution and that of the covered portion, is

$$I_B = I_B^0 \left[1 - \theta_A + \theta_A \exp\left(-\frac{a_A \cos\vartheta}{\lambda_A}\right)\right] \tag{2.6.13}$$

where I_B^0 is the signal from a clean B substrate, λ_A is the inelastic mean free path, and ϑ the detection angle. Therefore,

$$\frac{I_A I_B^0}{I_B I_A^0} = \theta_A \left[1 - \theta_A + \theta_A \exp\left(-\frac{a_A \cos\vartheta}{\lambda_A}\right)\right]^{-1}. \tag{2.6.14}$$

XPS for Pt 4f levels:

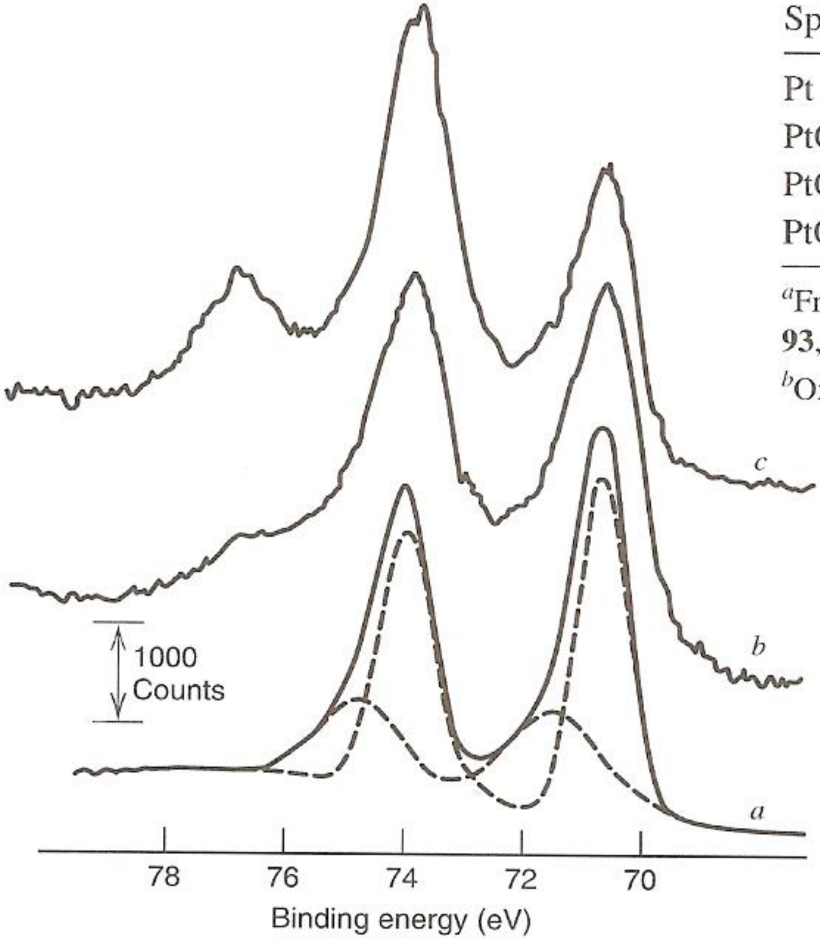

	Binding Energy, eV		Relative Peak Areas[b]		
Species	4f (7/2)	4f (5/2)	+0.7 V	+1.2 V	+2.2 V
Pt	70.7	74.0	56	39	34
PtO_{ads}	71.6	74.9	39	37	24
PtO	73.3	76.6	<5	24	22
PtO_2	74.1	77.4	0	0	20

[a] From K. S. Kim, N. Winograd, and R. E. Davis, *J. Am. Chem. Soc.*, **93**, 6296 (1971).

[b] Oxidation carried out at indicated potential (*vs.* SCE) for 3 min.

Electrochemical XPS (SNU)

UHV-XPS **Glove Box**

Ex-situ Analysis without Contamination

Ambient Pressure X-ray Photoelectron Spectroscopy

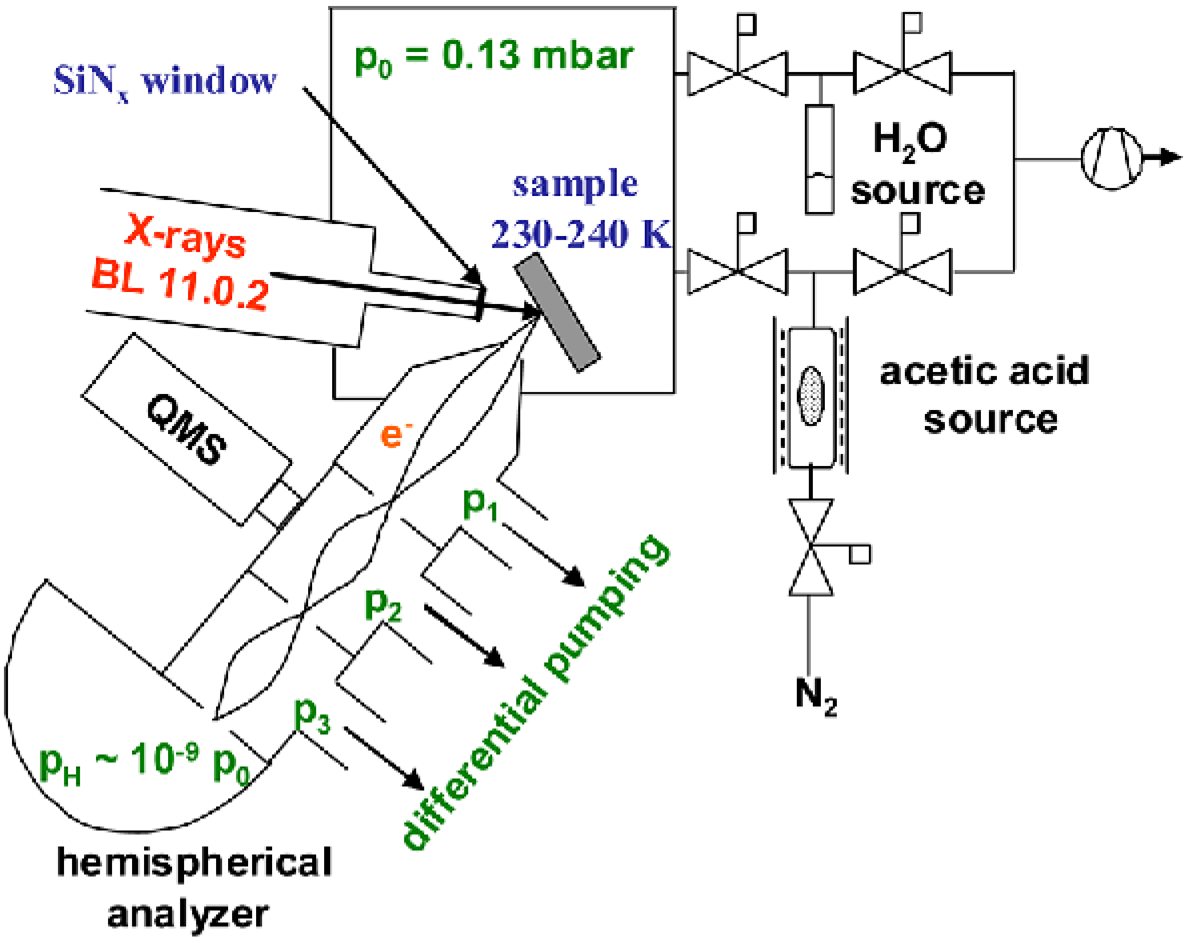

Published in The journal of physical chemistry. A 2013
DOI:10.1021/jp3102332

Ultraviolet photoelectron spectroscopy (UPS)

UV photons can excite photoemission from valence levels
Since valence electrons are involved in chemical bonding → UPS is well suited to the study of bonding at surfaces → work function, band structure of the solids, surface and adsorbed layers, bonding structure(σ or π)

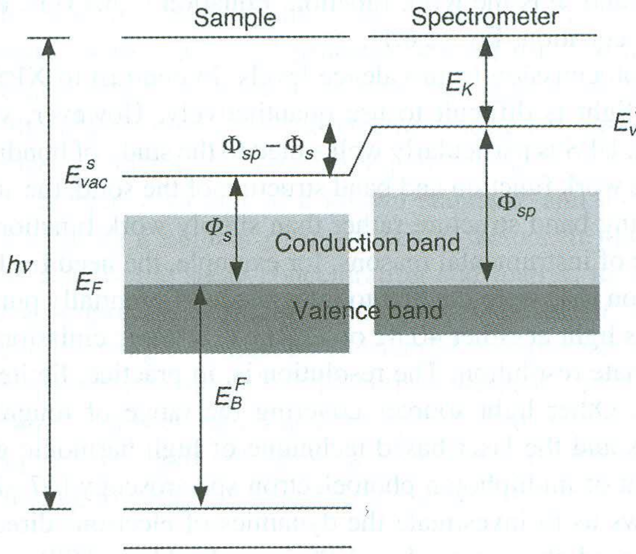

Figure 2.18 *The influence of the spectrometer work function, Φ_{sp}, on photoelectron spectra. Φ_s, work function of the sample; E_{vac}^{sp}, E_{vac}^{s} vacuum energies of the spectrometer and the sample, respectively; E_F, Fermi energy; E_K, electron kinetic energy; E_B^F, binding energy; h, Planck constant; ν, frequency of incident photon. Adapted from J. C. Vickerman,* Surface Analysis: The Principal Techniques, *John Wiley, Chichester, Sussex. © 1997 with permission from John Wiley & Sons, Ltd.*

$$E_{\mathrm{K}} = h\nu - E_{\mathrm{B}} - \Phi_{\mathrm{sp}}. \tag{2.6.16}$$

For excitation with a fixed photon energy $h\nu$, therefore, the maximum kinetic energy of photoelectrons is given by

$$E_{\mathrm{K,max}} = h\nu - \Phi_{\mathrm{sp}}. \tag{2.6.17}$$

Meanwhile the minimum kinetic energy is given by

$$E_{\mathrm{K,min}} = \Phi - \Phi_{\mathrm{sp}}. \tag{2.6.18}$$

The width of the spectrum,

$$\Delta E = E_{\mathrm{K,max}} - E_{\mathrm{K,min}} = h\,\nu - \Phi \tag{2.6.19}$$

is used to determine the work function of the sample

$$\Phi = h\,\nu - \Delta E \tag{2.6.20}$$

Auger electron spectroscopy (AES)

3 electron processes

(1) Core electron ejected
(2) Higher electron fills the core hole
(3) Exothermicity to eject 3rd electron (Auger electron)

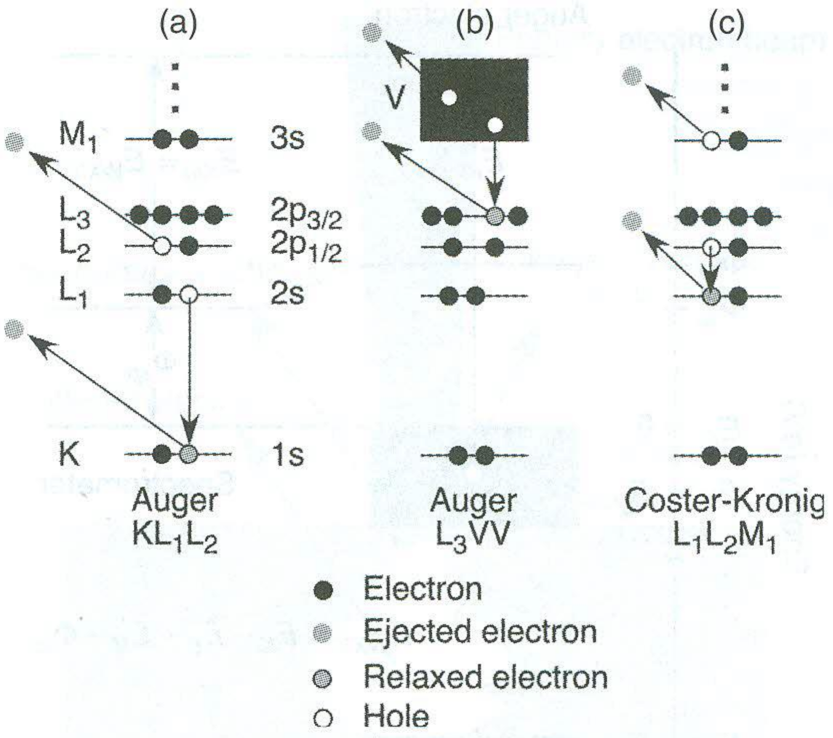

Figure 2.22 *A detailed depiction of Auger transitions involving (a) three core levels; (b) two core levels and the valence band; and (c) a Coster-Kronig transition in which the initial hole is filled from the same shell.*

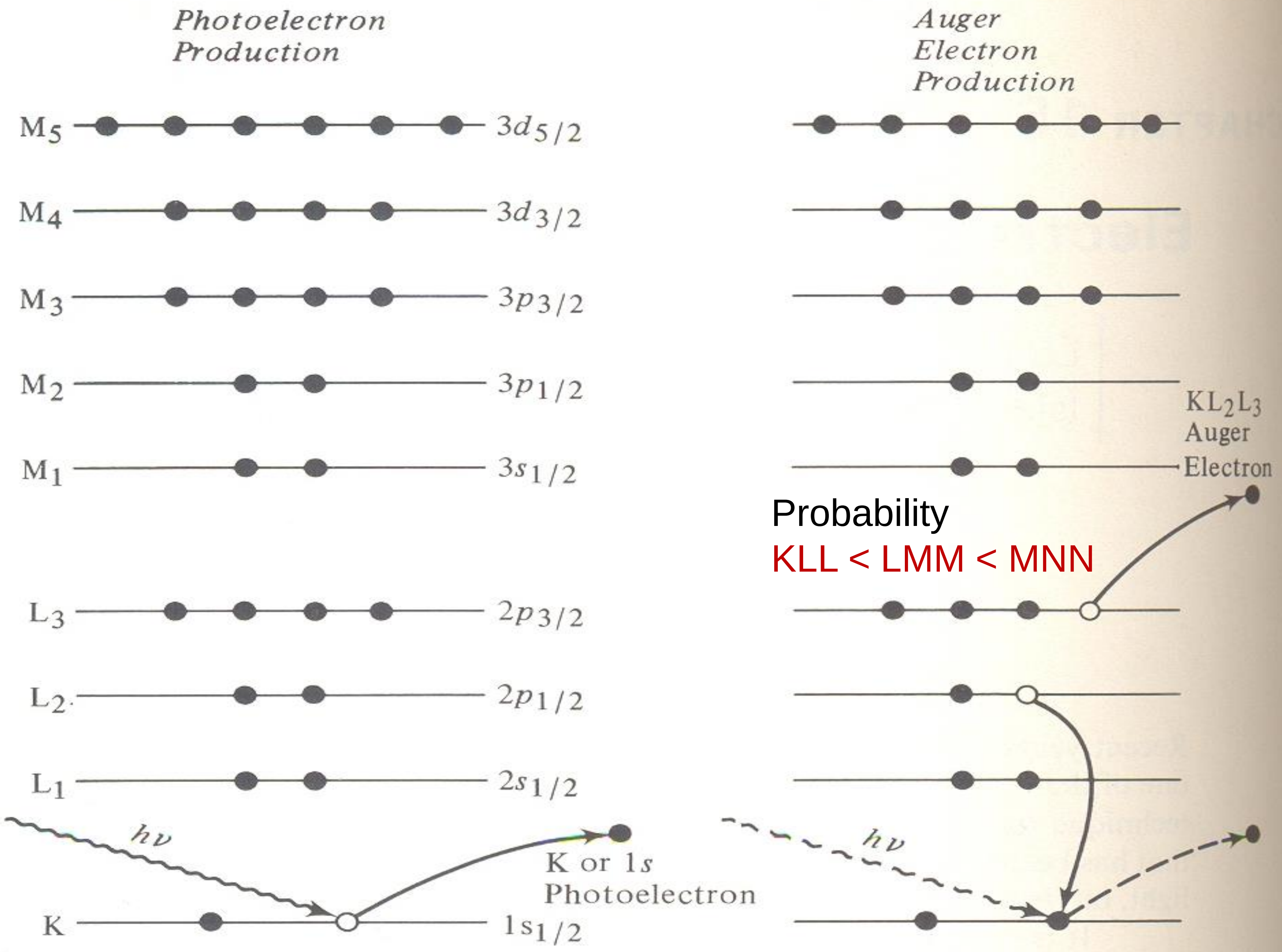

Probability

KLL < LMM < MNN

$$E_{WXY} = E_K - E_L - E_V - \phi_{sp}$$

or

$$E_{KL1L2} = (E_K - E_{L1}) - E_{L2}$$

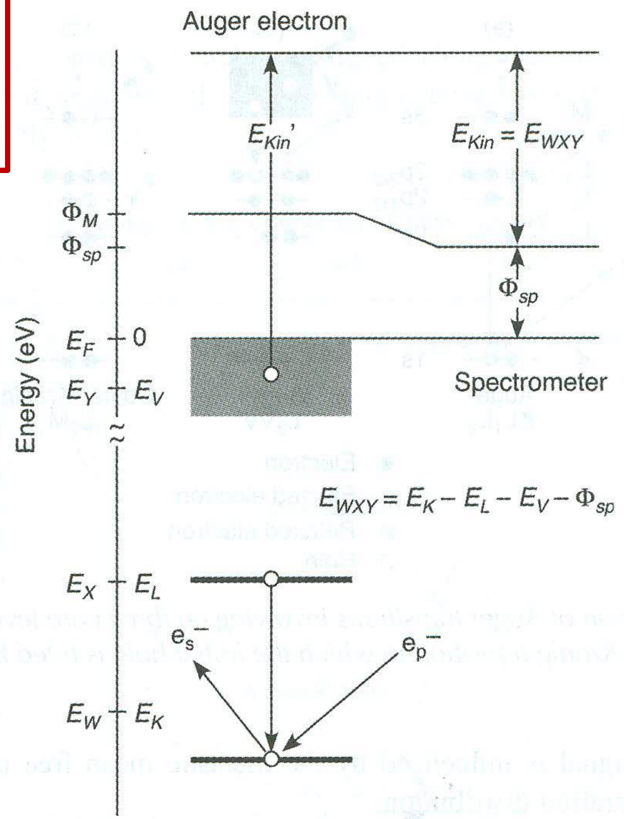

Figure 2.23 *Energy levels for a KLV Auger transition, including the influence of the spectrometer work function* Φ_{sp}*. Adapted from J.C. Vickerman,* Surface Analysis: The Principal Techniques, *John Wiley & Sons, Chichester. © 1997 with permission from John Wiley & Sons, Ltd.*

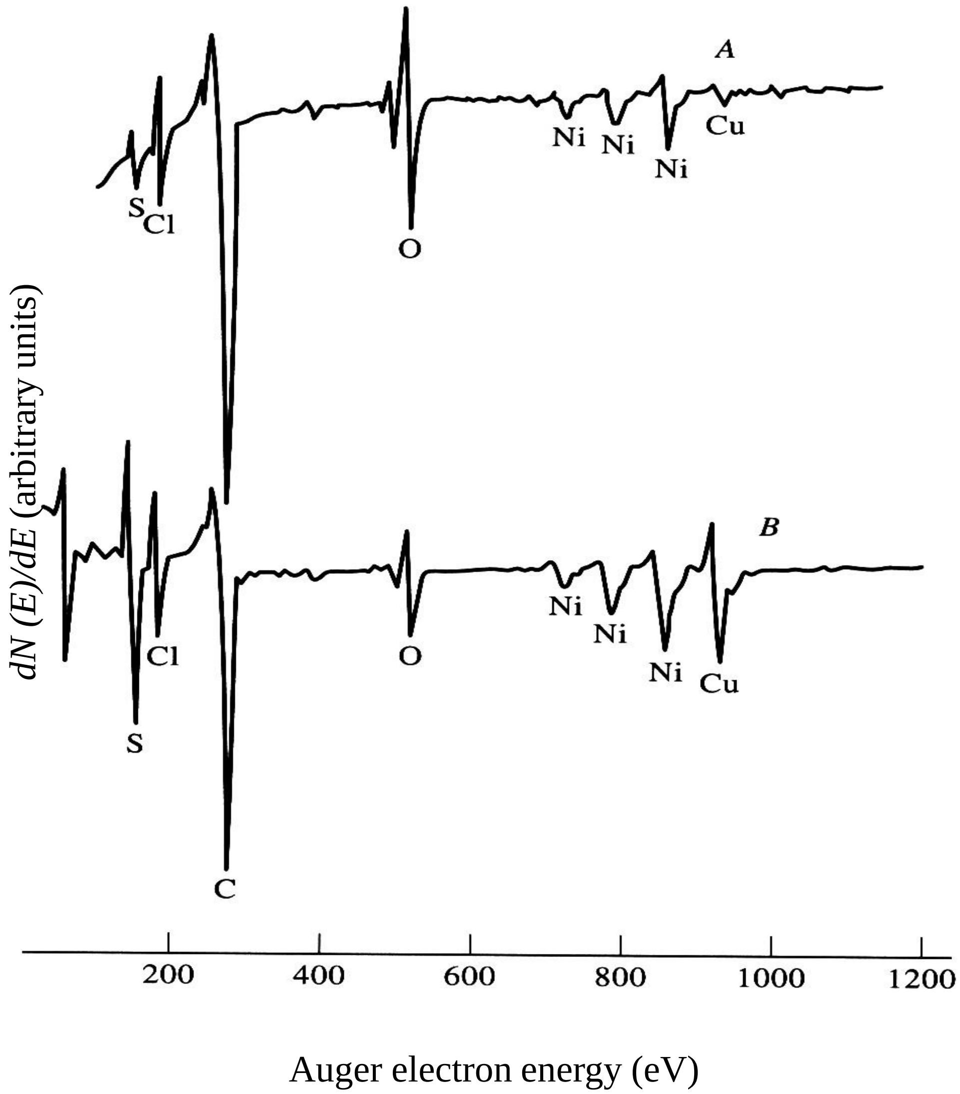

Auger Electrons

→ element analysis

Oxidation state

Structure

Quantitative analysis

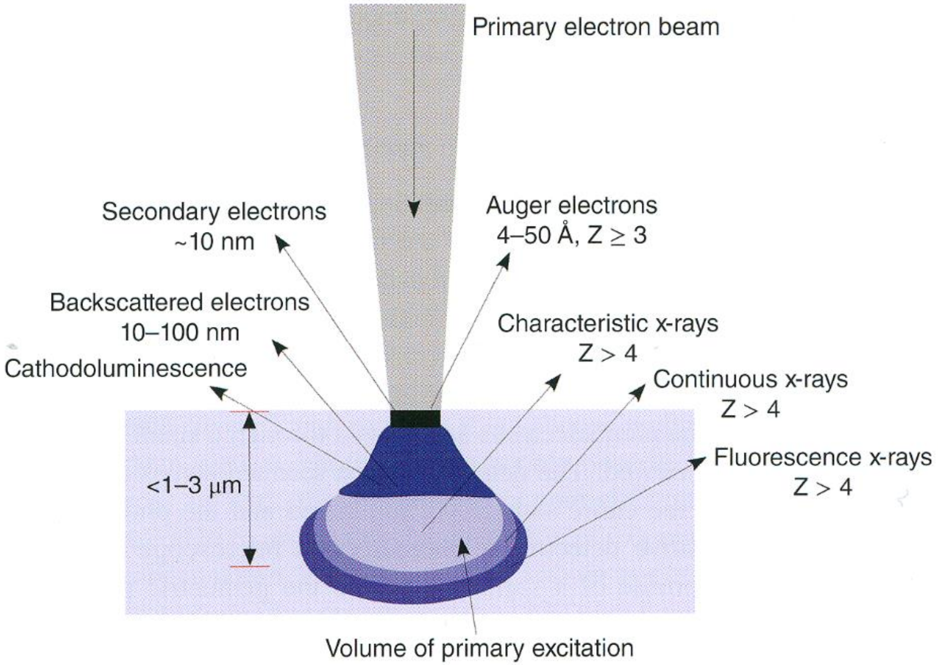

Figure 2.24 *The geometry of Auger electron spectroscopy. A primary electron beam excites the formation of Auger electrons as well as X-ray fluorescence. Backscattered and secondary electrons are also created in the process.*

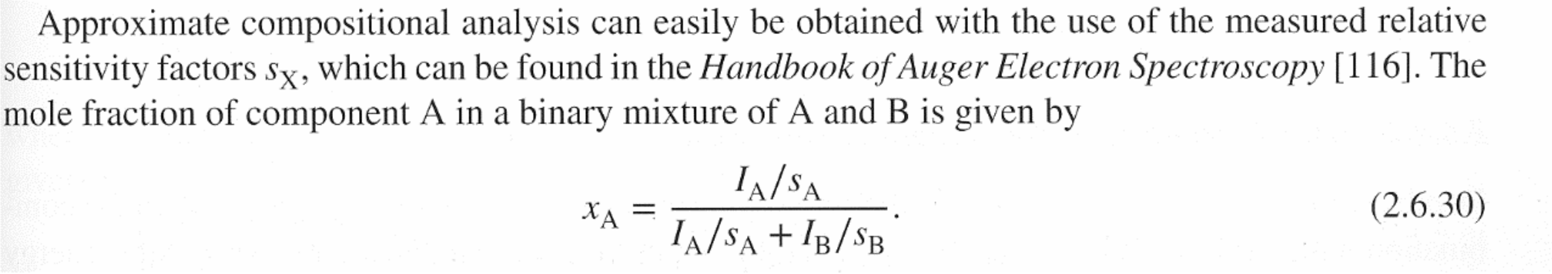

Approximate compositional analysis can easily be obtained with the use of the measured relative sensitivity factors s_X, which can be found in the *Handbook of Auger Electron Spectroscopy* [116]. The mole fraction of component A in a binary mixture of A and B is given by

$$x_A = \frac{I_A/s_A}{I_A/s_A + I_B/s_B}. \qquad (2.6.30)$$

AES depth profile: ion sputtering

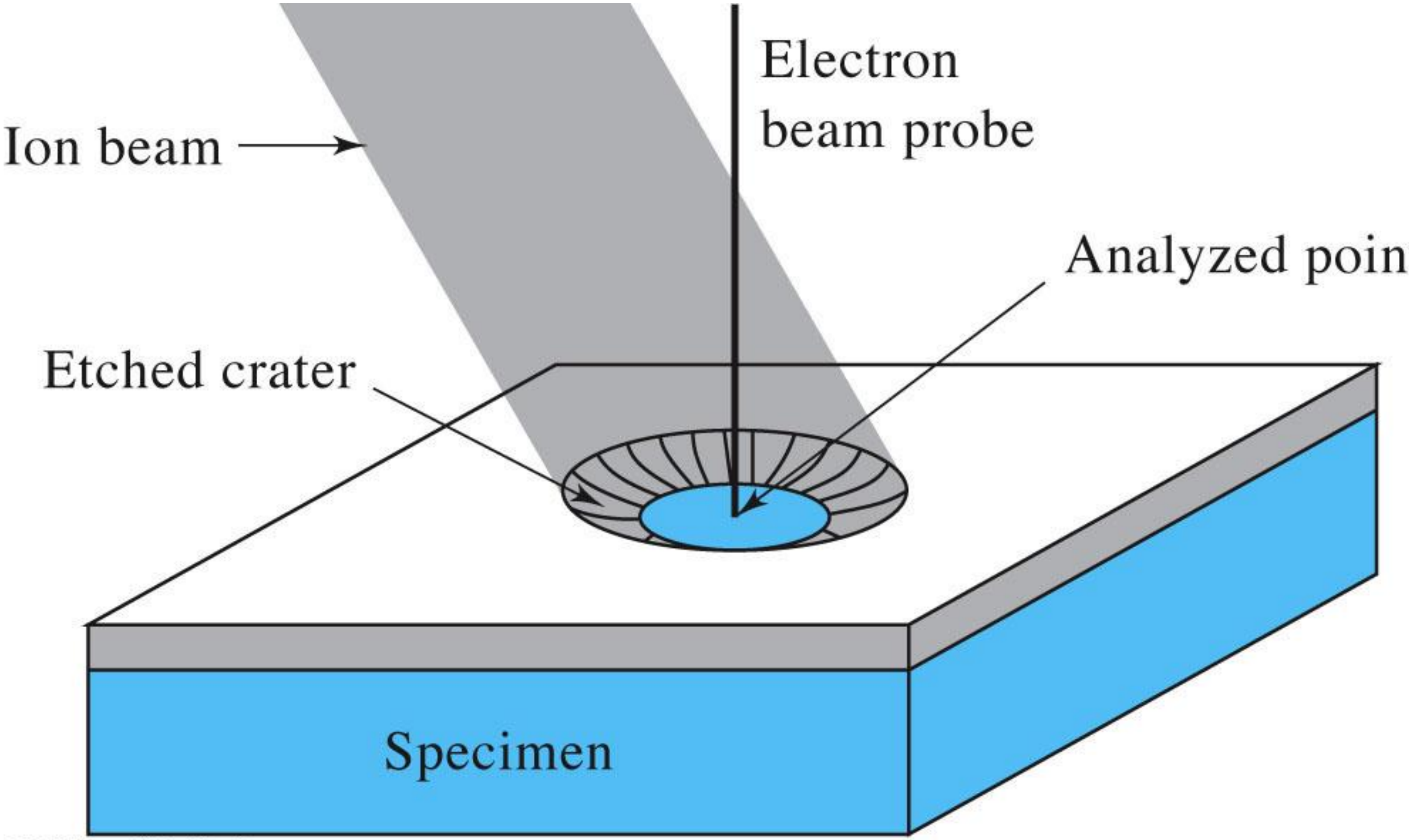

Skoog, Holler, Crouch, Principles of Instrumental Analysis (Thomson)

AES depth profiles: GaAs

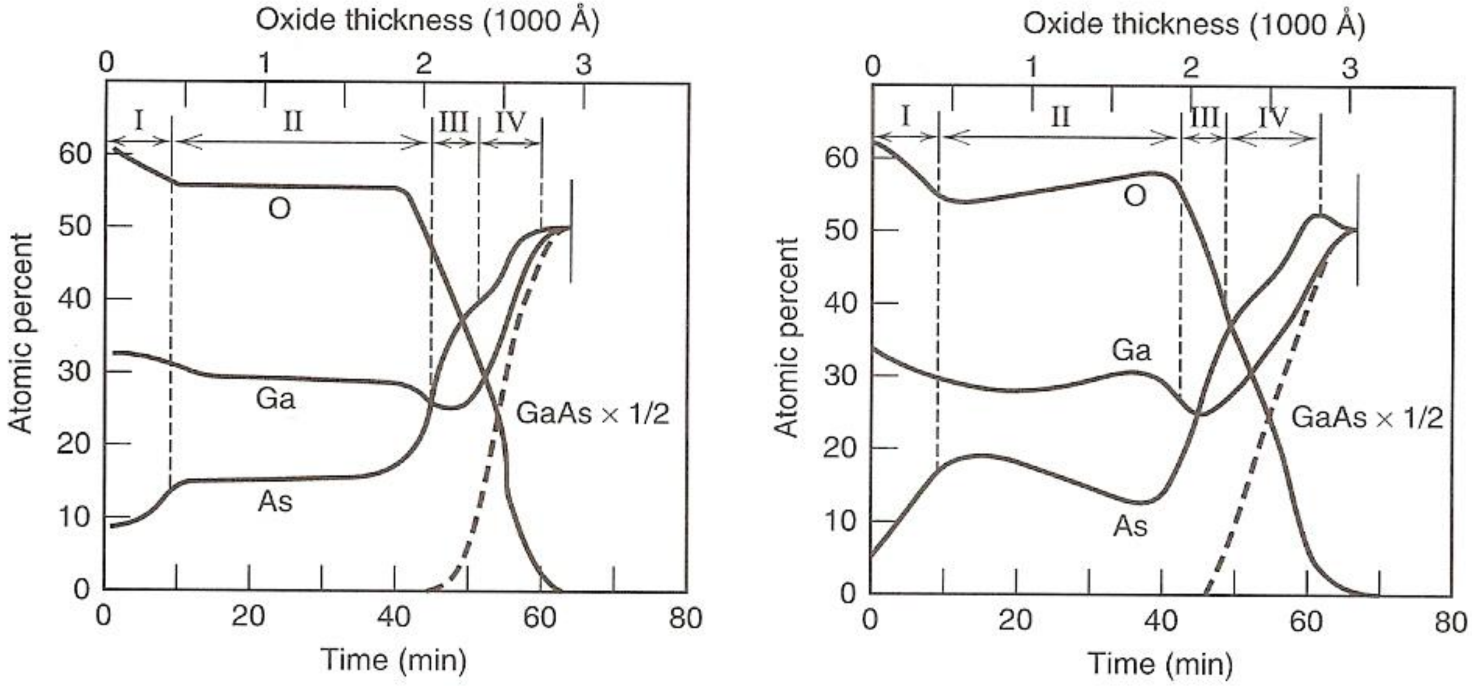

(*a*) (*b*)

Vibration spectroscopy

Vibration motions → IR absorption, electron energy loss, Raman, sum frequency generation, inelastic neutron tunneling, He scattering

Energy of electromagnetic field: oscillating electric & magnetic disturbance

$$\boxed{E = h\nu = h\,c/\lambda}$$

h; Planck constant (6.6 x 10^{-34} Js)
speed of light (c); 3 x 10^{8} m/s,
wavelength (λ); distance between the neighboring peaks of wave,

$$1\ \text{Å} = 0.1\ \text{nm} = 10^{-10}\ \text{m}$$

frequency (ν, Hz = 1 s^{-1}); number of times per second

$$\lambda\nu = c$$

wavenumber (cm^{-1}, reciprocal cm), ν-bar = $\nu/c = 1/\lambda$
cf) 1 eV ~ 8066 cm^{-1}

Wavelength (λ, nm) = 1240/band gap energy (eV)

Widely used IR spectroscopy: mid-IR (670~4000 cm^{-1}(2.5 ~ 14.9 µm))

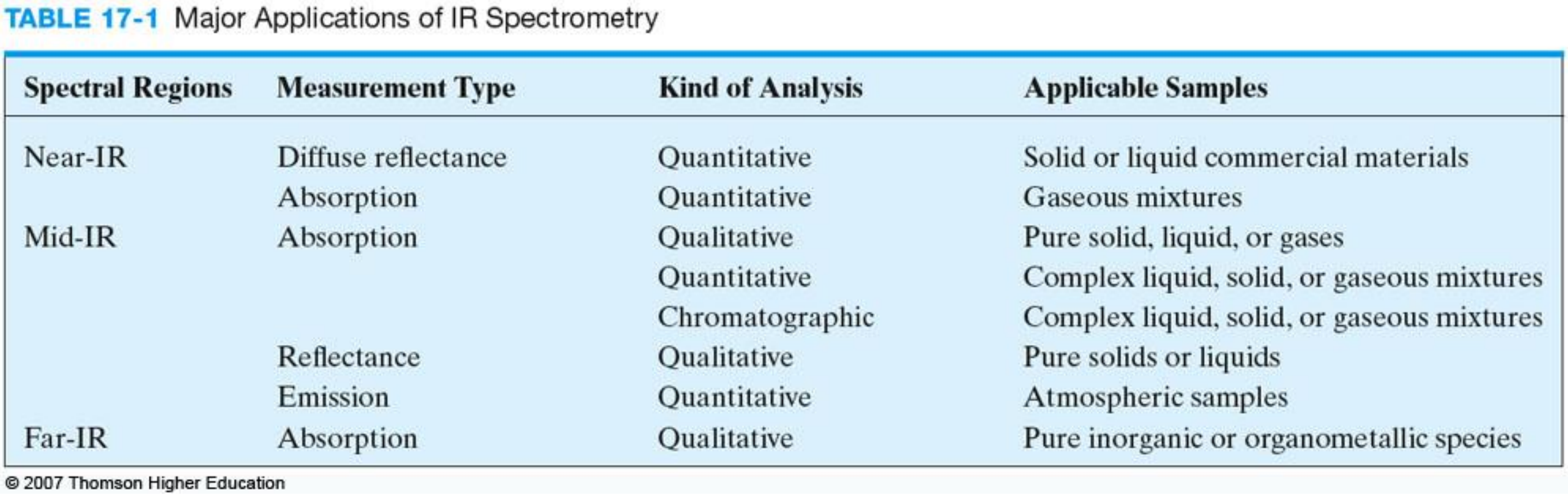

TABLE 17-1 Major Applications of IR Spectrometry

Spectral Regions	Measurement Type	Kind of Analysis	Applicable Samples
Near-IR	Diffuse reflectance	Quantitative	Solid or liquid commercial materials
	Absorption	Quantitative	Gaseous mixtures
Mid-IR	Absorption	Qualitative	Pure solid, liquid, or gases
		Quantitative	Complex liquid, solid, or gaseous mixtures
		Chromatographic	Complex liquid, solid, or gaseous mixtures
	Reflectance	Qualitative	Pure solids or liquids
	Emission	Quantitative	Atmospheric samples
Far-IR	Absorption	Qualitative	Pure inorganic or organometallic species

Skoog, Holler, Crouch, Principles of Instrumental Analysis (Thomson)

Electromagnetic spectrum

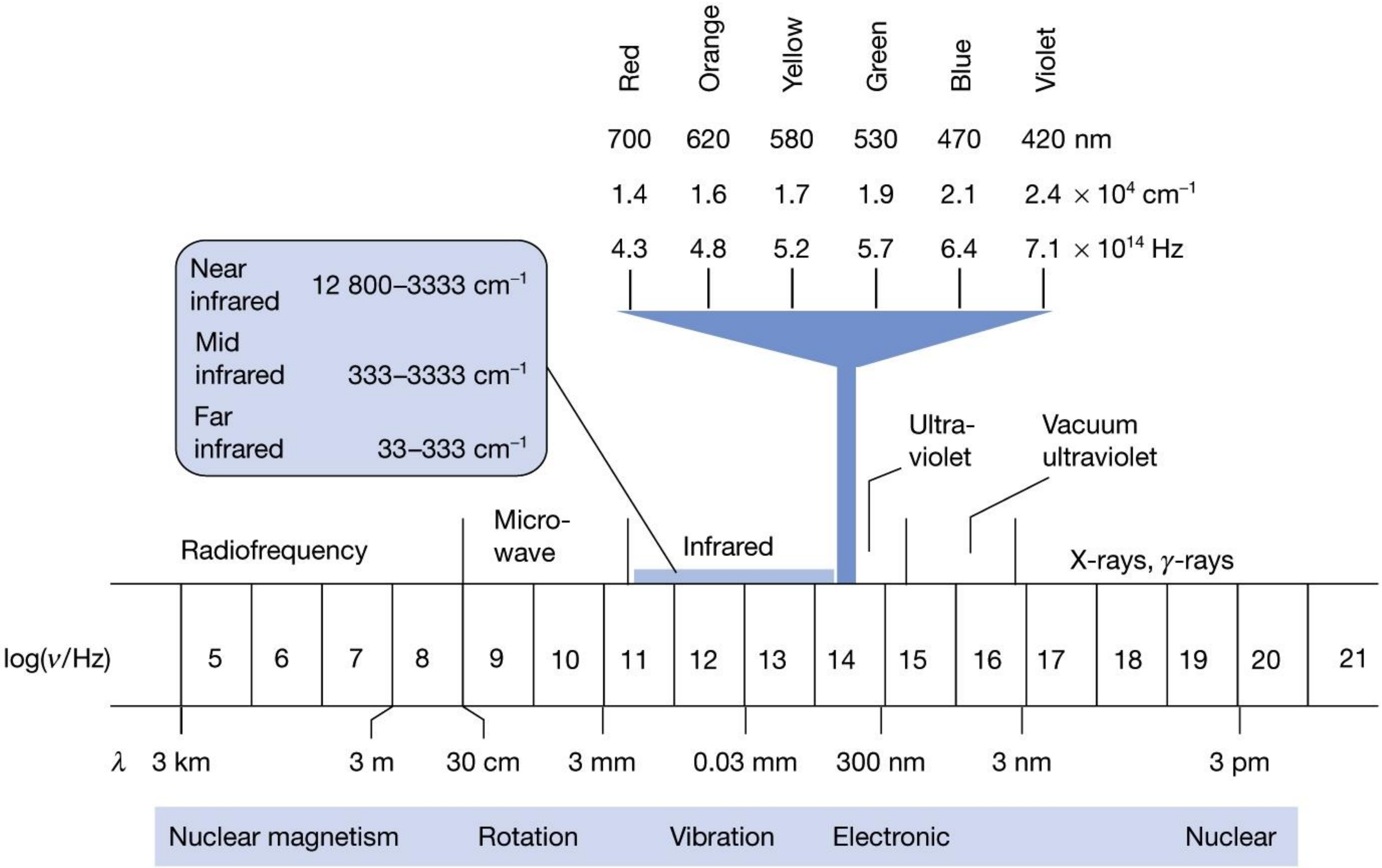

IR radiation ~ energy differences for vibrational & rotational states

For absorption of IR radiation: dipole moment change during vibration

Dipole moment is determined by the magnitude of the charge difference and the distance between two centers of charge
e.g) H-Cl (o)
O-O (x)

Types of vibration: stretching & bending


Symmetric
Asymmetric

(a) Stretching vibrations

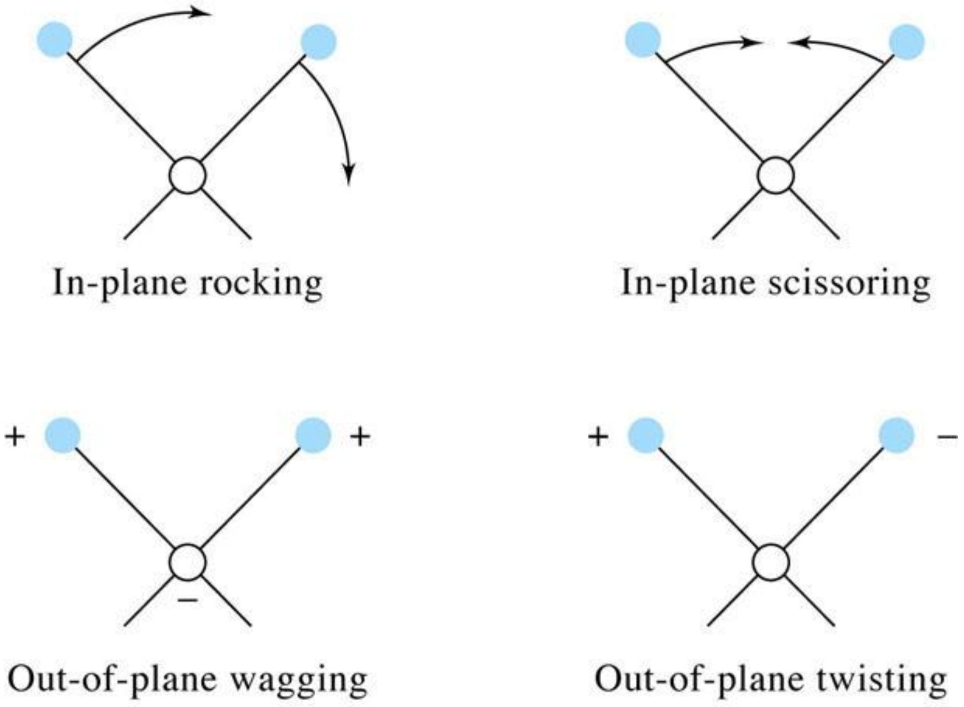

In-plane rocking
In-plane scissoring
Out-of-plane wagging
Out-of-plane twisting

(b) Bending vibrations

Harmonic oscillator

$F = -ky$ Hooke's law

k: force constant

-: opposite direction for the force

Potential energy:

$$E = \tfrac{1}{2}ky^2$$

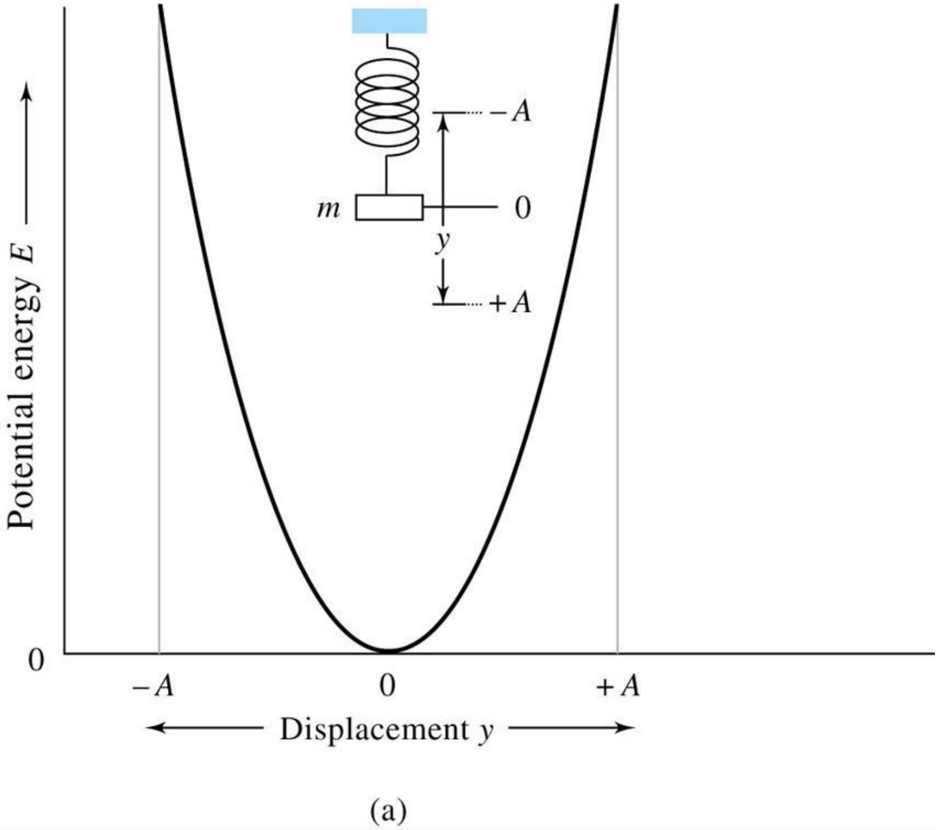

(a)

Vibrational frequency

$F = ma = m(d^2y/dt^2) = -ky$

$y = A\cos(2\pi vt)$

Frequency of mechanical oscillator

$v = (1/2\pi)\sqrt{(k/m)}$

Reduced mass: $\mu = m_1m_2/(m_1 + m_2)$

$v = (1/2\pi)\sqrt{(k/\mu)}$

Quantum treatment of vibration:

$$\boxed{E = (v + \tfrac{1}{2})(h/2\pi)\sqrt{(k/\mu)} = (v + \tfrac{1}{2})\hbar\omega_0}$$

h: Planck’s constant, v: vibrational quantum number

Transition v=0 to v=1
$\Delta E = hv = (h/2\pi)\sqrt{}(k/\mu)$

Ground state at v = 0:

$E_0 = ½\ hv$

1st excited state (v= 1)

$E_1 = 3/2\ hv$

Required radiation energy:

$(3/2 – ½)hv = hv$
$= (h/2\pi)\sqrt{}(k/\mu)$

Wavenumber (cm^{-1}):
v-bar = $(1/2\pi c)\sqrt{}(k/\mu)$
$= 5.3 \times 10^{-12}\sqrt{}(k/\mu)$

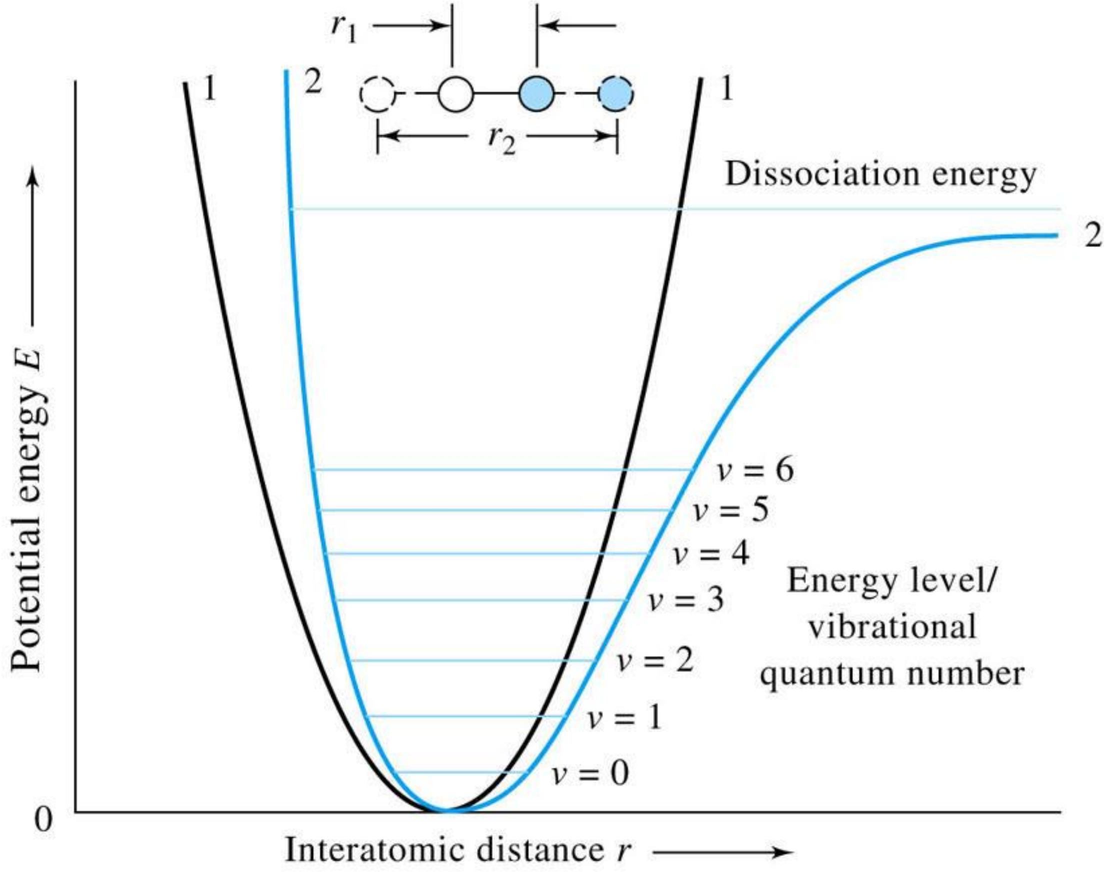

(b)

© 2007 Thomson Higher Education

1. Harmonic oscillator
2. Anharmonic motion

IR spectroscopy

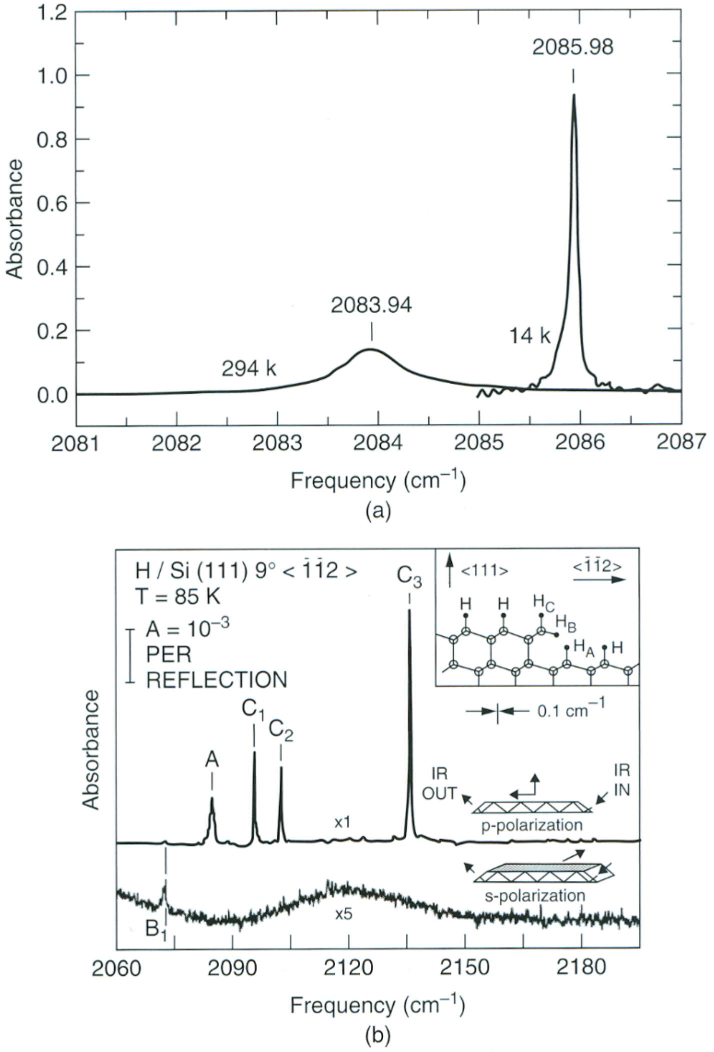

(a)

(b)

Figure 2.26 *The IR spectrum of H adsorbed on chemically prepared (a) flat and (b) stepped Si(111) surfaces. Source: Reproduced with permission. Panel (a) from R. Honke, et al.,* Phys. Rev. B ***59*** *(1999) 10996. ©1991 American Physical Society. Panel (b) reproduced from P. Jakob, Y. J. Chabal, K. Raghavachari, S. B. Christman,* Phys. Rev. B, ***47*** *(1993) 6839. ©1993 American Physical Society.*

IR spectroscopy

Transmission
Reflection
Diffuse reflection
Internal reflection

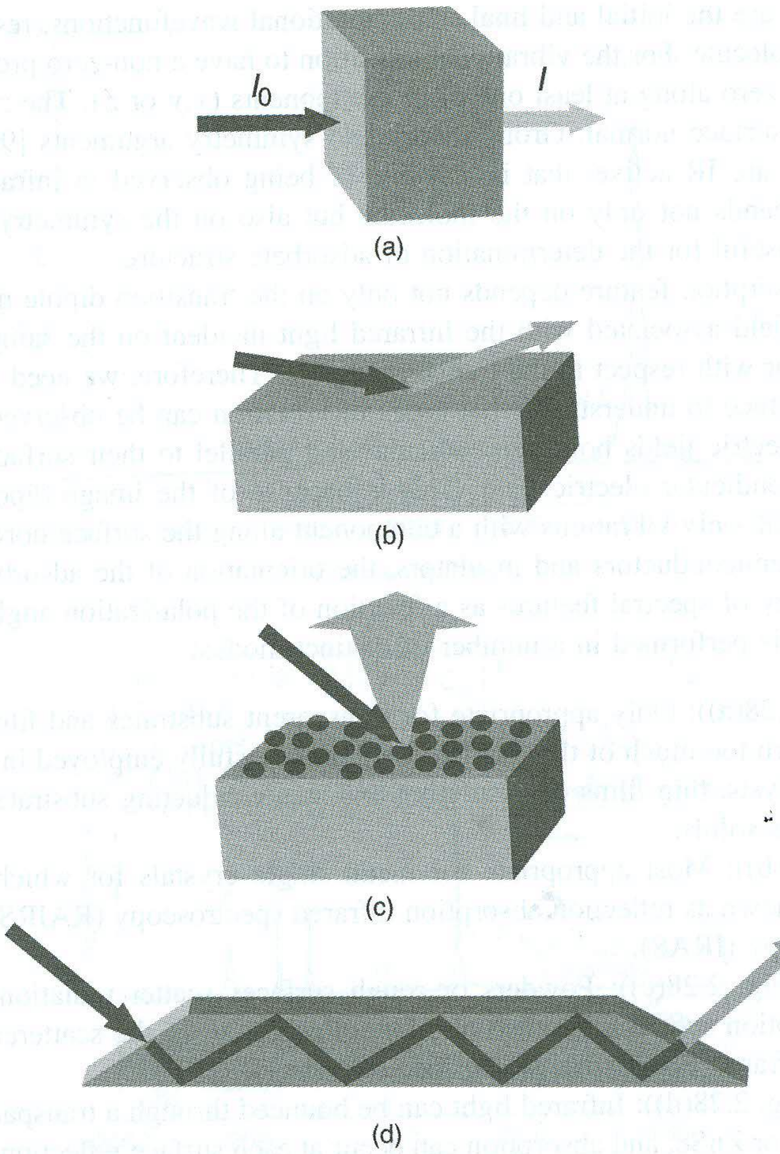

Figure 2.28 *The modes of IR spectroscopy.*

$$T = I/I_0 \tag{2.7.5}$$

or absorbance

$$A = -\log T = \log(I_0/I) \tag{2.7.6}$$

where I_0 is the incident intensity and I is the transmitted intensity. In the absence of reflection and scattering, the transmittance is given by

$$T = 10^{-acl} = \exp(-\alpha l) \tag{2.7.7}$$

where a is the absorptivity, c the concentration and l the path length. The absorption coefficient, α, is related to the absorptivity by

$$\alpha = 2.3026 \ \ ac \tag{2.7.8}$$

which is, in turn, related to the imaginary part, κ, of the complex refractive index, $\tilde{n}$, by

$$\alpha = 4\pi\kappa/\lambda_0 \tag{2.7.9}$$

where λ_0 is the vacuum wavelength of the infrared light and κ is defined through

$$\widetilde{n} = n + i\kappa. \tag{2.7.10}$$

It follows that absorbance is linearly proportional to concentration and the path length

$$A = acl. \tag{2.7.11}$$

IR reflection spectroscopy

Specular reflection: smooth surface
Diffuse reflection
Internal reflection

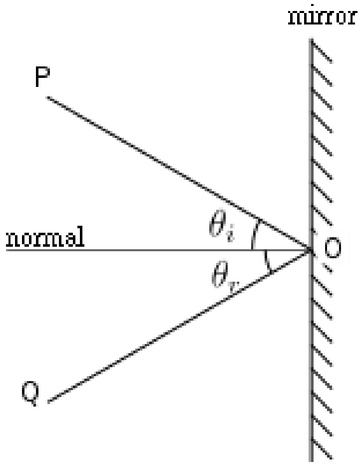

Specular reflection

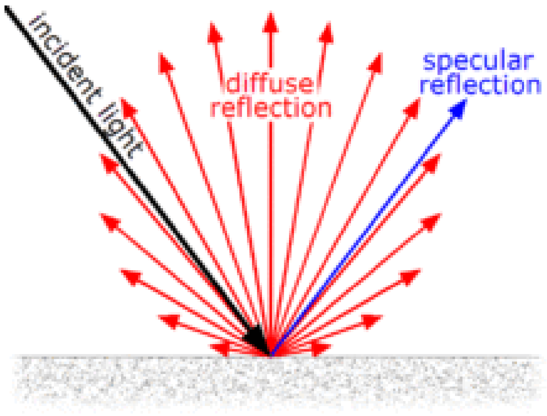

Diffuse reflection

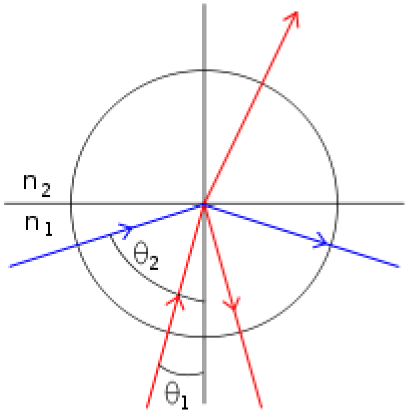

Internal reflection
(blue line)

Diffuse reflection

Diffuse-reflectance attachment

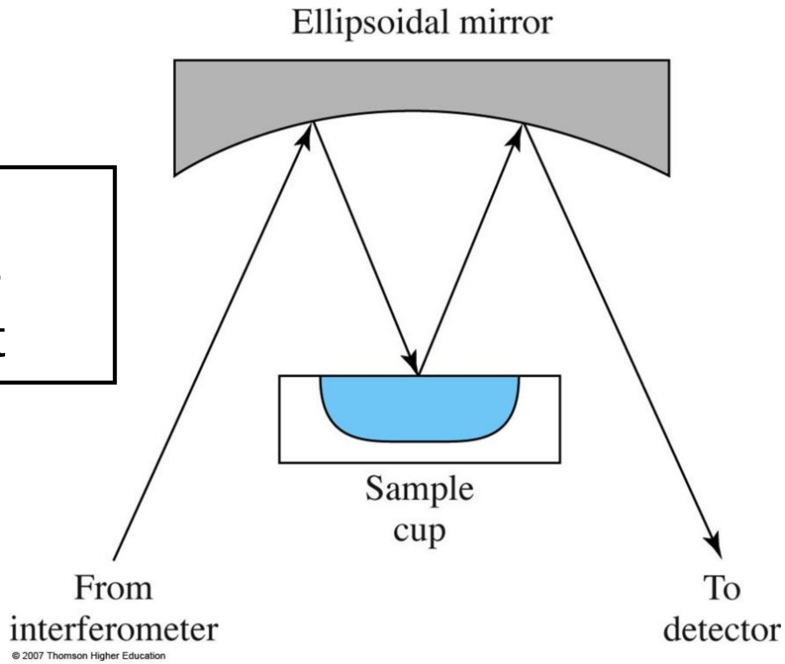

© 2007 Thomson Higher Education

- Diffuse Reflectance Infrared Fourier Transform Spectroscopy (DRIFT)

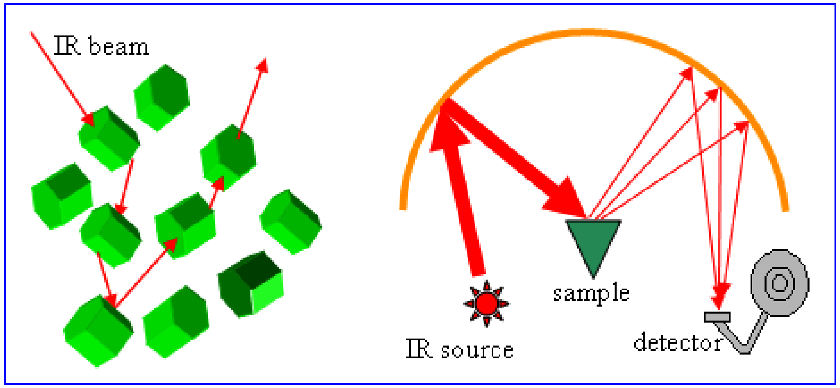

Powder sample

Electron energy loss spectroscopy (EELS)

Electron backscattered from surface → lose energy of the surface and adsorbed layer → vibrational transitions (1 meV = 8.064 cm^{-1})

$$\boxed{E = E_0 - \hbar\omega}$$

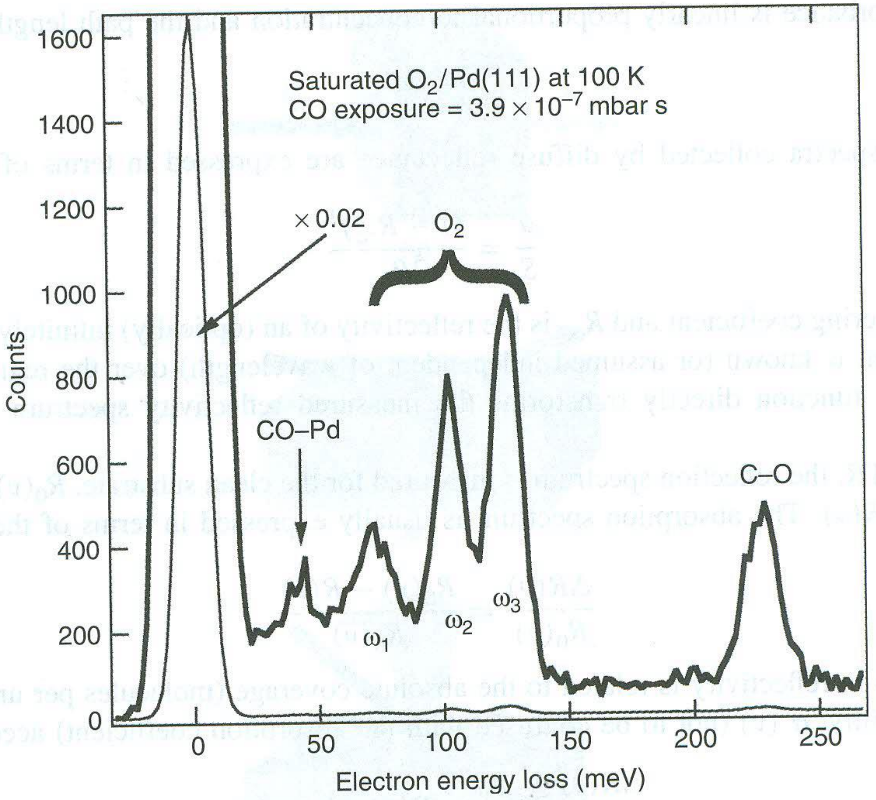

Figure 2.29 *The electron energy loss spectrum of co-adsorbed* $O_2 + CO$ *on Pd(111). The species associated with* ω_1, ω_2 *and* ω_3 *are illustrated in Fig. 3.8. Adapted from K.W. Kolasinski, F. Cemič, A. de Meijere, E. Hasselbrink,* Surf. Sci., *334, 19. © 1995 with permission from Elsevier.*

High resolution electron energy loss spectroscopy

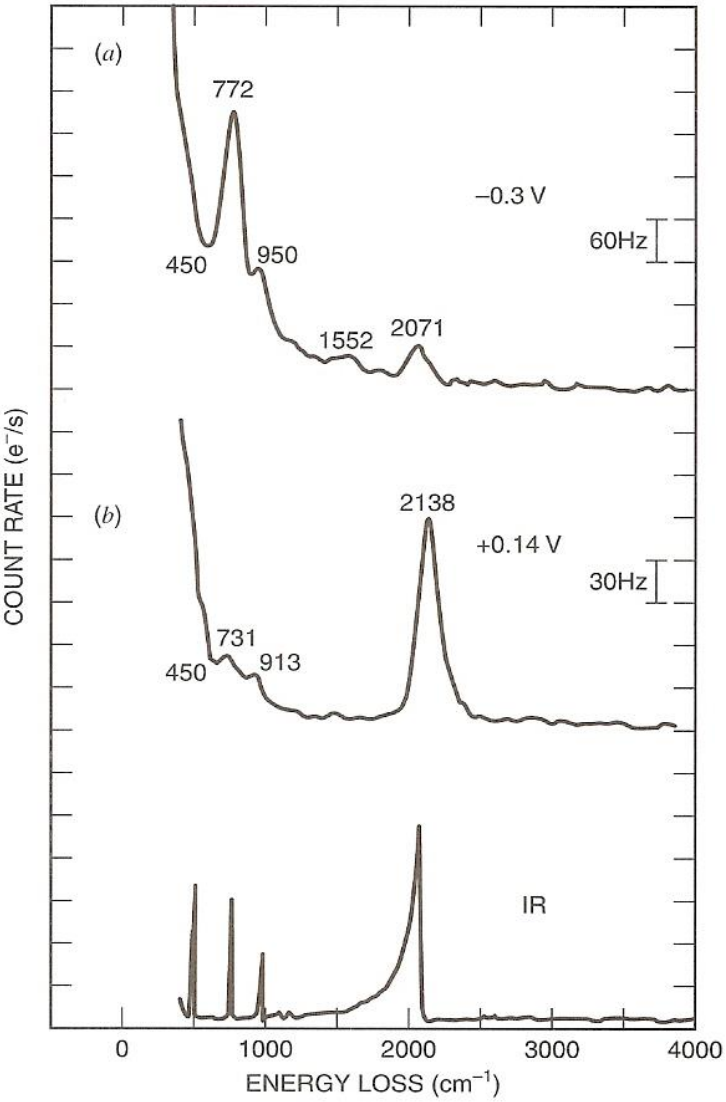

SCN$^-$ on Ag(111)

(a) -0.3 V
(b) +0.14 V

Second harmonic and sum frequency generation

SHG & SFG are two closely related techniques → application in surface and interface science → laser light illuminates an interface between two phases A and B → excites a non-linear polarization responses

1) Two photons at same frequency ω, can be mixed together to form a 3rd photon at frequency $\omega = \omega_1 + \omega_2$
→ "second harmonic generation"

2) Two photons with distinct frequencies ω_1 and ω_2 and angle of incidence θ_1 and θ_2 can mix together to form 3rd photon $\omega = \omega_1 + \omega_2$ which depart at θ_3
→ "sum frequency generation"

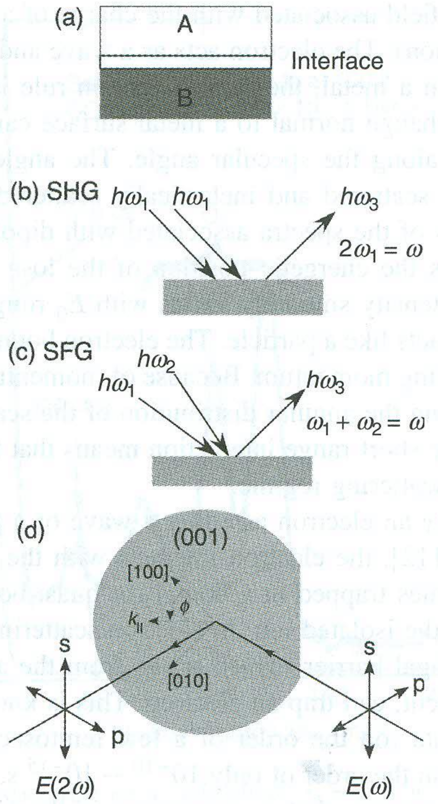

Figure 2.30 *(a) Two bulk materials joined by an interfacial region. (b) Two photons of the same frequency are mixed in second harmonic generation (SHG). (c) Two photons of different frequency are mixed in sum frequency generation (SFG). (d) The polarization components s and p are shown for a laser incident on a surface.*

Second harmonic spectroscopy

Second harmonic generation (SHG): ω → 2ω
Second harmonic generation (SHG): noncentrosymmetric crystals
If symmetry is broken at the solid/liquid interface → SHG signal

SHG signal is sensitive to species at the interface: used to detect adsorbed species, reaction intermediates etc

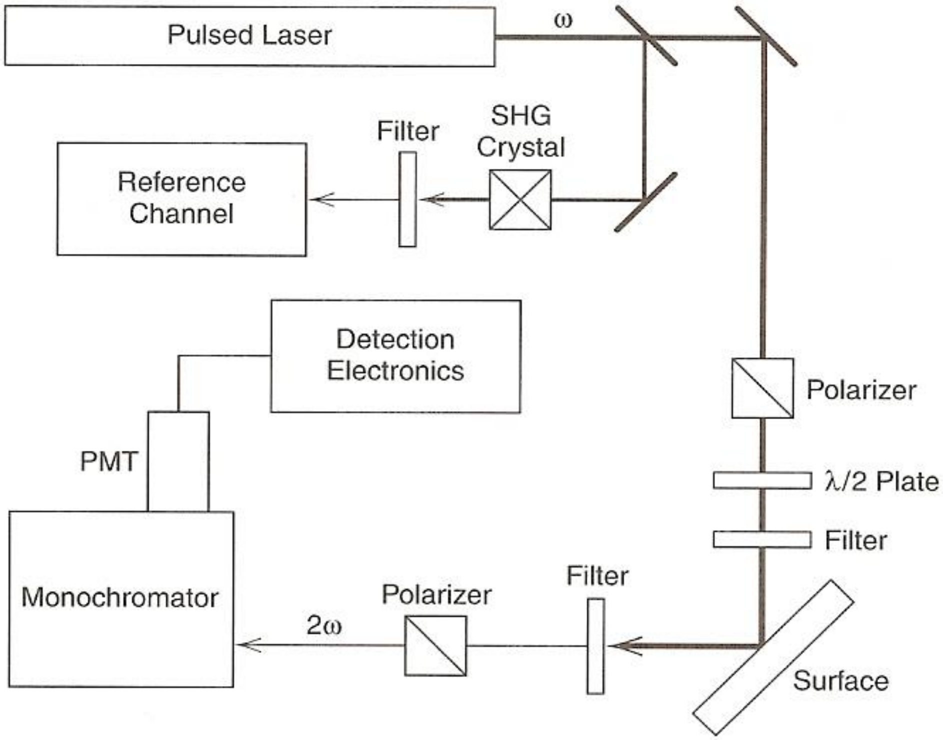

Summary

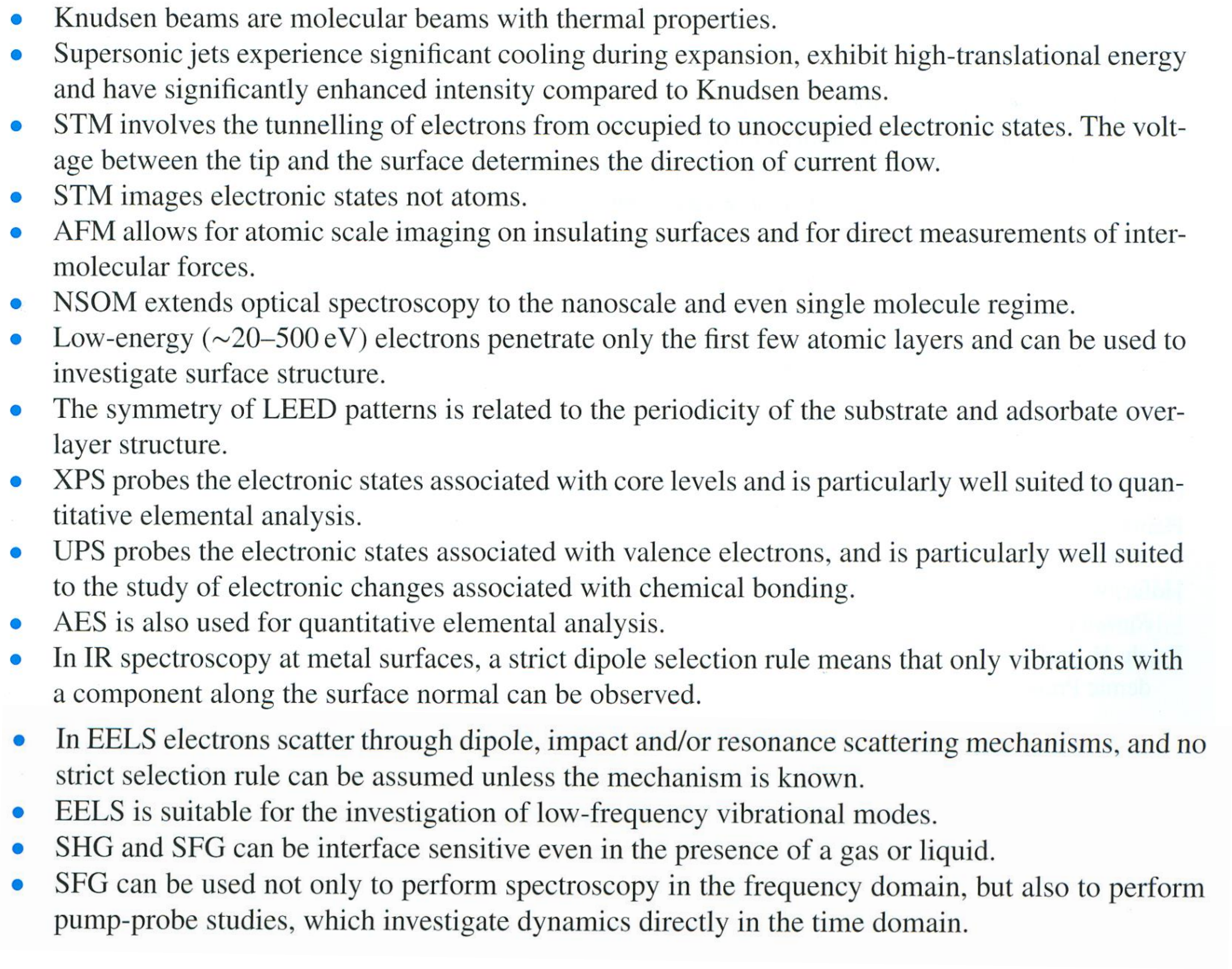

- Knudsen beams are molecular beams with thermal properties.
- Supersonic jets experience significant cooling during expansion, exhibit high-translational energy and have significantly enhanced intensity compared to Knudsen beams.
- STM involves the tunnelling of electrons from occupied to unoccupied electronic states. The voltage between the tip and the surface determines the direction of current flow.
- STM images electronic states not atoms.
- AFM allows for atomic scale imaging on insulating surfaces and for direct measurements of intermolecular forces.
- NSOM extends optical spectroscopy to the nanoscale and even single molecule regime.
- Low-energy (~20–500 eV) electrons penetrate only the first few atomic layers and can be used to investigate surface structure.
- The symmetry of LEED patterns is related to the periodicity of the substrate and adsorbate overlayer structure.
- XPS probes the electronic states associated with core levels and is particularly well suited to quantitative elemental analysis.
- UPS probes the electronic states associated with valence electrons, and is particularly well suited to the study of electronic changes associated with chemical bonding.
- AES is also used for quantitative elemental analysis.
- In IR spectroscopy at metal surfaces, a strict dipole selection rule means that only vibrations with a component along the surface normal can be observed.
- In EELS electrons scatter through dipole, impact and/or resonance scattering mechanisms, and no strict selection rule can be assumed unless the mechanism is known.
- EELS is suitable for the investigation of low-frequency vibrational modes.
- SHG and SFG can be interface sensitive even in the presence of a gas or liquid.
- SFG can be used not only to perform spectroscopy in the frequency domain, but also to perform pump-probe studies, which investigate dynamics directly in the time domain.